UBIQUITIN MODULATES TOLLIP'S PTDINS3P BINDING AND DISSOCIATES THE DIMERIC STATE OF C-TERMINAL CUE DOMAIN

Sharmistha Mitra

Thesis submitted to the Faculty of the Virginia Polytechnic Institute and State University in partial fulfillment of the requirements for the degree of

Doctor of Philosophy
In
Biological Sciences

Daniel G. S. Capelluto (Chair)
Glenda Gillaspy
Liwu Li
Michael Klemba

June 10, 2013
Blacksburg, Virginia
Keywords: Tollip, phosphoinositides, ubiquitin, endocytosis

UBIQUITIN MODULATES TOLLIP'S PTDINS3P BINDING AND DISSOCIATES THE DIMERIC STATE OF C-TERMINAL CUE DOMAIN

SHARMISTHA MITRA

ABSTRACT

Ubiquitylation is a highly controlled post-translational modification of proteins, in which proteins are conjugated either with monoubiquitin or polyubiquitin chains. Ubiquitin modifications on target proteins are recognized by ubiquitin-binding domains, which are found in several effector proteins. In this study, we describe for the first time how ubiquitin controls the function of the Toll-interacting protein (Tollip), which is an effector protein in the innate immune signaling pathway and an adaptor protein for endosomal trafficking. We have demonstrated that the central C2 domain of Tollip preferentially interacts with phosphoinositides with moderate affinity. Remarkably, we found that ubiquitin modulates Tollip's lipid binding. We have observed an ubiquitin dose-dependent inhibition of binding of Tollip to phosphoinositides and it does so specifically by blocking Tollip C2 domain-phosphoinositide interactions. This led us to discover that the Tollip C2 domain is a novel ubiquitin-binding domain. In addition, we have biophysically characterized the association of the Tollip CUE domain to ubiquitin and compared it with Tollip C2 domain-ubiquitin binding. The Tollip CUE domain reversibly binds ubiquitin with affinity higher than C2 domain and at a site that overlaps with that corresponding to the Tollip C2 domain. We have also found that ubiquitin binding to dimeric Tollip CUE domain induces a drastic conformational change in the protein, leading to the formation of a heterodimeric Tollip CUE-ubiquitin complex. These

data suggest that ubiquitin binding to the Tollip C2 and CUE domains and ubiquitin-mediated dissociation of CUE dimer reduces the affinity of the Tollip protein for endosomal phosphoinositides, allowing Tollip's cytoplasmic sequestration. Overall, our findings will provide the structural and molecular basis to understand how Tollip works inside the cell and commit itself to cytosolic signalling or endosomal trafficking in a ligand dependent manner.

DEDICATION

The thesis is dedicated to my parents Late Subal Mitra and Late Rita Mitra, whose accidental death from fatal diseases inspired me to be a researcher in the area of Biological Sciences.

ACKNOWLEDGEMENTS

The thesis represents my four and a half years long endeavor through the roads of science and research on which I had walked, stumbled, learned, relearned from mistakes and ultimately grown to become a researcher from a mere graduate student. All these years, I came across many faces - some new, some old. I am grateful to many of them for my achievement today.

First and foremost, I will express my sincere gratitude to Dr. Daniel Capelluto, my supervisor, whose immense patience, encouragement and excellent scientific guidance helped me to grow as a researcher over years. I am especially thankful to him for giving me enough space to share my own research ideas with him, discuss research specific problems, prepare for national and college level research grants and last but not the least to learn the phrase - 'never-ever give up'! My thanks goes to Dr. Carla Finkielstein who was always there beside me whenever I needed any professional advice- be it an experimental research problem, fixing of FPLC instrument or applying to a postdoctoral position. Her extreme enthusiasm and endless passion towards biological science research made her as a role model to me. I want to thank all of my committee members and Capelluto-Finkielstein lab members, both past and present for their guidance, suggestions and support over last few years. My special thanks goes to Iriscilla Ayala, my lab mate, who eventually became a great friend of support in my life.

I am grateful to the American Heart Association (AHA), Philanthropic Educational Organization (PEO), Fralin Life Sciences Institute, College of Science and Graduate Student Association at Virginia Tech who supported me financially with Predoctoral Fellowship, International Peace Scholarship, Fralin Fellowship, Roundtable Scholarship and Graduate Research and Development Award during my Ph.D. study.

I would like to take this opportunity and give my heartiest thanks to some of the family members and friends who became a vital part of my life during last five years. First and foremost, my sincere love to my sister Manjushree Palit for standing beside me throughout these years of ups and downs. Any problem I faced - professional or personal, she was there as my sister-best-friend-philosopher and guide. I sincerely acknowledge her support and love, without which, I would not have succeeded this journey. My love and gratitude will always be with my uncle late Mr. Tapas Kumar Ghosh who was of great support to me throughout his lifetime. Among others, Sanghamitra Sen, Tannishtha Maiti, Poulomi Laha and Bireswar Laha were some incredible people I met here at Blacksburg who made this place ‘a home away from home’ to me.

In a nutshell, I must say that I spent some most wonderful years of my life in Virginia Tech surrounded by some great people, who all-together made this journey a momentous one!

TABLE OF CONTENTS

LIST OF TABLES

LIST OF FIGURES

ABBREVIATIONS

AD	Atopic dermatitis
AMP	Adenosine monophosphate
AP-1	Activator protein 1
AUC	Analytical ultracentrifugation
BAR	Bin/Amphysin/Rvs
BTK	Bruton's tyrosine kinase
C2	Conserved 2
CARD	Caspase recruitment domain
CBL	Calcium binding loop
CD	Circular dichroism
CD14	Cluster of differentiation 14
CLRs	C-type lectin-like receptors
Cox-2	Cyclooxygenase-2
$cPLA_2$	Cytosolic phospholipase A_2
CREB	Cyclic-AMP response element binding protein
CUE	Coupling of ubiquitin binding to endoplasmic reticulum degradation domain
DAMPs	Danger associated molecular patterns
ECD	Ectodomain
EE	Early endosomes
ERK	Extracellular-signal regulated kinase
EPS 15	EGFR substrate 15

Epsin 1	EPS15 interacting protein 1
ESCRT	Endosomal sorting complex required for transport
GPI/AP	Glycosylphophatidylinositol-anchored protein
HECT	Homologous to the E6-AP C-terminus
HOPS	Homotype fusion and vacuole protein sorting
HRS	Hepatocyte growth factor regulated tyrosine kinase substrate
IFN	Interferon
Ik-β	Inhibitor of kappa-β
IKK	Inhibitory kappa-β-kinase
IL-1	Interleukin 1
IL-1R	Interleukin 1 receptor
ILVs	Intraluminal vesicles
IRAK	IL-1 receptor associated kinase
IRF	Interferon regulatory factor
ISRE	IFN-sensitive response element
ITAM	Immunereceptor tyrosin-based activation motif
JNK	c-Jun-N-terminal kinase
KD	Kinase domain
LBA	Liposome binding assay
LBP	Lipopolysaccharide binding protein
LE	Late endosomes
LPOA	Lipid protein overlay assay

LPS	Lipopolysaccharide
LRR	Leucine rich repeat
MAL	Myeloid differentiation protein 88 adapter-like protein
MAPK	Mitogen activated protein kinase
MD2	Myeloid differentiation factor 2
MEKK	MAP/ERK kinase kinase
MKK	MAPK kinase
MVBs	Multivesicular bodies
MyD88	Myeloid differentiation protein 88
NEMO	NF-kβ essential modulator
NFkβ	Nuclear factor kappaβ
NLRs	Nucleotide-binding oligomerization domain like receptor
NSF	N-ethylmaleimide-sensitive factor
NOD	Nucleotide-binding oligomerization domain like receptor
NMR	Nuclear magnetic resonance
PAMPs	Pathogen associated molecular patterns
PIs	Phosphoinositides
PI3K	Phosphatidylinositol-3-kinase
PKC	Protein kinase C
PP-InsPs	Inositol pyrophosphates
ProST	Proline-Serine-Threonine
PRRs	Pattern recognition receptors

PS	phosphatidylserine
PTEN	Phosphatase and tensin homolog
PtdIns	Phosphatidylinositol
PtdIns3*P*	Phosphatidylinositol-3-phosphate
PtdIns(4,5)P_2	Phosphatidylinositol-(4,5)-bisphosphate
PtdIns(3,4,5)P_3	Phosphatidylinositol-(3,4,5)-trisphosphate
RIP-1	Receptor interacting protein-1
RLRs	Retinoic acid-inducible gene (RIG)-like receptors
ROS	Reactive oxygen species
TAB1/TAB2	TAK-1 binding protein 1/2
TAK-1	Transforming growth factor b-activated kinase 1
TBD	Tom 1 binding domain
TIR	Toll/IL-1 receptor
TLR	Toll like receptor
TNFα	Tumor necrosis factor-α
TOM1	Target of Myb1
TRAF-6	Tumor necrosis factor associated factor 6
TRAM	TRIF related adaptor molecule
TRIF	TIR-domain containing adaptor inducing interferon beta
TRIKA-1	TRAF-6-regulated IKK-activator-1
Tpl2	Tumor progression loci 2
SIGIRR	Single immunoglobulin IL-1-related protein

SEC	Size exclusion chromatography
SNARE	N-ethylmaleimide-sensitive factor soluble attachment protein receptor
ST-2	Suppressor of tumorigenicity 2
SPR	Surface plasmon resonance
Ub	Ubiquitin
UBC	Ubiquitin conjugating enzymes
Ubc13	Ubiquitin conjugating enzyme 13
Uev1A	Ubc-like protein ubiquitin E2-variant 1A
Vps/Vsp	Vacuolar sorting protein

ATTRIBUTIONS

CHAPTER III THE C2 DOMAIN OF TOLLIP, A TOLL LIKE RECEPTOR SIGNALING MODULATOR, EXHIBITS BROAD PREFERENCE FOR PHOSPHOINOSITIDES

The article was published in *Biochem J* 435, 597-608 in the year 2011 and reproduced in the thesis with due permission. Following is the list of people who have contributed towards this work:

- *Daniel Capelluto*, Ph.D. (Department of Biological Sciences & Department of Chemistry, Virginia Tech) served as the committee chair and director for the project. He also helped in designing the experiments and analyzing the data. He wrote the manuscript.
- *Gayatri Ankem*, M.S. (Department of Chemistry, Virginia Tech) purified proteins, performed liposome binding assays, nuclear magnetic resonance experiment, protein lipid overlay assays and circular dichroism experiments. She was the first-co-author for the paper.
- *Furong Sun*, Ph.D. (Department of Chemistry, Virginia Tech) purified mutant protein.
- *Anna Moreno*, B.S. (Department of Biological Sciences, Virginia Tech) purified proteins.
- *Boonta Chutviraskul*, M.S. (Department of Chemistry, Virginia Tech) designed the constructs and purified proteins.
- *Hugo Azurmendi*, Ph.D. (Department of Chemistry, Virginia Tech) assisted

nuclear magnetic resonance experiments and helped to analyze the NMR data.

- *Liwu Li*, Ph.D. (Department of Biological Sciences, Virginia Tech) provided necessary reagents and constructs needed for this project.

CHAPTER IV - BACKBONE ^{1}H, ^{15}N, AND ^{13}C RESONANCE ASSIGNMENTS AND SECONDARY STRUCTURE OF THE TOLLIP CUE DOMAIN

The paper was published in *Mol Cells* 30, 581-585 in the year 2010 and reproduced in the thesis with due permission. Below is the list of people who has contributed towards this project.

- *Daniel Capelluto*, Ph.D. (Department of Biological Sciences & Department of Chemistry, Virginia Tech) served as the director for this project. He helped in designing the experiments and analyzing the data. He also wrote the manuscript.
- *Hugo Azurmendi,* Ph.D. (Department of Chemistry, Virginia Tech) carried out the NMR resonance assignment experiments and analyzed the data.
- *Iriscilla Ayala,* B.S. (Department of Biological Sciences, Virginia Tech) performed the crosslinking experiment.
- *Carla Finkielstein,* Ph.D. (Department of Biological Sciences, Virginia Tech) served as the co-director of the project.
- *Liwu Li*, Ph.D. (Department of Biological Sciences, Virginia Tech) served as the co-director of the project.

CHAPTER V UBIQUITIN INTERACTS WITH THE TOLLIP C2 AND CUE DOMAINS AND INHIBITS TOLLIP'S PHOSPHOINOSITIDE BINDING**.**

The study detailed in this chapter is under the review process by *Journal of Biological Chemistry*. Following are the list of people who has contributed towards this work.

- *Daniel Capelluto*, Ph.D. (Department of Biological Sciences & Department of Chemistry, Virginia Tech) was the director for the project. He also helped in designing the experiments, analyzing the data and wrote the results and discussion sections of the manuscript.
- *Alicia Traughber*, B.S. (Multicultural academic opportunities program scholar and VT-PREP scholar at Virginia Tech) performed the lipid protein overlay competition assay.
- *Stephanie Gomez*, B.S. (Department of Biological Sciences, Virginia Tech) purified proteins and performed the size exclusion chromatography experiment.

CHAPTER I: LITERATURE REVIEW

The thesis evolves around a protein named the Toll-interacting protein (Tollip). Tollip was identified as a negative regulator of Toll-like receptor signaling pathway. Later, the protein was found to be important in other cellular pathways such as endosomal trafficking of protein and protein sumoylation. The following literature review outlines the pathways in which Tollip participates and provides background information on Tollip's function in cell. Following the literature review, a brief description of specific aims is documented which allows the reader to understand the scope and importance of the study performed. The results section of the thesis documents related works published in peer-reviewed journal followed by conclusion and future directions of the project.

PART I. THE TLR SIGNALING PATHWAY AND TOLLIP

1.1. Introduction to the TLR Signaling Pathway

Vertebrate immune system provides protection from infectious diseases and is mediated by cells and molecules of innate and adaptive immune system. The innate immune system is the immediate first line of defense mechanism and is found in all multicellular organisms including insects, plants, and mammals (*1*). Adaptive immunity, on the other hand, is a highly evolved mechanism and is able to distinguish and recognize closely related pathogenic molecules as well as remember and respond vigorously to the repeated exposure of the same molecule (*2*). The innate immune

sensor system is genetically programmed to detect invariant features of invading pathogens. Pattern recognition receptors (PRRs) are germ-line encoded innate immune sensors, which recognize pathogen-associated molecular patterns (PAMPs) and danger-associated molecular patterns (DAMPs) (*2*). PRRs are ubiquitously expressed in different professional and non-professional immune cells such as macrophages, dendritic cells and epithelial cells. Upon recognition of PAMPs or DAMPs, PRRs initiate a cascade of signaling events that lead to the production of inflammatory cytokines and chemokines. They also induce the expression of co-stimulatory molecules by antigen presenting cells conjugating the innate immune response with the adaptive immunity.

Currently, there are four classes of PRRs identified in mammals. They are i) Toll-like receptors (TLRs); ii) C-type lectin receptors (CLRs); iii) Retinoic acid-inducible gene (RIG)-like receptors (RLRs); and iv) Nucleotide-binding-oligomerization domain (NOD)-like receptors (NLRs).

CLRs are transmembrane-receptors and recognize carbohydrates on viruses, bacteria and fungi. They either contain immunereceptor tyrosine-based activation motif (ITAM) or upon ligand binding recruits ITAM domain harboring adaptors. The signaling cascade activated by these receptors induces the production of pro-inflammatory cytokines (*3*).

RLRs are cytoplasmic receptors that recognize genomic RNA of dsRNA viruses and dsRNA as the replication intermediate of ssRNA viruses. Structurally they are composed of N-terminal caspase recruitment domain (CARD), a middle DEATH box helicase/ATPase domain and C-terminal regulatory domain (*4*). Upon recognition of short dsRNA (upto 1kb) or long dsRNA (more than 2 kb), RLRs induces the production

of type I interferons (IFNs). Another member of RLR family, lacks a CARD and acts as negative regulator of RIG-I responses by either sequestering dsDNAs or inhibiting conformational changes of RIG-I (*4*).

NLRs mostly recognizes bacterial cell wall components. There are two types of NLRs- NOD1 and NOD2 and they differ in their ligand specificity. Structurally, they are composed of a central nucleotide-binding domain and C-terminal leucine-rich repeats. Upon recognition of ligand, NLRs activate Nuclear factor-kappaβ (NF-κβ), MAP-kinase p38, extracellular signal-regulated kinase (ERK) and c-Jun N-terminal kinase (JNK) pathways, which induce the production of proinflammatory cytokines (*5*). Recently it has been found that NOD2 specifically recognizes 5'-triphosphate RNA from respiratory syncytial viruses and provides defense response against them (*5*).

1.2. The TLRs

1.2.1. General introduction, location, and ligands

TLRs are the best-studied innate immune receptors and play important role in the regulation of innate and adaptive immunity. The protein was first identified in insect *Drosophila melanogaster*, where it was known for its role in dorso-ventral pattern formation in the embryos. In 1996, the protein was reported to be critical in flies for its role against *Aspergillus fumigatus* infection. The following year, a mammalian homolog of the *Drosophila* Toll receptor (TLR4) was identified (*6*). Later, it was found that a point mutation in the TLR4 gene rendered the mice unresponsive to bacterial infection.

Therefore, the connection between mammalian TLRs and innate immunity became obvious (*6*).

There are 10 TLRs in human and 13 in mice. TLRs 1-9 are conserved in human and mice. TLR 10 is found only in humans, whereas TLR11 is functional only in mice (*6*). The biological roles and the signaling mechanisms for TLR1-9 have been defined, albeit not so much is known for TLR10, 11, 12, and 13 signaling and functions (*7*). Table 1 provides an overview of different TLRs along with their chromosomal locations and ligand diversity.

Table 1. TLRs, their chromosomal maps, and ligands. ND, Not determined

Receptor	**Chromosomal location**	**Ligand**
TLR1	Close to 4p14	Triacyl lipopeptides
TLR2	4q32	Lipopeptides, lipoproteins, peptidoglycan, lipotechoic acid, glycolipids, zymosan, heat-shock protein 70
TLR3	4q35	Double stranded RNA
TLR4	9q32-33	Lipopolysaccharide,

		taxol, heat-shock protein 60, heat-shock protein 70, fibrinogen
TLR5	1q33.3	Flagellin
TLR6	Close to 4p14	Diacyl lipopeptides, lipotechoic acid, zymosan
TLR7	Located in tandem in Xp22	Single stranded DNA
TLR8	Located in tandem in Xp22	Single stranded DNA
TLR9	3p21.1	CpG-containing DNA
TLR10	ND	ND
TLR11	ND	Toxin from uropathogenic bacteria, profilin-like proteins

TLRs are widely expressed in many cell types including epithelial cells, endothelial cells, macrophages, neutrophils, and dendritic cells (*7*). Within the cells, TLRs are compartmentalized so that TLR 1, 2, 4, 5 and 6 are plasma membrane-bound and TLR 3, 7, 8 and 9 are found in endosomes (*8*). TLR4 is the best-characterized cell surface

TLR. In resting cells, TLR4 is located in the Golgi apparatus. Upon activation by the ligand, TLR4 is translocated to the plasma membrane where it commences the early signaling phase of TLR4-mediated immune response. TLR4 is also found in early endosomes from where it initiates the late signaling phase of immune response. The translocation of TLR4 from plasma membrane to endosomes is clathrin-dependent (*8*). TLR 1, 2, and 6 are exclusively expressed on the plasma membrane. In contrast to plasma membrane bound TLRs, the intracellular TLRs 3, 7, and 9 are present within the endoplasmic reticulum (ER). Within the ER, the chaperone protein Gp96 promotes the proper folding of TLRs 3, 7, and 9. The TLRs then follow the conventional secretory pathway and traffic through Golgi to endosomes. Within the endosomal compartment, TLR 7 and 9 are cleaved in their ectodomains (ECDs) by lysosomal cysteine proteases.

1.2.2. Structure of TLRs

The TLRs are type I integral membrane glycoproteins with average molecular weight of 90-115 kDa. They harbor an N-terminal leucine-rich-repeat (LRR), which binds to ligand, a single α-helical transmembrane domain and C-terminal intracellular domain that interacts with the adapter molecules upon ligand binding (*6*). The ectodomain of TLRs contains a single block of a 24-amino acid motif (LRRs), which is capped with cysteine-rich structures at the amino and carboxyl terminal (*9*). The N-terminal caps are structurally variable among different TLRs, whereas the C-terminal caps are highly conserved. The ECD structure folds into a curved solenoid in which the conserved residues form the concave beta-face of the solenoid. The outer convex side of the

solenoid is formed by variable residues (*10*). In addition, the LRRs of TLR-ECDs contain two important insertions at positions 10 and 15. The consensus at position 10 is often replaced by residues Cys, Ser or Thr. This insertion lies in a position that connects the concave or β-face with the convex structure. Insertion at position 15 lies mostly in the convex structure (*11*). In addition to these two frequently found insertions, there are insertions specific to each of the TLRs. These insertions often provide flexibility to the rigid horseshoe structure of TLR ECD so that it could interact with large PAMPs or other accessory molecules (*11*). The TLR C-terminal domain is homologous to the intracellular domain of interleukin 1 receptor (IL-1R) and hence is called Toll/IL-1 (TIR) domain. The TIR domain is approximately 160 amino acids long and contains three important regions named as Box 1, Box 2 and Box 3. Structurally, this domain is composed of a five-stranded β-sheet surrounded by five α-helices. The loop in Box 2 that connects the second β-sheet and the second α-helix, also termed as BB loop and is important for TLR dimerization and adaptor recruitment upon ligand recognition (*6*). In support of the importance of BB loop, it was found that G676L substitution interfered with signaling by the TLR1 (*6*). Particularly, the mutation of a single proline residue to histidine (P681H) does not induce any structural changes in the TIR domain but rather physically disrupts the interaction between the TIR domain of TLR2 and its adaptor molecule (*6*).

1.3. The TLR signaling pathway

There are three major steps involved in TLR signaling:

1) Ligand binding and conformational changes in the TLRs: Upon ligand recognition, TLRs form homodimer or heterodimer and initiates the signaling cascade (*12*). The structural basis of TLRs-ligand recognition has been well studied for TLRs 1, 2, 4 and 9. Several TLRs bind to their respective PAMPs directly, yet notably, TLR4 needs some additional co-receptor molecules for proper LPS recognition (*13*). The lipid A moiety of bacterial LPS is recognized by acute phase protein LPS-binding protein (LBP). This LBP-LPS complex then interacts with another soluble and secreted protein called cluster of differentiation 14 (CD14). With the aid of CD14, LPS is then transferred to the myeloid differentiation protein 2 (MD2)/TLR4 complex (*14*). MD2 is a secreted glycoprotein that acts as an extracellular adaptor protein for the recognition of LPS by TLR4. It is proposed that LPS binds to MD2, which then interacts with the LRR of TLR4. The crystal structure of LPS-MD2-TLR4 has been solved (*15*). The two antiparallel β-sheets forms a hydrophobic β-cup fold structure to which LPS binds and mediates the dimerization of the two TLR4-MD2 complexes. It has been shown that the two tyrosine residues in MD2 (Tyr22 and Tyr131) are phosphorylated by Lyn kinase and that this phosphorylation is important for downstream signaling by TLR4 receptor (*16*). In case of TLR9, the ligand binding induces a conformational change in the TLRs homodimers leading to the close approximation of the TIR domains. TLR3 signals followed by a ligand induced formation of multimers (*11*). In additional to conformational changes, TLR4 is also known to be tyrosine phosphorylated in its TIR domain at Tyr674 and Tyr680 residues by Lyn kinase after LPS induction (*17*). Additionally, the PGV714-

716AAA mutation in the TIR domain abolishes tyrosine phosphorylation of the TIR domain. Interestingly, it has been found that the Bruton's tyrosine kinase (BTK) interacts with the TIR domains of TLRs 4, 6, 8, and 9 and is involved in the respective signaling pathway (*18*).

2) The activated TLR signaling: The most extensively studied TLR signaling pathway is the TLR4 signaling pathway activated by LPS. Depending on types of TLR4 mediated response whether early or delayed response, TLR4 receptor recruits different sets of adaptor molecules (*19*). There are two types of TLR signaling cascade: a) Myeloid differentiation factor 88 (MyD88)-dependent signaling cascade and b) MyD88-independent signaling cascade.

a) MyD88-dependent signaling cascade: MyD88 is a universal adapter protein utilized by all the TLRs except TLR 3. In this pathway, MyD88 works in coordination with another adaptor protein, the TIR domain containing adaptor protein (TIRAP) (also known as MyD88 adaptor-like protein [Mal]) (*20*). Followed by ligand induced receptor dimerization and/phosphorylation, TLR4 is recruited to the phosphatidylinositol-(4,5)-P_2 [PtdIns(4,5)P_2]-enriched lipid rafts, a phenomenon mediated partly by NADPH oxidase mediated reactive oxygen species (ROS) generation (*21*). In resting cells, TIRAP localizes within the membrane ruffles through its N-terminal PtdIns(4,5)P_2 binding domain, a process which is independent of TLR signaling. Therefore, followed by receptor activation, it co-localizes with TLR4 to the lipid rafts (*22*). At this stage, C-terminal TIRAP TIR domain interacts with TLR4 by TIR-TIR interactions (*23*). In resting cells, MyD88 is present throughout the cytosol as discrete condensed particles.

Following the TLR4 activation, TIRAP functions as a sorting adaptor and recruits MyD88 to the receptor cytosolic side in a TIR-dependent manner (*24*). It is now known that TIRAP and MyD88 interact to a non-overlapping region of TLR4. After forming a complex of TLR4-TIRAP, MyD88 recruits the kinase interleukin receptor-associated kinase 4 (IRAK-4) (*25*). Human IRAKs contains four members - IRAK-1, IRAK-2, IRAK-4, and IRAK-M. Each member has a N-terminal death domain (DD), a middle ProlineSerineThreonine (proST) domain, a conserved kinase domain (KD) and a C-terminal domain (IRAK-4 lacks the C-terminal domain) (*26*). IRAK-4 is a serine/threonine kinase that associates with MyD88 via DD-DD interactions (*25*). Once associated with MyD88, IRAK-4 recruits another kinase, IRAK-1 or IRAK-2 (IRAK-1 and IRAK-2 plays redundant roles in signaling) (*27*). In this assembly, IRAK-4, MyD88,and IRAK-2 form a large protein complex known as Myddosome. Structurally, this is mediated by a single stranded left-handed helix of DDs of six MyD88, four IRAK-4, and four IRAK-2 proteins (*28*). It has been shown that a single threonine residue in the DD region of IRAK-1 (Thr66) is responsible for stable interactions with IRAK-4. IRAK-4 then autophosphorylates itself and phosphorylates IRAK-1 to its kinase domain at Thr209 and Thr387 residues, which are present in the activation loop. Hence this phosphorylation event leads to the conformational change in the protein making IRAK-1 active. Activated IRAK-1 then autophosphorylates at its proST region. Upon this hyper-phosphorylation, IRAK-1 is released from the receptor complex and associates with downstream proteins for further signaling (*6*). It has been noted that although IRAK-1 and IRAK-2 work redundantly in the TLR4 signaling, IRAK-2 is critical in late-phase TLR

responses, whereas IRAK-1 is not. Also, IRAK-2 contains an asparagine residue instead of an aspartate residue (which is present in canonical IRAKs kinase family members such as IRAK-1 and IRAK-4) in its kinase domain. However, it is shown that residue Lys237, in its ATP binding pocket, can be phosphorylated by IRAK-4 and thus triggers the kinase activity of IRAK-2 (*29*).

The C-termini of IRAK-1 and IRAK-2 contain motifs (Glu544, Glu587 and Glu707 in IRAK-1; Glu528 and Glu559 in IRAK-2) that interact with tumor necrosis factor receptor-associated factor 6 (TRAF-6) - a RING domain-containing E3 ubiquitin ligase. TRAF-6 is a member of TRAF family proteins and contains two C-terminal TRAF domains (TRAF-N and TRAF-C) and N-terminal RING- and Zinc-finger domains. Activated IRAK-1 or IRAK-2 binds to the TRAF domain of TRAF-6. TRAF-6 works in combination with a heterodimeric E2 enzyme complex known as TRIKA1 (TRAF-6-regulatated Inhibitory-kappaβ-kinase [IKK] activator 1) (*30*). This complex consists of ubiquitin conjugating enzyme 13 (Ubc13) and Ubc-like protein ubiquitin E2-variant 1A (Uev1A). TRAF-6 and TRIKA1 together promotes Lys63-mediated polyubiquitination of TRAF-6 (*30*). These polyubiquitin chains are then recognized by zinc finger ubiquitin binding domains of transforming growth factor-β-activated kinase 1 (TAK1) binding protein 1 (TAB1) and TAB2 or TAB3, which is present in TAK-1-TAB1-TAB2/3 complex. This activates the kinase activity of TAK 1, which then acts as common activators of several downstream signaling molecules. Activated TAK1 is now in close proximity to the IKK complex, which is made up of catalytic subunits IKKα, IKKβ and an essential regulatory subunit NF-κB essential modulator (NEMO) (*6*). TRAF-6-TRIKA1 complex then mediates Lys63-

linked polyubiquitination of NEMO. The polyubiquitination of IKK induces TAK1 to phosohorylate its IKKβ subunit, which leads to the activation of IKK. Activated IKK then phosphorylates the NF-κB inhibitor (IκB) proteins. Phosphorylated IκB is recognized by a F-box protein bTrCP, which is a subunit of E3 ubiquitin ligase $SCF^{\beta TrCP}$ (*31*). The E3 ubiquitin ligase then polyubiquitinates IκB proteins, which is then degraded by proteosomes. As the inhibition is removed, the NF-κB p50 and p65 subunits then translocate to the nucleus and turn on pro-inflammatory genes (*32*). TAK1 then phosphorylates 2 members of mitogen activated protein kinase 2 (MAP2K) family-MAPK kinase 3 (MKK3) and MKK6. MKK3 phosphorylates the stress activated protein kinase p38 and MKK6 phosphorylates JNK (*33*). JNK activates the transcription factor, activator protein-1 (AP-1), whereas p38-signaling pathway mediates the phosphorylation of cyclic-AMP response elements binding (CREB) protein. The NF-κB and the AP-1 pathway together regulate the expression of type 1 interferons (IFNs), including IFNα and IFNβ. CREB mediates the induction of pro-inflammatory genes such as cyclooxygenase-2 (Cox-2) and the tumor necrosis factor α (TNFα) (*33*). Interestingly, p38 also mediates phosphorylation of histone H3 of IL-8 promoter and enhances the binding of NF-κB to it. Very interestingly, it has been found that IRAK-1 can directly regulates and facilitates NF-κB mediated gene expression. A pool of IRAK-1 has been found to translocate to the nucleus, binds to the promoter region of NF-κB dependent gene IκB-α and phosphorylates Ser10 of H3 of this gene. This phosphorylation enhances the binding of p65 subunit to the promoter region of IκB-α (*34*).

b) MyD88 independent signaling cascade: The MyD88 independent signaling cascade utilizes TIR-containing adaptor protein inducing interferon-β (TRIF) and TRIF-related adaptor molecule (TRAM) (*35*). In resting cells, TRIF is diffusely expressed in the cytosol and TRAM is localized in the plasma membrane and in early endosomes. Upon LPS stimulation, TRIF moves to endosomes and colocalizes with TRAM. It is known that during endocytosis, the PtdIns(4,5)P_2 concentration drops in the plasma membrane (*36*). This leads to the dissociation of TLR4 from TIRAP, which then translocates to the endosomes and initiates the MyD88-independent signaling pathway from early endosomes (*36*). TRAM contains a bipartite sorting signal sequence (a myristoylation motif followed by a polybasic region) at its N-terminus that controls its movement from plasma membrane to the endosomes (*36*). TRIF-TRAM complex interacts and activates TAK1 binding kinase-1 (TBK-1). TBK-1 together with IKK phosphorylates interferon regulatory factor 3 (IRF3), which dimerizes, translocates to the nucleus, and binds to the interferon-sensitive response element (ISRE). This leads to the induction of a subset of genes including IFNβ and TNFα (*37*). TRIF can also interact with TRAF6 and TRAF3. TRAF6 mediates early TRIF signaling through TAK1-MAPK pathway and TRAF3 mediates the later phase of TRIF signaling. The C-terminal domain of TRIF also interacts with receptor-interacting protein (RIP-1), which mediates NF-κB activation (*32*).

1.4. Negative regulators of TLR signaling pathway

Activation of the TLR signaling is required to eliminate invading pathogens. However, prolonged activation of this pathway leads to severe immunopathological conditions such as endotoxin shock, sepsis, lupus, and chronic inflammatory disorders such as asthma (*51,52*). Extensive TLR signaling could also contribute to cardiovascular disease conditions such as atherosclerosis, cardiac hypertrophy and dilated cardiomyopathy (*53,54*). Therefore, tight regulation of the TLR signaling is needed in order to avoid overwhelming immune activation. In past few years, several negative regulators of TLR signaling have been discovered. These regulators work in concert with each other and invoke an orchestral response to keep TLR signaling under tight control. There are three levels of regulation of TLR signaling pathway.

a) Extracellular regulation: Soluble decoy TLRs (sTLRs) that compete with TLR agonists are highly effective in blocking TLR signaling (*39*). The soluble form of TLR4 consists of 86 amino acids, which are identical to the extracellular domain of TLR4 and rest 36 amino acids bear homology with mouse Phosphatidylinositol-3-kinase (PI3K). sTLR is able to inhibit LPS-induced NF-κB activation and proposed to do so by blocking the interaction between TLR and co-receptor molecules, MD2 and CD14. Six isoforms of soluble TLR2 have been found human milk and plasma. They are the results of post-translational modification of the transmembrane receptor with molecular weights of 20-85 kDa. They have been found to inhibit IL-8 and TNF production through a direct interaction with co-receptor sCD14 molecule (*39*).

b) Transmembrane protein regulators: There are four transmembrane regulators, which either sequester TLR adapter proteins or interfere with the binding of the TLR ligands (*40*).

ST2: Suppressor of tumorigenicity (ST) 2 is a type I transmembrane protein with 3 extracellular immunoglobulin-like domains and an intracellular TIR domain (*41*). There are two forms of this protein - ST2L and the soluble form sST2. It mainly works by sequestering adapter proteins and studies have suggested a direct interaction between ST2L and MyD88 and Mal through their TIR domains. ST2L also negatively regulates inflammatory responses. It binds to macrophages through a putative ST2 receptor. Although the exact mechanism by which sST2 works in TLR signaling pathway is unknown, but following the addition of sST2 to LPS-stimulated macrophages, there was a significant reduction in TLR1 and TLR4 mRNA expression (*41*).

SIGIRR: Single immunoglobulin IL-1-related protein (SIGIRR) is also an orphan receptor and is characterized by a single extra cellular immunoglobulin-like domain and a cytoplasmic TIR domain (*40*). It has been suggested that SIGIRR works in MyD88-dependent pathway and forms a complex with IRAK1 and TRAF-6. Therefore, it is speculated that SIGIRR interfere with the formation of receptor complexes and negatively regulates MyD88 dependent TLR signaling pathway (*39*).

RP105: Radioprotective 105 (RP105) is a TLR4 homolog and directly interacts with TLR4/MD2 complex and sequesters LPS binding sites (*39*).

TRAILR: TNF-related apoptosis-inducing ligand receptor (TRAILR) does not have a TIR domain but belongs to TNF superfamily. It is proposed that TRAILR stabilizes inhibitor

of kappa-βα (Iκβα) and decreases the nuclear translocation of NF-κβ. Therefore, it does not inhibit early TLR signaling but affects the Iκβα-mediated NF-κβ activity in the later phase (*41*).

c) Intracellular regulators: Table 2 shows the diversity of intracellular negative regulation of TLR signaling pathway. The table has been designed from the information provided in references 39-43.

Table 2. Diversity of intracellular negative regulation of TLR pathway

Regulator	Possible mechanism
Short MyD88 lacking the linker sequence between DD and C-terminal	Antagonizes with MyD88 homodimer formation and favors MyD88-MyD88s heterodimer formation
Sterile armadillo motif (SARM)	Interacts with TRIF and prevents the recruitments of downstream molecules
IRAK-2c, IRAK-2d and IRAK-M	IRAKM prevents the dissociation of IRAK-1/IRAK-4 from MyD88 receptor complex; IRAK-2c and IRAK-2d inhibits NF-κB activation
TRAF4	With the help of NADH oxidase p47phox, it associates with TRAF-6 and inhibits it

A20	Deubiquitinates TRAF-6
Triad 3A	Lys48 linked polyubiquitination and degradation of TLR4, TLR9, RIP-1, TRIF and Mal
Suppressor of cytokine signaling –1 (SOCS-1)	Polyubiquitinates and degrades Mal, suppresses IRAK-1 kinase activity
PI3K	Inhibits p38, JNK and NF-κB
Beta-arrestins	Prevents IκB phosphorylation and degradation; binds to TRAF-6 and prevents K63 linked polyubiquitination
TGF-β	Degradation of MyD88
Activating transcription factor-3 (ATF-3)	Binds histone acetylation sites on chromatin structure and prevents NF-κB binding to it
Flightless I homolog (Fliih)	Associates with the TIR domains of TLR4 and MyD88 and prevents the formation of receptor complex
FLN29	Interacts with TRAF-6 and prevents downstream complex formation
Cyclindomatosis (CYLD)	Interacts with TRAF-6 and TRAF-7 in an deubiquitination dependent manner
SH-2 containing protein tyrosine	Binds to N-terminus of TABK1 and

phosphatase 2 (SHP-2)	suppresses TABK1 mediated phosphorylation.
Deubiquitinating enzyme A (DUBA)	Selectively binds and cleaves K63-linked polyubiquitin chains on TRAF-3

1.5. Tollip as a negative regulator of TLR signaling

Tollip was identified as IL-1R accessory protein through a yeast-two-hybrid screen assay (*44*). Later, it was found that Tollip is able to interact with other proteins involved in TLR signaling such as TLR2, TLR4, and IRAK-1. Tollip is a modular protein with N-terminal Tom-1 binding domain (TBD), a central C2 domain and a C-terminal coupling of ubiquitin binding to endoplasmic reticulum degradation (CUE) domain (*45*) (Figure 1.1).

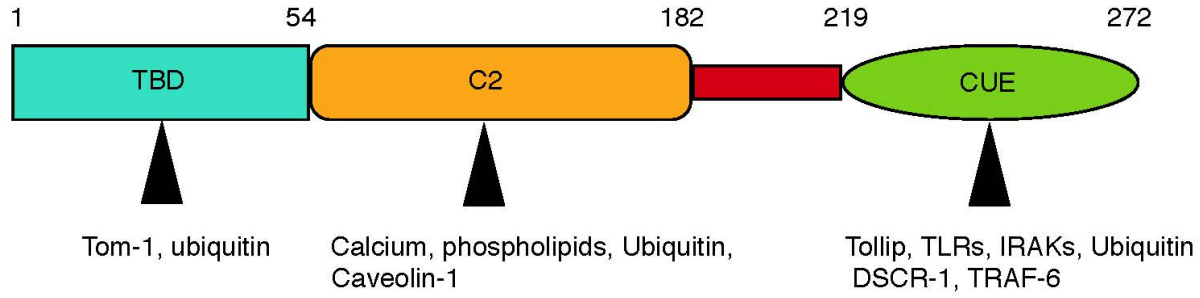

Fig 1.1. The modular architecture of Tollip. Black arrows indicate the ligands for the three different domains of the protein as found in this and other studies.

Tollip consists of 274 amino acids and is encoded by a gene located on chromosome 11p15.5 region in human (*46*). Four isoforms of Tollip has been found so far with truncations in their C2s and TBDs, but their precise function is yet to be known (*46*). In resting cells, Tollip associates with TLR4/TLR2 TIR domain and IRAK-1 via its CUE domain (*47*). The association of Tollip to TLRs TIR domains inhibits further receptor complex formation in TLR signaling, whereas its association to IRAK-1 inhibits IRAK1 phosphorylation (*48*). Thus, in resting cells, Tollip acts as a negative regulator of TLR signaling pathway. When the cell is being challenged by pathogens, the Tollip-IRAK-1 complex is recruited to the myddosome. Activated IRAK-1 then phosphorylates Tollip on its CUE domain, which dissociates Tollip from the complex. IRAK-1 further autophosphorylates itself and activate the downstream signaling components. It has been shown that a mutant version of Tollip (K150E), which is unable to bind to lipid is also unable to inhibit LPS-induced NF-kβ activation (*49*). However, the detailed molecular mechanism by which Tollip precisely acts as a negative regulator of the TLR signaling pathway is still not known and an intriguing area of study.

1.6. TLRs and diseases

TLRs signaling play a major role in initiating the innate immune responses against pathogenic infection and also required for effective secondary immune responses. Pertinent to the importance of TLRs and their signaling, it is not surprising that specific polymorphisms in genes encoding the TLRs and their downstream signaling players are associated with diseased state (*50*).

a) TLRs and immunity related diseases: The D299G mutation in TLR4 has been shown to be associated with higher risk for sepsis, a syndrome associated with severe lethal bacterial infection (*51*). The same mutation has been found to be associated with asthma and an increased severity to atopic syndrome. The R753Q polymorphism in TLR2 is associated with *Staphylococcus* infection or tuberculosis and R677W mutation in the same TLR enhances the susceptibility to leprosy or tuberculosis in human (*51*). A truncated version of IRAK-4 lacking the amino acids 287-293 failed to drive IRAK-1-dependent NF-κB activation and is associated with *Staphylococcus aureus* or S. *pneumoniae* infection in children. In a condition known as immunotolerance or immunosuppression, where cells previously exposed to LPS has shown decreased capacity to respond to a second challenge, there has been less phosphorylation of IRAK proteins or decrease in the association of TLR4 with MyD88 (*52*). Interestingly, the apoptosis of T and B cells in septic patient is directly correlated with TLR4 signaling independent of NF-κB pathway (*52*). Mutations in the *NEMO* gene have been found to be associated with anhydrotic extrodermal dysplasia (AED) and immunodeficiency (*52*). Signaling through TLR9 has been found to be associated with systemic lupus erythematosus (SLE), a severe autoimmune condition in which the body produces autoantibodies against self-antigens such as against nucleic acid (*52*).

b) TLRs in cardiovascular diseases: Recently, it has been proposed that TLRs can be activated by host derived molecules and, thus, could be involved in non-immune related human diseases. Thereafter, investigations revealed that activation of TLR signaling pathway has major role in the development and progression of several cardiovascular

diseases such as atherosclerosis, septic cardiomyopathy, ischemia and reperfusion injury, cardiac hypertrophy, and congestive heart failure (*53*). An increased level of circulating TLR4 positive monocyte has been observed in patients with unstable angina and acute myocardial infraction (*53*). The resident cells and the migrating leukocytes to the arterial wall in atherosclerosis plaques have been found to be associated with several TLRs (1, 2, 4, and 5). *MyD88-Apoe* double knockout mice had 60% reduction in atherosclerosis lesion (*53*). Mice, deficient in TLR4 or IRAK-1 are protected from cardiac dysfunction (*54*). Interestingly, TLR4 knockout mice are protected from ischemia perfusion injury (*54*). IRAK-1 deletion is associated with cardiac TLR signaling and protects against contractile heart dysfunction (*54*).

c) TLRs and neurodegenarative diseases: Components of central nervous system such as glial cells express TLRs (*55*). In addition, neuronal cells have been found to express certain TLRs. Two neurodegenarative diseases, Alzheimer's disease and multiple sclerosis (MS), are directly related with TLRs signaling (*55*). TLRs, together with other cell surface receptors such as CD47 or scavenger receptor-A, recognize the fibrillar amyloid-β and favor the production of reactive oxygen species, nitrogen radicals, which are toxic to the cells (*55*). Higher severity of MS has been observed in TLR-/- mice (*55*).

d) TLRs and tumorigenesis: Sequence variants of several TLRs (TLR1, 4, 6, and 10) are associated with cancer risk (*56*). Several human tumor cell lines (melanoma, breast, colon) have been found to express multiple TLRs. It seems that TLRs signaling induce tumor cells to produce immunosuppressive agent, anti-apoptotic and metastatic agents such as matrix metalloproteases, which turns the cells from benign to malignant (*56*).

PART II. ENDOCYTOSIS AND ROLE OF UBIQUITIN IN ENDOSOMAL TRAFFICKING

2.1. Introduction to the process of endocytosis and endosomal trafficking

The term 'endocytosis' defines a process where cells internalize small molecules, macromolecules, and particles and target them to specific organelle within the cytoplasm (*57*). The phenomenon is associated with several physiological processes such as uptake of nutrients, viruses, and toxins inside the cell, regulation of cell surface receptors expressions, lipid homeostasis and antigen presentation. Therefore, defects in the endocytosis process have been found to be associated with severe diseased conditions such as prion disease, atherosclerosis, and Alzheimer's disease (*57, 58*). The first key step of the endocytic process is the internalization of the molecules inside the cells using complex machinery of protein-lipid system. In the second phase, depending on the nature of the molecules, they can either recycle back to plasma membrane, go to lysosome and degraded or being transported to other organelle such as Golgi bodies (*58*).

2.2. The process of endocytosis

Step I - Different ways to enter inside the cells

I) Macro-scale endocytosis: In this process, particles typically larger than 500 nm in size (phagocytosis) or a large volume fraction of the extracellular bulk phase (pinocytosis) are ingested. In mammals, phagocytosis is performed by specialized cells

such as macrophages, monocytes, and neutrophils. The process involves a stepwise activation of Rho-GTPases, actin polymerization, and the formation of a zipper-like structure around the invading macromolecules. Pinocytosis or fluid-phase uptake also involves GTPases and actin reorganization but instead of zippering up along a particle, the membrane protrusion collapse onto extracellular milieu and fuse with the plasma membrane (*59*). This has been seen in antigen presenting cells such as in immature dendritic cells. Several pathogens also utilize this process to inject virulence factors.

II) Microscale endocytosis: In this process, small molecules are internalized and trafficked through the cytoplasm (*59*). It can be divided into three major distinct pathways: clathrin-mediated endocytosis, caveolae-mediated endocytosis and clathrin-caveolae independent endocytosis.

The clathrin-caveolae-independent pathway does not require specific coat proteins or a particular pinching system (*60*). The internalization of IL-2 receptors is not recruited to any coat proteins but requires dynamin to form vesicular 50-100 nm sized endocytic pit. Another outer leaflet membrane protein glycosylphophatidylinositol-anchored protein (GPI-AP) lacks cytosolic extensions and thus is unable to bind to any cytosolic adaptors. It has been suggested that lipid based sorting mechanisms and actin polymerization are the two key factors for the formation of endosomal compartments with GPI-AP. ARF6 positive endosomes have been found to be important in trafficking of MHC I proteins. Other clathrin and caveolin independent pathways utilize special class of proteins such as flotillins and tetraspanins (*60*).

Caveolaes are specialized lipid rafts and forms flask-shaped invagination at the plasma membrane. The structure is extensively found in vascular endothelial cells (ECs), adipocytes, fibroblasts, and epithelial cells. The main structural coat protein is caveolin (Cavs), which together with the supporter protein cavin forms caveolae structures (*60*).

Clathrin-mediated endocytosis is the most well defined endocytic pathway found in mammalian cells. Mostly, the transmembrane receptors and their bound ligands are incorporated into 'coated pits' formed by the assembly of coat proteins- clathrin. Three clathrin heavy chains (CHC) together with three light chains (CLC) first assemble into a polygonal lattice and deform the overlying plasma membrane into a coated pit. Heterotetrameric adaptor complex 2 (AP2) is then recruited to clathrin structures. The α-adaptin subunit targets AP2 to the plasma membrane, the β-2 subunit helps in clathrin assembly and μ-2 subunit interacts with the sorting motifs on the cargo complex. Finally, dynamin, a GTPases is recruited to the neck of the pits, assembles into a spiral fashion and pinches off the clathrin coated vesicles into cytoplasm (*59*).

Step II - Trafficking through the cytoplasm - the endosomal trafficking

After cargo is internalized from the plasma membrane, vesicles containing cargo reach ealy endosomes (EE). EEs are short-lived (~10 min) tubulovesicular structures having tremendous fusogenic property. EEs can be divided into two distinct pools depending on the nature of the cargo molecules. Recycling endosomes (REs) are EEs having the molecules that need to be recycled back to the plasma membrane. These are tubular structures and are dispersed throughout the cytoplasm. Optimal pH and cholesterol-rich microdomains present in EEs are important for regulation of recycling

through these endosomes (*58*). Sorting endosomes (SEs) transport cargo destined for lysosomal degradation as well as recycling molecules. SEs have a slightly lower pH (~5.9-6.0) than the REs (pH ~6.4-6.5). Acidification is an essential property for proper sorting of molecules from these endosomes to either REs or to endolysosomes (*58*). One of the less understood concepts in EEs dynamics is how molecules are precisely sorted to their destined places. It has been suggested that the sequence of the retained protein, the geometry and shape of the molecules or spatial arrangement of the molecules in specific locations within the EEs are all important (*58*).

In the next phase of endosomal trafficking, EEs mature into late endosomes (LEs). During this maturation process, the EEs undergo some subtle changes. These include i) loss of tubular structures and gain of oval shape, ii) Rab5 is exchanged for Rab7. Other Rabs such as Rab4, 11, and 22 are lost whereas Rab9 is added, iii) reduction in luminal pH, and more importantly, iv) ubiquitinated cargo brings special machinery of proteins called endosomal sorting complex required for transport (ESCRT), which in a stepwise process induce budding of the limiting membrane and forms intralumenal vesicles (ILVs). ILVs containing LEs are also called multivesicular bodies (MVBs). They harbor membrane proteins and lipids targeted for degradation. Also the recycling receptors are lost and the recycling process has been stopped. The fusogenic property of EEs is also changed in LEs. At this stage, they are no longer able to fuse with EEs, instead, they acquire tethering complexes and can fuse with each other, or with lysosomes. They also move towards the perinuclear region of the cell (*57*).

In the last phase of endosomal trafficking, LEs fuse with pre-existing lysosomes and delivers its content there for degradation. The mechanistic steps involved in endosome-lysosome fusion are still not fully understood yet experiments with cell-free system and cultured cells established the important protein compartments involved in this event. First, homotype fusion and vacuole protein sorting (HOPS) interacts with syntaxin and Rab7 and tether the endosome to lysosome. Following the tethering a trans-SNARE complex is formed which involves N-ethylmaleimide-sensitive factor (NSF) and N-ethylmaleimide-sensitive factor soluble attachment protein receptor (SNARE). This trans SNARE complex induces the fusion of the phospholipid bilayer of endosome and lysosome. The result is the formation of a hybrid organelle, often referred to as 'cell stomach' that contains a mixture of lysosomal enzymes and the cargo from MVBs, in which the digestion occurs (*61*).

2.3. Ubiquitin and endocytosis

2.3.1. Introduction to Ubiquitin

Ubiquitin is a 76 amino acid-containing protein, which is highly conserved in eukaryotes. Only four of its amino acid residues differ among yeast, plants, and animals. It is absent in prokaryotes (including *E. coli*) but present in archaebacteria (*62*).

The role of ubiquitin-system as a protein degradation machinery was discovered in early 1980's. Since the discovery of the protein, several scientific researches have established the importance of ubiquitin in numerous basic cellular functions such as cell signaling, DNA damage repair, histone modification, and endocytosis. In human,

ubiquitin protein is encoded by four different loci, *UbA80*, *UbA52*, *UbB* and *UbC*. The last one, *UbC*, often contains tandem repeats of different nucleotide sequences but translate to the same ubiquitin protein. Also, there are some ubiquitin fusion genes, which encode ubiquitin protein fused to unrelated ribosomal proteins. This fused precursor protein is then cleaved by proteases and results in the production of mature ubiquitin monomer (*63*). The protein is composed of an alpha helix of three and one-half turns and five beta-strands forming a beta sheet (*64*). The core between alpha helix and beta sheet is exclusively hydrophobic whereas all the acidic and basic residues are lying on the surface. This includes all of the seven lysine residues that are known to be important in polyubiquitin chain formation and its proteolytic function. Side chains of some of them are solvent exposed (such as Lys6, Lys33 and Lys63) while the others are engaged in forming hydrogen bonds or salt bridges (Lys11, Lys27, Lys29 and Lys48). There are amino acids whose hydrophobic side chains are also exposed on the surface (Leu8, Ile44, and Val70) forming a hydrophobic patch, which is important for proteolytic targeting or endosomal function of the protein (*64*).

2.3.2. The process of 'Ubiquitin tagging to proteins' - Ubiquitylation

Ubiquitylation (or ubquitination) is a post-translational modification of proteins in which the C-terminal carboxyl group of Gly76 of ubiquitin forms an isopeptide bond with the ε-amino group on the substrate protein (*62*). Attachment of ubiquitin to its substrate protein occurs via three steps. An ubiquitin-activating-enzyme (E1) first, in an ATP requiring reaction generates a thio-ester bond between the carboxyl terminus of G76

and a cysteine residue present in the catalytic core of the enzyme producing E1-S~ubiquitin. So far, only one E1 is known to exist. This step is also called ubiquitin activation and is the only energy-requiring step in whole process. The activated ubiquitin is then transferred to ubiquitin-conjugating enzyme (UBCs), E2, in which a second thio-ester bond is formed between carboxyl group of G76 and side chains of catalytic cysteine producing the intermediate E2-S~ubiquitin. In the last step, E2, together with an ubiquitin-ligase (E3) then transfers the activated ubiquitin to a lysine side chain of the substrate. Ubiquitin can be conjugated to protein either as monoubiquitin or polyubiquitin chains (*65*). Monoubiquitylation results in conjugation of a single ubiquitin molecule onto one or more lysine residues (multimonoubiquitylation) on the protein surface. Multi-ubiquitin chain forms when carboxy-terminal glycine of ubiquitin is attached to one of the seven-lysine residues (Lys6, Lys11, Lys27, Lys29, Lys33, Lys48 and Lys63) of the preceding ubiquitin. Polyubiquitin chains can be linear, in which the ubiquitin is attached to the other with no more than one amino group or it can be branched in which at least one ubiquitin is attached to other ubiquitins via two or more different amino acid groups (*65*). The ubiquitylation of a substrate is a reversible phenomenon. Covalently attached monoubiquitin or multiubiquitin chains can be removed or disassembled by deubiquitinating enzymes (DUBs), which are proteases that cleave the isopeptide bond between mono/polyubiquitin chains and the target proteins. Multiubiquitin molecules or monoubiquitin fused with ribosomal proteins are also cleaved by deubiquitinases and produce single ubiquitin molecules. Functional significance and diversity of mono or polyubiquitylation has been well characterized

(*66*). Lys48- and Lys63-linked polyubiquitin chains have distinct cellular functions. For example, Lys48 drives several nuclear cytosolic and ER membrane proteins degradation by the 26S proteasome (*66*). Lys63-driven polyubiquitination is associated with endocytosis of plasma membrane-associated proteins. Similarly, monoubiquitin also serves as an excellent source for intracellular transport of proteins (*66*). Chains containing Lys29, Lys11, Lys6, and Lys27 linkages are less characterized, however, they are associated with non-proteolytic signals (*65*).

2.3.3. Role of ubiquitin in endocytosis

During the process of endocytosis, ubiquitin acts at the plasma membrane for receptor endocytosis and at the endosome for sorting of cargo in the MVBs (*67*). In yeast, monoubiquitination or Lys63-linked polyubiquitylation have been shown to facilitate the endocytosis of many plasma membrane proteins. Although the situation is less clear in mammalian cells, several types of receptors such as receptor tyrosine kinases (RTKs), TGF-β receptors, G-protein coupled receptors (GPCRs), notch receptors, ion-channels, junctional proteins, and transporters are found to be endocytosed on a ubiquitin dependent fashion. Ubiquitylation also modulates the endocytic internalization route of the receptors and decides the fate of the receptors between signal transduction from endosomes or receptor down-regulation (*68*). Several studies have shown that ubiquitylation is a signal for degradative receptor sorting into MVBs and for lysosomal degradation. For example, transferrin receptors are usually

recycled back to the plasma membrane but the ubiquitin-fused receptor does not undergo recycling and is targeted for endosomal degradation instead (*69*).

2.4 Ubiquitin binding domains

The ubiquitin modification on target proteins is recognized by ubiquitin binding domains (UBDs) or ubiquitin receptors that harbors at least one UBD in their structure (*70*). The majority of the UBDs bind to a hydrophobic patch formed by Ile44/Leu8/His68/Val70 and surrounding residues. The other UBDs interacting regions of ubiquitin are made up of Ile36/Leu71/Leu73 or Gln2/Phe4/Thr12 patches and the C-terminal residues of ubiquitin (*71*). UBDs show variety of structural features and adopts different structural conformations in solution depending on monoubiquitin or polyubiquitin chain selection. The ubiquitin structure is quite rigid yet recently performed structural studies indicate that UBD:ubiquitin binding changes the conformation of ubiquitin and its binding partner (*71*). Most of the monobiquitin binding UBDs have diverse affinities for ubiquitin in the micromolar range (*72*). Table 3 gives an account of our current understanding of UBDs, their structure and affinities.

Table 3. An overview of UBDs, their structures and possible functions. Abbreviations, mUbi, monoubiquitin; pUbi, polyubiquitin. The table is reconstructed using information provided in 68, 73-74.

UBDs	Structure	Function	Ubiquitin	Affinity for

			binding property	binding
Ubiquitin associated (UBA) domain	Compact three-helix bundle	Proteosomal degradation, regulation of kinase activity and autophagy	Recognizes mUbi, Lys48 and Lys63-linked poly ubi; mainly Ile44 patch is the interaction surface	(~15 - 400 μM)
Coupling of Ubiquitin binding to endoplasmic reticulum degradation domain (CUE)	Three helix-bundle	Endocytosis and regulation of kinase activity	Mostly mUbi binding motif, binds to Ile44 patch. Binds either as dimer or monomer to ubiquitin	(~1 - 200 μM)
Ubiquitin interacting motif (UIM)	Single alpha helix, often tandem repeats in protein	DNA repair, protesosomal degradation, endocytosis	mUbi, Lys48 linked and Lys63 linked chain; binds to Ile44 patch	(~0.03 - 1.6 mM)
Motif interacting	Single alpha	Mainly	Mainly mUbi	~30 μM)

with ubiquitin (MIU)	helix	endocytosis	and Ile44 patch	
Double sided UIM (DUIM)	Two UIM sequences are interlaid on a single helix	MVB biogenesis	mUbi binding motif, binds two ubiquitin moieties simultaneously to Ile44 patch	~200 μM
GGA [Golgi-localized, gamma-ear-containing, ADP-ribosylation-factor-binding protein] and ToM1 [target of Myb1] binding domain (GAT)	Three helix bundle	Endocytosis and MVB biogenesis	Binds to mUbi and precisely to Ile44 patch through two distinct sites	100 μM
Np14-zinc-finger domain (NZF)	Four beta strands contains a single zinc-finger site	Endoplasmic reticulum associated degradation, regulation of	Binds to mUbi to Ile44 patch and Lys63 lined pUbi	100 μM

		kinase activity and endocytosis		
Zinc finger domain of A20 (ZNF A20)	Zinc finger	Regulation of kinase activity and endocytosis	Binds to mainly Asp58 patch; mUbi or Lys63 linked pUbi	~30 μM
Polyubiquitin - associated zinc binding (PAZ) domain	Large protein with single zinc finger site, contains a deep cleft and pocket in which the ubiquitin tail is inserted	Proteosomal degradation and autophagy	The C-terminal region of ubiquitin interacts of with tunnel like cleft, supplemented by Ile36 patch, but no interaction with Ile44 patch. Binds to unanchored pUbi	~3 μM
Ubiquitin binding ZNF (UBZ) domain	Zinc finger domain with ββαfold	NF-kβ signaling and DNA damage tolerance	Mainly binds to Ile44 patch and binds to both	No known

			mUbi and pUbi	
Ubiquitin conjugating enzymes (UBC) related domain	α/β fold	Transfer of ubiquitin	Binds to mUbi to Ile44 patch	~300 μM
Ubc E2 variant (UEV) domain	α/β fold	DNA repair, regulation of kinase activity and MVBs generation	Same as UBC	~500 μM
Ubiquitin binding motif (UBM)	Helix turn helix and is centered on an invariant L-P pair	DNA damage tolerance	It binds to mUbi to Leu8 patch	~180 μM
GRAM [glucosyl transferases, Rab-like GTPase activators and myotubularins) like ubiquitin binding in EAP45 (GLUE)	Split-pleckstrin homology (PH) domain	MVB biogenesis	Binds to mUbi to Ile44 patch	Not reported

domain				
Pleckstrin like receptor for ubiquitin (PRU) domain	Plecktrin homology domain and the three loops bind to ubiquitin	Proteosomal degradation	Binds to mUbi to Ile44 patch and also to Lys48 linked pUbi	Not reported
Jab1/MPN domain	Catalytically inactive domain of Jab1/MPN family	RNA splicing	Binds to mUbi to Ile44 patch	Not reported
PLAA [phospholipase A2 -activating] family ubiquitin binding (PFU) domain	Four beta strands and two alpha helices	Endoplasmic reticulum associated degradation	Binds to mUbi to Ile44 patch and also pUbi	Not reported
SH3 [Src homology 3] variant	Beta barrel fold where the hydrophobic grooved	Endocytosis	Binds to Ile44 patch of mUbi	Not reported

	binds to ubiquitin			
Ubiquitin binding in ABIN [A20 binding inhibitor of NF-kb] and NEMO [NF-kb essential modulator] domain (UBAN)	Coiled coil dimer	Cell signaling, apoptosis	Binds to both Ile44 patch and Phe4 patch; binds to liner pUbi chains	Not reported

2.5. UBDs in endocytosis

UBDs are important both in early steps of endocytosis as well sorting of endosomal cargo proteins in EE (*68*). EGFR substrate 15 (EPS15), EPS15-interacting protein 1 (epsin1), and epsin 2 contain UIMs and interact with monoubiquitin (*73*). They also interact with the clathrin adaptor complex and help forming the clathrin-coated vesicles. The limiting membranes of EE also contain UBD containing proteins. These proteins bind to ubiquitinated receptors and direct their sorting into MVBs. The machinery of ESCRT complex contains several UBDs that cooperatively participate in ubiquitinated cargo sorting in MVBs (*73*). There are also other proteins such as endosome-localized EPS15, EPS15β associate with ESCRT-0 and participate in

endosomal protein sorting. There are adaptor proteins for endosomal trafficking such as GGA proteins and TOM1, which bind to polyubiquitinated receptors and bring them to EE for sorting into MVBs (*75*). The precise molecular mechanism of role of UBDs in endosomal trafficking is yet to be investigated.

Regulation of ubiquitin recognition by UBDs

As seen from Table 3, UBDs bind to ubiquitin with low-moderate affinity. This is surprising together with the fact that the cellular concentration of ubiquitin is relatively high. However, this should not come as surprise when one considers increased avidity for ubiquitin by multiple other phenomena (*71*). The processes that regulate ubiquitin recognition by UBDs and ensure proper sorting of ubiquitinated cargo protein are as follows:

1) Multivalent interactions increased the binding avidity: More than one ubiquitin binding sites on a single UBD increased the binding affinity for ubiquitin. One of the examples is the UIM domain of hepatocyte growth factor regulated tyrosine kinase substrate (HRS), which is a component of ESCRT complex that binds to two ubiquitin moieties with equal affinity (*68*). Most of the ESCRT components contain more than one UBD within a single protein, associate with each other, and hence, form supracomplexes bound to multiple ubiquitin moieties simultaneously (*68*). Cargo proteins also undergo multivalent ubiquitination. Epidermal growth factor receptor (EGFR) is ubiquitinated on multiples sites by monoubiquitin moieties as well as modified by Lys63-linked polyubiquitin. This

modification allows multivalent interaction surfaces to UBD binding proteins during endosomal sorting (*68*).

2) Combinatorial use of modular domains in ubiquitin binding proteins: Most often ubiquitin binding proteins contain modular domains that modulate the oligomeric state and this oligomerization then leads to high-avidity interactions. Modular domains sometime additionally bind to other partners and help to increase the proximity of ubiquitinated cargo to UBD containing proteins. One of the examples is provided by HRS, which captures the UBD-ubiquitin bound cargo protein onto sorting endosomes via its FYVE domain interaction to endosomal PtdIns3*P*. This also increases the local concentration of cargo in microdomains of endosomes.

3) Combinatorial use of UBDs in ubiquitin binding proteins: In addition to the presence of tandem UBDs and membrane binding domain as seen in HRS, the UBD itself can act as lipid-binding modules and contribute in efficient trafficking of proteins to endosomes. The ELL associated protein 45 (EAP45) is involved in endocytic sorting and binds to ubiquitin via its GLUE domain. This domain has a PH domain-like fold and hence able to bind to phosphoinositides simultaneously. This dual binding provides efficient trafficking of ubiquitinated cargos by EAP45 (*72,73*).

4) Coupled monoubiquitylation: Some of the UBD-containing proteins undergo monoubiquitylation that is dependent on their UBDs. This coupled monoubiquitylation results in an intramolecular inhibition of the adaptor proteins in endocytosis and the protein cannot bind to ubiquitinated cargo (*68*).

2.6 CUE domain as an UBD

The CUE domain was first identified as a small (~40 amino acids in length) motif that is similar to a region of the yeast Cue1 protein (*78*). The authors proposed that this module participates in the ER degradation pathway and acts as a scaffold for interaction with UBCs. Later, however, it was demonstrated that CUE domains are indeed monoubiquitin-binding motifs engaged in arrays of cellular functions including membrane trafficking and inducing coupled monoubiquitylation (*79*). Proteins can have one or more CUE domains and, in some instances, such as in yeast Vps9p, CUE domain binds to Lys48-linked polyubiquitin chains (*79*). Some of the CUE domains, such as Cue1, might need UBCs in order to bind to ubiquitin, whereas others such as yeast Vps9p and Cue2, can directly bind to ubiquitin (*79*). CUE domains bind to ubiquitin Ile44 patch through their conserved MFP and LL motifs (*79*). There are two known CUE-ubiquitin structures. The solution structure of yeast Cue2 protein CUE-ubiquitin complex reveals canonical hydrophobic interaction between conserved MFP patch of CUE domain to Ile44/His68/Leu8 patch on the ubiquitin surface. The interaction is also stabilized by electrostatic interactions and hydrogen bonding between the two partners. On the other hand, the crystal structure of yeast Vps9p CUE domain reveals that it binds to ubiquitin as a domain-swapping dimer (*80*). In this crystal lattice, CUE dimer forms a basket-like structure, in which it wraps around ubiquitin via its concave high-affinity basket surface and interacts with two different patches of ubiquitin made up of Ile44 and Leu73 patches, respectively. The ‘left-over’ low-affinity convex sides of the CUE dimer interact with the secondary ubiquitin molecule to the same patches.

2.7 Tollip in endocytosis

Tollip in association with other adaptor proteins, such as Tom1 and clathrin, takes important role in EE cargo trafficking. Tollip itself binds to ubiquitin via its C-terminal CUE domain and brings polyubiquitiated cargo to EE. Tollip is proposed to interact with the Tom 1 GAT domain through its N-terminal TBD (*81*). Tom 1 binds to polyubiquitinated cargo through its GAT domain and recruits the whole complex to the EE. In the EE, Tollip might bind to endosomal membranes via C2 domain-PtdIns3*P* interactions. Interestingly, when the CUE domain and/or TBD were deleted (Tollip ΔCUE, Tollip ΔTBD, and Tollip ΔCUE/ΔTBD), the proteins were still associated with early endosomal structures (*77*). This suggested that CUE domain or TBD binding to Tom 1 is not sufficient enough for Tollip's endosomal localization and that C2 domain of Tollip also has important role in the endosomal function of Tollip. The endosomal role of Tollip becomes evident forms studies that demonstrate that Tollip recruits IL-1 receptor and TGF-β receptor to EE (*82, 83*).

Part III. PHOSPHOINOSITIDES, C2 DOMAIN, AND ENDOSOMAL TRAFFICKING

3.1 Introduction

Lipids are group of organic compounds, which are ubiquitous, structurally well diverse and participate in arrays of cellular structures and functions such as structural components of cellular membranes, signaling pathways and energy storage. Phosphoinositides (PIs) are major class of membrane-associated phospholipids. The parent molecule for PI is phosphatidylinositol (PtdIns) - a cyclic polyol D-*myo*-inositol to which a phosphate is attached at number one position (1-monophosphate headgroup) and this monophosphate headgroup is coupled to 1-stearoyl 2-arachidonoyl diacylglycerol (DAG) (*84*). The structural features of PIs allow for their suitable positioning in biological membranes in which the inositol headgroup is facing the cytosol (or any other hydrophilic environment), whereas the esterified fatty acyl chains are anchored to the hydrophobic membrane core. Among the five free hydroxyl group (D2 through D6) present in the inositol ring, only three (D3, D4 and D5) can be phosphorylated *in vivo* by lipid kinases and phosphatases that can generate seven different PIs (*84, 85*).

3.2 Cellular PI maps

PIs are synthesized in the ER, from where they are transported to different cellular compartments via lipid-transfer proteins (*86*). The spatial distribution and

temporal activation of PtdIns-specific kinases and phosphatases spatially restricts PIs in different cellular compartments. Plasma membrane is enriched with PtdIns(4,5)P_2, PtIns(3,4,5)P_3, and PtdIns(3,4)P_2; the cytosolic face of the limiting membrane of endosomes and the intraluminal vesicles of MVBs contain PtdIns3*P*, whereas limiting membranes of LE are characterized by the presence of PtdIns(3,5)P_2; PtdIns4*P*, and PtdIns(4,5)P_2 are present in the *trans*-Golgi network and ER, whereas nuclear membranes contain PtdIns5*P* (*86*).

3.3 Functions of PIs

PIs are the minor components of membrane lipids, albeit they have important functions in cell. i) PI specific lipases work on PIs and generate second class of inositol containing compounds such as inositol pyrophosphates (PP-InsPs), which regulate many cellular processes such as vesicular trafficking, apoptosis, and cytoskeleton dynamics (*87*); ii) PIs can also be a part of ion-channels and regulate their functions; so far forty PtdIns(4,5)P_2-regulated integral proteins have been identified, with many of them being membrane channels (*85*); iii) III) PIs recruit binding proteins to specific sites on cellular compartments and initiate cellular signaling cascades (*88*).

3.4 PIs in endocytosis

Many intrinsic properties of the membrane, such as thickness, asymmetry, and curvature, are determined by its lipid composition. Also lipid-binding soluble proteins interact with membrane lipids and this initiates arrays of cellular signaling pathways.

Therefore, lipids play crucial role in the formation and function of dynamic structures such as clathrin coated pits and endosomes during endocytosis (*89*). During endocytosis, clathrin coated pits are formed at the plasma membrane and the invagination process requires PtdIns(4,5)P_2 pool. Several coat adaptor proteins such as AP2, AP3 and the epsins also interact with PtdIns(4,5)P_2 and initiate the formation of pits (*90*). In the second step of endocytosis, during the formation of EEs, the PtdIns(4,5)P_2 concentration drops because of the activity of 5-phosphatases. PtdIns3*P* is being synthesized in EEs by the action of class III PI3K from PtdIns. It is also present in the MVBs and is involved in several steps of endocytosis such as docking, fusion, and motility of EEs (*91*). Several early endosomal adaptor proteins and the proteins of ESCRT complexes contain PtdIns3*P* binding motifs and ubiquitin binding motifs (*92*). In this case, ubiquitin and PtdIns3*P* work in concert for setting up proper destination to endocytosed moieties. In the next step, the conversion of PtdIns3*P* to PtdIns(3,5)P_2 occurs in the MVBs or late endosomes by the PIKf*yv*e kinase (*89*). PtdIns(3,5)P_2 is involved in cargo sorting within MVBs and also budding of vesicles from late endosomes. PtdIns3*P* also works together with sorting nexins and induce the tubulation of recycling endosomes (*84*).

3.5 Synthesis and breakdown of the two key PIs

Among PIs, PtdIns3*P* and PtdIns(4,5)P_2 are the two key players involved in endocytosis. Interestingly, both PIs have been identified as key targets of Tollip C2 domain in our study. The major pathways of synthesis and breakdown of PtdIns3*P* and

PtdIns(4,5)P_2 and their cellular functions are summarized in Table 4 (taken from references 85-86, 88-89 and 93)

Table 4. Synthesis, breakdown and functions of PtdIns3*P* and PtdIns(4,5)P_2

PtdIns	Synthesis	Breakdown	Function
PtdIns3*P*	From cellular PtdIns by the action of Class III PI3kinases: I) Vps34/Vps15/Rab 5 (endocytosis) II) Vps34/Vps15/Beclin-1/UVRAG (autophagy)	Dephosphorylation by Myotubularin (MTM) and MTM related protein (MTMR)	Mainly involved in three important cellular pathways: I) Endocytic-trafficking II) Autophagy and III) Mammalian target of rapamycin 1C (mTOR1C) pathway
PtdIns(4,5)P_2	A) From PtdIns4*P* by the action of	A) Dephosphorylation	Mainly involved in cellular

	type I PIP kinases and from PtdIns5*P* by the action of type II PIP kinases B) From PtdIns(3,4,5)P_3 by phosphatase and tensin homolog (PTEN)	by 5-phosphatase of the Synaptojanin family- (SYNJ1, SYNJ2) and OCRL1 which converts PtdIns(4,5)P_2 to PtdIns4*P* B) Conversion to PtdIns(3,4,5)P_3 by the action of Class I PI3K	trafficking pathway. A) Involved in membrane invagination during clathrin coated pit formation at plasma membrane B) Immobilizing secretary granules and in controling synnaptic vesicles during membrane fusion.

3.6 Introduction of PI-binding domains

Catimel *et al.* conducted a lipid based proteomic study, in which they used PI-containing liposomes or beads as bait and pulled down proteins that bound to lipid

vesicles/beads from an cytoplasmic protein extracts. They identified 388 proteins of different cellular functions containing different lipid-binding domains (*94*, *95*). These 'conditionally peripheral membrane proteins' displayed some general characteristics (*92, 96*):

i) They are either spatially or temporally restricted. This means, they selectively bind lipids, which are present in specific subcellular compartments. The binding event is transient in nature, triggered by either synthesis of specific lipids or by the presence of another molecule (such as Ca^{2+}), which aids in membrane recognition. ii) The interaction between binding domains to membranes is mainly nonspecific and electrostatic in nature. Therefore, mostly positively charged cationic residues from the protein form electrostatic interactions with the negatively charged cytosolic headgroup of the PIs. In some specific scenarios, geometric identification such as membrane curvature of the biological membrane becomes important as well. This is the case for domain Bin/Amphysin/Rvs (BAR) domain, which is an extended helical bundle protein that promotes and senses the curvature of the associated membrane. For the endo-lysosomal network, many of the ESCRT complex proteins contain features, which allow lumenal membrane of endosome to bend inward and form multivesicular bodies. iii) Most of the PI-binding domains target more than one partner, which secure their binding to the membrane. One of the examples includes protein kinase C (PKC) α C2 domain, which binds simultaneously to phosphatidylserine (PS) and PtdIns(4,5)P_2. This phenomenon, which is called 'coincidence detection' (*96*), ensures binding of signaling

molecule to the specific components of the membrane and allows the integration of the signaling processes.

3.7 C2 domain as a PI-binding domain

The C2 domain is the second most abundant lipid-binding domain after the PH domain. It was first identified as the second of the four conserved domains (C1 through C4) in mammalian Ca^{2+} dependent PKC (*97*). Later, it was found that PKCs that apparently did not have this domain were unable to bind to Ca^{2+}. It was later revealed that these 'non-classical' PKCs (such as PKCθ, PKCε, PKCη, PKCδ) contain C2 domains, which are Ca^{2+}-independent (*98*). C2 domains are independently folded modules, consisting of ~130 amino acids, which are found in nearly 100 human proteins. They are mostly found in signaling molecule or membrane trafficking proteins. A number of these proteins contain more than one C2 domains. The functional significance of multiple C2 domains in proteins remains elusive. It is suggested that either they increase the lipid affinity in the full-length protein by additive or co-operative manner or they are independently involved in individual membrane recognition (*99*). Most of them are soluble, conditionally peripheral membrane bound proteins but there are a few cases in which the domain is present in transmembrane proteins.

Ca^{2+}-dependent C2 domains

Many of the Ca^{2+}-dependent C2 domains function as cellular Ca^{2+} effectors (*100*) such as Synaptotagmin, an integral Ca^{2+} sensor found in synaptic vesicles and in

secretory granules of endocrine cells (*101*). Other examples include the N-terminal C2 domain of cytosolic phospholipase A_2 ($cPLA_2$), C2 domain of rabphilin-3A, a protein that binds small GTPase Rab3A during vesicular trafficking (*100*,*102*,*103*). There are high-resolution structures published for C2 domains, which fall into two slightly different topologies designated as topology I and II (*104*). In general, C2 domains have a common eight-stranded antiparallel beta sandwich consisting of a pair of four-stranded beta-sheets, which are connected by surface loops. The two topologies of C2 domain structures differ in their β-strand connectivity and are easily inter-convertible (*104*). Majority of the C2 domains contain a cationic patch on a concave surface of beta-sandwich and is referred to as beta-cationic groove. The Ca^{2+} binding region is defined by three calcium binding loops (CBL 1-3) and several aspartic acid residues present in these loops participate in Ca^{2+} binding (*99*). Structural and biochemical studies suggest that fully saturated C2 domains bind at least two metal ions. In Synaptotagmin C_2A, crystallopgraphic and NMR studies provide an excellent view of the two Ca^{2+} coordination (*105*). The two Ca^{2+} ions bind to C2A domain with different micromolar affinity. A set of four aspartic acid residue side chains provides binding surfaces for each of the Ca^{2+} ions. Additionally, solvents oxygen, and backbone carbonyl oxygen also provides coordination for Ca^{2+} binding (*105*). Multiple Ca^{2+} binding has been proposed to increase the positive cooperativity for Ca^{2+} sensing by C2 domains where Ca^{2+} binding has been proposed to facilitate the lipid binding by these domains. There are three models that describe the importance of Ca^{2+} binding in Ca^{2+}-independent C2 domains (*103*); In the first model, also termed as 'Ca^{2+} bridge model', there is a ternary

complex formed in which Ca^{2+} is coordinated by protein and phospholipid residues. This model is supported by the PKCα-C2-PS complex, in which the lipid binds simultaneously to the Ca^{2+} ions and another basic residue in the loop region. In the second model, the introduction of a positively charged residue such as Ca^{2+} in the protein induces an electrostatic potential in the protein and helps in recognizing the negatively charged lipids. The third extreme model proposes that Ca^{2+} binding induces local conformational changes in the protein exposing some hydrophobic residues and hence facilitates the lipid binding by the protein. This model is supported by several studies including that for the C2 domain of $cPLA_2$, in which the Ca^{2+} induced conformational changes were detected by an intrinsic fluorescence approach (*103*). Also the C2A domain of Piccolo protein undergoes a drastic conformational change in the structure upon Ca^{2+} binding and this triggers the insertion of the nine amino acid residues present on the other side of the CBL to be inserted into the membrane (*103*). Irrespective of these three models, it has been found that several residues present on the CBL determine the selectivity of lipid binding in C2 domains. Sometimes, the aromatic and aliphatic residues present in the CBL select non-ionic phospholipids. This is the case for $cPLA_2α$ and 5-lipooxygenase C2 domains, in which the tryptophan residue selects for phosphatadylcholine (PC) instead of PI when bound to the membrane. Apart from CBL the β-cationic groove play important roles in lipid binding in absence of Ca^{2+}. This is exemplified by the binding of C2B domains of synaptotagmin I and II to PI (*99, 100*).

Ca^{2+}-independent C2 domains

There are major classes of C2 domain containing proteins, which are Ca^{2+} independent in terms of lipid binding. They either have very little or almost no affinity for Ca^{2+}. Examples of this class of C2 domains are non-conventional PKCs such as PKCθ, δ, ε, and η (*98*). Some of them have been found to bound to membranes, others are either non-functional or involved in protein-protein interactions (*99*). Often, these non-classical C2 domains lack one or more of the aspartic acid residues present in CBL (*99*). In some Ca^{2+}- independent C2 domains such as from PLCδ4, PTEN and Rsp5, the CBL play important function in lipid selectivity and binding (*99*). In other cases the β-cationic groove has been found to be important in PI selection, as observed for the C2 domain of PKCθ and $cPLA_2$ (*98*).

3.8 The Tollip C2 domain as a PI-binding domain:

In a study by Li *et. al.* Tollip was found to bind two major PIs - PtdIns3*P* and PtdIns(3,4,5)P_3 (*49*). They also found a key lysine residue Lys150 within the C2 domain critical for PI binding. Further, the functional assays on a K150E mutant of Tollip shows no effect on NF-kβ activation (*49*). Given this property of the protein to bind to PIs, it is necessary to biophysically characterize the lipid binding by the Tollip C2 domain and to elucidate the functional significance of this binding.

PART IV - TOLLIP IN LITERATURE: FROM ENDOCYTOSIS TO HUMAN DISEASES

4.1 Tollip, a multitasking protein involved in endocytosis and protein sumoylation

One of the classic examples of Tollip's involvement of endosomal trafficking came from the evidence that Tollip associates with ubiquitinated IL-1 receptor via its CUE domain MF motif in LEs and lysosomes, where it promotes IL-1 receptor degradation (*82*). Consistent with this finding, very recently it has been shown that Tollip is a suppressor of TGF-β signaling pathway and it does by specifically interacting with Smad7 via its C2 domain (*83*). It was also found that Tollip interacts with ubiquitinated Type I TGF-β receptor through its CUE domain and TBD (*83*). This association triggers early endosomal localization and subsequent degradation of the receptor. Related with these observations, there were not many molecular studies to describe Tollip's role in endosomal trafficking. Tollip interacts with Tom1 family proteins including Tom L1 via its TBD (*77, 81*). This interaction is mutually exclusive to that of Tom1 proteins binding to ubiquitin. Hence it was also proposed that Tom1 is involved in the later part of endosomal sorting after ubiquitinated cargo is transferred to Tom1 from Tollip (*77*).

Interestingly, Tollip has been found to be a major player in protein sumoylation (*106*). Protein sumoylation is a post-translational modifications of proteins in which proteins are tagged with small ubiquitin-like modifier (SUMO) proteins. Often times, protein sumoylation and ubiquitination happen to involve the same lysine residues on the protein and the two processes antagonize one with each other. Sumoylated proteins are

also usually associated with nucleus (*107*). Tollip interacts with sumoylation enzymes, sumoylates itself potentially to the central C2 K162 residue and mediates IL-1 receptor sumoylation (*106*). In addition, sumoylated Tollip was found to be associated with nucleus. The crosstalk, if any, between ubiquitination and sumoylation in Tollip, has not been yet tested.

4.2 From basic to translational research- Tollip in human diseases

Tollip is one of the endogenous negative regulators of TLR signaling pathway. There is also direct evidence that Tollip is related to the progression of several immune and non-immune diseases. Patients with inflammatory bowl diseases are unable to up-regulate Tollip expression and this can lead to chronic inflammation (*107*). Atopic dermatitis (AD), a common inflammatory disorder has been found to be correlated with Tollip gene polymorphism. In a study it was found that an amino acid exchange in exon 6 (A222S) and two polymorphisms in intron I and in 3'UTR are all related to AD patients (*109*). Using neonatal cardiomyocytes, Tollip has been shown to suppress the development of cardiac hypertrophy (*110*). Very recently it has been found that polymorphisms within Tollip allele associated with decreased level of mRNA expression and increased IL-6 production, are related to susceptibility of tuberculosis in Vietnamese population (*111*). Altogether, these studies suggest that Tollip has novel functions in controlling the development and progression of several immune and non-immune diseases, albeit how Tollip is involved in these processes is still unknown.

CHAPTER II - SCOPE AND SPECIFIC AIMS

The presence of both lipid and protein binding domains within a single protein places Tollip in a group of modular protein category in which, the protein and lipid binding partners of Tollip might interdependently control Tollip's function. Therefore, in this study we chose to describe the biophysical basis of Tollip's association with its potential protein and lipid partners, and how these interaction can modulate Tollip's role in endosomal trafficking. Here we have biophysically characterized i) Tollip C2 domain binding to key endosomal phospholipid, PtdIns3*P; ii*) Tollip CUE domain binding to ubiquitin; iii) Novel properties of Tollip C2 domain binding to ubiquitin; and iv) how ubiquitin binding modulates CUE domain's dimeric state and targets Tollip to membrane. Using several biophysical and biochemical techniques such as nuclear magnetic resonance spectroscopy (NMR), surface plasmon resonance (SPR), analytical ultracentrifugation (AUC), size exclusion chromatography (SEC), liposome binding assay (LBA), lipid protein overlay assay (LPOA), and circular dichroism (CD) spectroscopy we have identified the key residues from Tollip C2 domain engaged in PtdIns3*P* and ubiquitin association, compared the binding of Tollip CUE to ubiquitin with Tollip C2 to ubiquitin and kinetically characterized the bindings. In some endosomal adaptor proteins, ubiquitin binding modulates the oligomeric state or other partner recognition. Interestingly we have found that there is a competition of protein and lipid binding in Tollip. More interestingly, we have also found that ubiquitin modulates Tollip CUE domain's dimeric state. Overall, the specific aims of the study were as follows:

Aim 1: To characterize the binding mechanism of Tollip C2 domain to PtdIns3P and PtdIns(4,5)P_2: This specific aim was designed to biophysically characterize the binding between Tollip C2 domain and its lipid partners. First, we tested several phospholipids to identify lipid partners of Tollip C2 domain using LBA. NMR and SPR reinforced the specific binding of Tollip C2 domain to two key PIs, PtdIns3*P* and PtdIns(4,5)P_2. SPR further kinetically characterized the binding between wild-type (WT) protein and its lipid partners. The shared binding sites for PtdIns3*P* and PtdIns(4,5)P_2 on the surface of Tollip C2 domain was confirmed using competition LPOA. Mutant constructs of the protein were designed based on sequence conservation among different Tollip C2 domains and tested using LPOA and LBA. Structural integrity of the mutants was tested using CD spectroscopy and tyrosine fluorescence study. The calcium binding of Tollip C2 domain was monitored using NMR. LPOA was performed to see the effect of calcium binding on PtdIns3*P* recognition in Tollip C2 domain.

Aim 2: To characterize the novel ubiquitin binding mechanism of Tollip C2 domain and compare it with Tollip CUE domain ubiquitin binding: The novel nature of ubiquitin binding by Tollip C2 domain was investigated and confirmed using SPR and NMR. Two-dimensional heteronuclear single quantum coherence (2-D-HSQC) spectroscopy was employed to identify the residues of ubiquitin engaged in Tollip C2 domain recognition. SPR was performed with wild-type Tollip C2 domain and ubiquitin. The WT protein association was compared with Tollip deficient mutants of ubiquitin (identified from NMR study. In order to confirm the importance of specific residues in the formation of a stable Tollip C2 domain-ubiquitin complex, ubiquitin and PtdIns3*P* binding

sites on Tollip C2 domain surface was compared by testing the binding of lipid deficient Tollip C2 domain mutants (identified from aim 1) to ubiquitin. As mentioned in Aim 1, mutants were subjected to CD spectroscopy in order to confirm that the induced mutation does not alter the secondary structures but more precisely target the functions of the proteins.

Aim 3: To biophysically characterize ubiquitin modulation of CUE domain's dimerization and Tollip's membrane targeting: We further seek the significance of ubiquitin binding by two different domains of Tollip in terms of its oligomerization and membrane targeting. The initial evidence that ubiquitin might modulate Tollip oligomerization by dissociating CUE dimer came from SEC experiment which was further confirmed using sedimentation velocity AUC. Ubiquitin was also shown to inhibit protein binding to PtdIns3*P* and PtdIns(4,5)P_2. SPR kinetically characterized this inhibition and the IC_{50} value for this inhibition was estimated. The ubiquitin and lipid binding kinetics of the full-length Tollip was compared. Finally a model was constructed to describe ubiquitin modulation of Tollip's function.

CHAPTER III: The C2 domain of Tollip, a Toll like receptor signaling modulator, exhibits broad preference for phosphoinositides

Gayatri Ankem [*,1], Sharmistha Mitra [*,1], Furong Sun [*],
Anna C. Moreno [*], Boonta Chutvirasakul [*], Hugo F. Azurmendi [†],
Liwu Li [‡], and Daniel G. S. Capelluto [*, 2]

[*] Protein Signaling Domains Laboratory, and [‡] Laboratory of Innate Immunity and Inflammation, Department of Biological Sciences,
and [†] Department of Chemistry, Virginia Polytechnic Institute and State University, Blacksburg, Virginia 24061, United States

Short Title: Lipid binding properties of the Tollip C2 domain

[1] These authors contributed equally to this work.

[2] To whom correspondence should be addressed (e-mail capellut@vt.edu)

The article was published in *Biochem J* in the year 2011 and reproduced with permission, from author(s), 2011, *Biochem J*, 435, 597-608.

CONTRIBUTION TO THE PROJECT

This project served as the groundwork for my thesis. The detailed biophysical characteristics of Tollip C2 domain binding to lipid was much needed in order to decipher the interplay between lipid and ubiquitin recognition by the full-length protein. Related with this project, I contributed to purify WT and mutant Tollip C2 domain proteins, performed LPOA with the mutants, SPR experiment and analyses with proteins, fluorescent study with WT protein and the SEC experiment.

ABSTRACT:

Toll-like receptors (TLRs) provide a mechanism for host defence immune responses. Activated TLRs lead to the recruitment of adaptor proteins to their cytosolic tails, which in turn, promote the activation of interleukin-1 receptor-associated kinases (IRAKs). IRAKs act upon their transcription factor targets to influence the expression of genes involved in the immune response. Toll-interacting protein (Tollip) modulates IRAK function in the TLR signaling pathway. Tollip is multimodular with a conserved C2 domain of unknown function. We found that the Tollip C2 domain preferentially interacts with phosphoinositides, most notably with phosphatidylinositol 3-phosphate (PtdIns3*P*) and phosphatidylinositol 4,5-bisphosphate (PtdIns(4,5)P_2), in a Ca^{+2}-independent manner. However, NMR analysis demonstrates that the Tollip C2 binds Ca^{+2}, which may be required to target the membrane interface. NMR and lipid-protein overlay analyses suggest that PtdIns3*P* and PtdIns(4,5)P_2 share interacting residues in the protein. Kinetic studies reveal that the C2 domain reversibly binds PtdIns3*P* and PtdIns(4,5)P_2 with affinity values in the low micromolar range. Mutational analysis identifies key PtdIns3*P*- and PtdIns(4,5)P_2-binding conserved basic residues in the protein. Our findings suggest that basic residues of the C2 domain mediate membrane targeting of Tollip by interaction with phosphoinositides, which contribute to the observed partition of the protein in different subcellular compartments.

INTRODUCTION

Toll-like receptors (TLRs) and interleukin-1 receptors (IL-1Rs) provide a mechanism for host defence responses by activating the innate and adaptative immune responses [1]. These receptors are single-transmembrane proteins with ectodomains largely composed of leucine-rich repeats and with a conserved cytosolic Toll/Interleukin-1 receptor (TIR) domain, which facilitates the recruitment of adaptor proteins [2]. They are broadly distributed on cells of the immune system and are the best-studied immune sensors of invading pathogens. There are at least eleven human TLRs (TLR1-TLR11) [3] that utilize the adaptor protein myeloid differentiation factor 88 (MyD88) to signal, with the exception of TLR3 and 4 [4]. TLR types 1, 2, 4, 5, and 6 are expressed on the cell surface and are involved in recognizing lipopeptides and proteins. On the other hand, the antiviral TLR types 3, 7, 8, and 9 are localized in endosomes [4]. Upon activation (*i.e.*, by microbial products), TLRs are believed to either homo- or heterodimerize followed by MyD88 binding to the cytosolic TIR domain of the TLR. This, in turn, promotes the activation of stress-activated protein kinases including the IL-1R-associated kinases (IRAKs) 1, 2, M, and 4. All these kinases bind to MyD88 by their death domains, facilitating the activation of the tumor-necrosis factor-receptor-associated factor 6 (TRAF-6), which forms a protein complex with two ubiquitin-conjugating enzymes--ubiquitin conjugating enzyme variant 1A and ubiquitin-conjugating enzyme 13. Activation of other kinases, including the inhibitor of Nuclear factor-kappaB (NF-κB) [IκB] kinases, leads to the release of the transcription

factor NF-κB from IκB and subsequent phosphorylation and ubiquitin-dependent degradation of IκB. NF-κB translocates to the nucleus, which promotes pro-inflammatory responses by mediating cytokine gene expression [5].

The Toll-interacting protein (Tollip) controls IRAK function in both TLR and IL-1 receptor signaling pathways [6-8]. In resting cells, Tollip regulates these pathways at two different levels. First, Tollip associates with IL-1 receptor, TLR2 and TLR4 after lipopolysaccharide (LPS) activation, inhibiting TLR-mediated cell activation [7]. Secondly, Tollip directly binds to IRAK, inhibiting IRAK autophosphorylation [6, 7]. Indeed, overexpression of Tollip leads to inhibition of TLR-mediated NF-κB activation [6, 7]. Following TLR signaling stimulation, the Tollip-IRAK complex associates with the cytosolic tails of IL-1 receptor and TLR. IRAK autophosphorylates and phosphorylates Tollip [7], thus, initiating downstream signaling [6]. In addition, Tollip is involved in protein sorting by association with Target of Myb1 (Tom1), ubiquitin, and clathrin [9]. Tollip is localized on early endosomes where it is required for both degradation of ubiquitin-conjugated proteins [8] and sorting of IL-1 receptor on late endosomes [10]. Recently, Tollip has been shown to be SUMOylated and to mediate IL-1R SUMOylation [11]. This novel function makes Tollip a putative regulator of nuclear and cytoplasmic protein trafficking.

Tollip is a modular protein containing an N-terminal Tom1-binding domain (TBD), a central conserved 2 (C2) domain, and a C-terminal

coupling of ubiquitin to endoplasmic reticulum degradation (CUE) domain [6]. Using the lipid-protein overlay assay, Tollip has been reported to bind to both phosphatidylinositol 3-phosphate (PtdIns3*P*) and phosphatidylinositol (3,4,5)-triphosphate (PtdIns(3,4,5)P_3) [12]. A lysine to glutamic acid mutation located within the C2 domain (K150E) abrogates phosphoinositide binding [12], suggesting that the Tollip C2 domain is engaged in lipid binding. The CUE domain is a ubiquitin-binding module [13] that has been shown to bind to and be phosphorylated by IRAK proteins [7]. The tertiary structure of the CUE domain from two yeast proteins reveals a helical conformation [14, 15] with the yeast Vps9p CUE domain being a dimer [14], whereas the CUE domain of the yeast Cue2 protein is monomer [15]. Two-hybrid studies shows that rat Tollip interacts with itself, suggesting that the protein forms oligomers [11]. Furthermore, we have recently shown that the CUE domain forms tight dimers, which can contribute to Tollip oligomerization and ligand recognition [16].

There are at least 200 C2 domains and, after the PH domain, they represent the second most common lipid-binding domain [17]. Numerous C2 domains mediate signaling in a Ca^{+2}-dependent membrane-binding manner, as is the case for the conventional protein kinase C and synaptotagmin I, in which ion binding occurs via three loops known as Ca^{+2}-binding regions (CBRs) (for a review, see [18]). Binding of Ca^{+2} potentiates C2 domain recognition to acidic phospholipid membranes by changing the overall electrostatic potential at the C2 domain surface [19]. However, the

C2 domain of cytosolic phospholipase A2 binds to neutral membranes in a Ca^{+2}-bound state [19]. A minor group of C2 domains shows a weak membrane affinity, and are usually engaged in protein-protein interactions or exhibit a structural function. A third group of C2 domains does not bind Ca^{+2} at all but binds to membranes or participates in protein-protein interactions [20-22]. The Tollip C2 domain lacks two aspartic acid residues necessary for Ca^{+2} binding [6]. However, recent studies of the C2 domain of synaptotagmin IV indicate that Ca^{+2} binding cannot always be predicted from sequence-based analysis [23].

The structure of C2 domains typically present eight–stranded antiparallel β-sandwiches consisting of two sets of four-stranded β-sheets [18]. The C2 domain surface loops connect the β-strands in two different topologies. The majority of the C2 domains present a cationic patch in the interior of the β-sandwich, which is known as β-groove. Due to the cationic natures of the β-groove and the Ca^{+2}-binding loops, both are proposed to be two different lipid-binding sites [18]. The C2 domains are known to bind a wide spectrum of phospholipids without a well-defined lipid-binding site [18]. In the absence of Ca^{+2}, the cationic β-groove provides lipid recognition, necessary for the vesicle fusion activity of host proteins [24].

In the present study, we demonstrate that the Tollip C2 domain is responsible for phosphoinositide recognition in Tollip. Remarkably, our findings support a broad range of specificity, in which the phosphoinositide moiety is a common

theme. Moreover our results indicate that two of the most preferred ligands, PtdIns3*P* and PtdIns(4,5)P_2 interact with basic residues in the Tollip C2 domain with affinities in the low micromolar range and that binding of Ca^{+2} to the C2 domain is dispensable for phosphoinositide recognition. Overall, our findings might provide an explanation for the underlying mechanism responsible for Tollip's partition into different subcellular membrane compartments.

EXPERIMENTAL

Chemicals

A list of chemicals used and their suppliers follows: 1,2-dioleoyl-sn-glycero-3-phosphocholine (PC), 1,2-dioleoyl-sn-glycero-3-[phosphor-L-serine] (PS), 1,2-dioleoyl-*sn*-glycero-3-phosphate (PA), 1,2-dipalmitoyl-sn-glycero-3-phosphoethanolamine (PE), 1,2-dipalmitoyl-*sn*-glycero-3-phospho-(1'-*rac*-glycerol) (PG), and phosphatidylinositol (PI) (Avanti-Lipids); PI3P, PI4P, PI5P, PI(3,4)P_2, PI(3,5)P_2, PI(4,5)P_2, and PI(3,4,5)P_3 (Cayman Chemicals); inositol 1,3-bisphosphate (Ins(1,3)P_2) and inositol 1,4,5-triphosphate (Ins(1,4,5)P_3) (Echelon); isopropyl -D-thiogalactopyranoside (IPTG) (Research Products International). All other chemicals were analytical reagent grade.

Cloning, expression, and purification of the Tollip constructs

The human full-length Tollip and its isolated C2 domain (residues 54-182) as well as the *Saccharomyces cerevisiae* Vam7p PX domain (residues 2-134) cDNAs were cloned into a pGEX4T3 vector (GE Healthcare) and expressed in *Escherichia coli* (Rosetta; Stratagene). Briefly, bacterial cells were

grown in Luria-Bertani media at 37ºC until they reached an OD of ~0.8. Induction of glutathione S-transferase (GST) fusion proteins resulted from the addition of 0.1 mM IPTG followed by 4 h incubation at 25ºC. Cell pellets were suspended in cold buffer containing 50 mM Tris-HCl (pH 7.3), 500 mM NaCl, 500mM benzamidine, 0.1 mg/mL lysozyme, 5 mM dithiothreitol (DTT), and 0.1% Triton-X-100. Suspensions were further processed by sonication (using a Branson sonifier 250 with a duty cycle of 30% and eight pulses of 30 s each) centrifuged (1940 ***g***, 30 min, 4°C) and the resultants supernatants loaded onto a Glutathione Sepharose 4B (GE Healthcare) column. In some cases, fusion proteins were eluted off the beads by addition of 20 mM Tris/HCl (pH 7), 500 mM NaCl, and 100 mM reduced glutathione. In other purifications, the GST tag was removed by incubation of the fusion protein with thrombin (EMD Biosciences) overnight at 4°C. Proteins were recovered in a buffer containing 20 mM Tris/HCl (pH 8) and 500 mM NaCl, concentrated using a 3-kDa-cut-off concentrator device (Millipore) and further purified by an ÄKTA FPLC system using a size-exclusion chromatography column (Superdex 75; GE Healthcare) equilibrated with 50 mM Tris/HCl (pH 8), 1 M NaCl, and 1 mM DTT. Protein peak fractions were pooled, exchanged in the corresponding buffer, and further concentrated for functional and structural analysis.

Liposome-binding assay

Stocks of phospholipids were prepared in organic solvents as described in manufacturer's instructions. Liposomes were prepared by a weight ratio of 1:1 PC/PE, and 5% of the phospholipid under investigations was used. Controls were prepared by

adjusting ratios with both PC and PE. Lipid films were generated by freeze-drying and hydrated in 50 mM Hepes (pH 6) and 100 mM NaCl to 1 mg/ml at 67ºC for 30 min and freeze-thawed three times. Liposomes were sonicated (using Branson sonifier 250 with a duty cyle of 30% and eight pulses of 30 s each), pelleted (15 000 ***g***, 20 min, 22°C and suspended at 5 mg/ml in the same buffer. A 10 µg portion of protein was incubated with 200 µg of total lipid for 30 min at room temperature (22°C). Liposome-bound and free-protein fractions were obtained by centrifugation and analyzed by SDS/PAGE(10% gel). Protein bands were quantified using the AlphaEase FC software.

NMR spectroscopy

NMR protein samples contained 150 µM of Tollip C2 domain, 90%H_2O/10% ^2H_2O, 20 mM $^2H_{11}$ Tris/HCl (pH 6.8), 150 mM KCl, 5 mM $^2H_{10}$ DTT, and 1 mM NaN_3. Double-resonance experiments were acquired at 25°C using a Bruker Avance III 600 MHz spectrometer (Virginia Polytechnic Institute and State University) equipped with inverse TXI probe with z-axis pulse field gradients. Additional NMR experiments were collected on a Bruker Avance 800 MHz spectrometer equipped with a cryoprobe at University of Virginia. Phospholipid head group and $CaCl_2$ titrations into the ^{15}N-labeled C2 domain were analyzed by ^1H-^{15}N heteronuclear single quantum coherence (HSQC) experiments. Spectra were processed with NMRPipe [25] and analyzed using nmrDraw [26].

CD spectroscopy

Far-UV CD spectra were generated using purified proteins (10 µM) in 5 mM Tris/HCl (pH 6.8), 100 mM KF,

and 0.1 mM DTT on a Jasco J-815 spectropolarimeter equipped with a Jasco PFD-425 S temperature control unit. Spectra were collected in a 1-mm path length quartz cell at 25°C. Spectra were obtained from five accumulated scans from 240 to 190 nm using a bandwidth of 1 nm and a response time of 1 s at a scan speed of 20 nm/min. Buffer backgrounds were used to subtract from the protein spectra. Secondary structure content of the proteins were estimated with the online server DICHROWEB [27] using the CDSSTR algorithm [28]. Near-UV CD spectra were collected using a 0.1-cm path length at 20 nm/min between 340 and 250 nm with a response time of 1 s and a data pitch of 0.5 nm. Owing to the weak molar absorptivity of the aromatic amino acids, 100 µM of protein was employed for the near-UV CD experiments. The thermal denaturation of the proteins (10 µM) were investigated in the range of 4-90°C following temperature-induced changes in ellipticity at 218 nm, where the temperature was increased 1°C/min, using a 1.5-nm bandwidth, an averaging time of 30 s, and an equilibration time of 2 min.

Fluorescence spectroscopy

Intrinsic tryptophan fluorescence spectroscopy measurements were carried out using a J-815 Jasco spectropolarimeter at 25°C in a 1-cm path length cuvette. The λ_{ex} was 295 nm, and the fluorescence emission spectra were recorded from 310 to 410 nm for each protein sample.

Surface plasmon resonance analysis

All measurements were carried out at room temperature in 20 mM Hepes (pH 6) and 100 mM NaCl using an L1 sensor chip on a BIAcore X100

instrument (BIAcore, Uppsala, Sweden). Liposomes containing PtdIns3*P*, PtdIns(4,5)P_2, or PE were made as described above with an additional extrusion step using 400-nm membranes. The surface of the sensor chip was preconditioned by injecting 40 mM N-octyll-β-D-glucopyranoside at a flow rate of 5 µl/min. The first flow cell was used as a control surface, whereas the second flow cell was employed as the active surface. Both flow cells were coated with 6000 resonance units (RU) of 1 mg/ml each of the liposomes tested at a flow rate of 2 µl/min. After liposome coating, 30 µl of a 10 mM NaOH solution at a flow rate of 30 µl/min was used to wash away any unbound liposome. Nonspecific binding sites at the sensor chip surface were then blocked with the injection of 250 µl of 0.1 mg/ml of fatty acid-free BSA (Sigma) at a flow rate of 5 µl/min. A range of concentrations of protein analytes was prepared in the same buffer and injected on both flow cell surfaces at a flow rate of 30 µl/min. Sensorgrams were obtained from at least five different concentrations of each of the tested proteins. The association and dissociation times for each protein injection were set to 120 and 600 s respectively. The remaining bound protein was washed away by the injection of 30 µl of 10 mM NaOH. The sensor chip surface was regenerated using 40 mM N-octyl-β-D-glucopyranoside and recoated with fresh liposomes for the next protein titration. Data were analyzed using BIAcore X100 evaluation software (version 2.0).

Lipid-protein overlay assay

Lipid strips were prepared by spotting 1 µl of the indicated amount of phosphoinositide dissolved in

chloroform/methanol/water (65:35:8) onto Hybond-C extra membranes (GE Healthcare). Membrane strips containing the immobilized phosphoinositide were blocked with 3% (w/v) fatty acid-free bovine serum albumin (BSA, Sigma) in 20 mM Tris/HCl (pH 8), 150 mM NaCl, 0.1% Tween-20 for 1 h at room temperature. Then, membranes were incubated with 0.1 µg/ml of protein in the same buffer without BSA overnight at 4°C. Following four washes with the same buffer, bound proteins were probed with rabbit anti-GST antibody (Santa Cruz Biotech) and donkey anti rabbit-horse radish peroxidase (HRP) (GE Healthcare). Protein binding was detected using enhanced chemiluminescence reagent (Pierce).

RESULTS

The Tollip C2 domain preferentially binds phosphoinositides

The C2 domain is a conserved module located between a N-terminal TBD and the C-terminal CUE domains in Tollip (Figure 3.1A). A recent report indicated that Tollip binds to both PtdIns3*P* and PtdIns(3,4,5)P_3 using the lipid-protein overlay assay [12] and that a mutation at Lys^{150}, a residue located within the C2 domain, abrogates phospholipid binding [12]. To determine whether the C2 domain of Tollip is responsible for phospholipid recognition, we isolated the Tollip C2 domain and investigated whether it binds phospholipids using liposomes, which closely resemble biological membranes. We found that the C2 domain preferentially bound to phosphoinositides compared with liposomes bearing other phospholipids including PC, PA, PG, PS, or PI (Figures 3.1B and 3.1C). These findings are in agreement with other C2 domains, which typically exhibit highly variable and relatively low lipid

specificity [18]. Phospholipid binding by the C2 domain was at the most ~60% of the total protein when compared with the Vam7p PX domain (Figure 3.1B), a PtdIns3*P* binding domain [29]. These results indicate that the Tollip C2 domain preferentially binds phosphatidylinositols with phosphates at their inositol rings.

To further validate our findings, we next compared phosphoinositide interactions using the head group of PtdIns3*P* and PtdIns(4,5)P_2, the most preferred lipid ligands of the Tollip C2 domain (Figures 3.1B and 3.1C), and NMR spectroscopy analysis. Initial NMR titration experiments using PtdIns3*P* and PtdIns(4,5)P_2 led to significant protein precipitation (results not shown). Several chemical shift perturbations of the C2 domain residues were detected after the addition of lipid head groups, Ins(1,3)P_2 (for PtdIns3*P*; Figure 3.2A) and Ins(1,4,5)P_3 [for PtdIns(4,5)*P*2; Figure 3.2B] in ^{15}N-^{1}H HSQC experiments. The rate of the association is in the fast exchange regime and the protein exhibits a low affinity for the head group, which was anticipated owing to the absence of a membrane interface. Most of chemical shift perturbations in each spectra are similar, suggesting that at least PtdIns3*P* and PtdIns(4,5)P_2 share some binding residues. These perturbations are absent from NMR samples of the Tollip C2 domain containing Ins1*P* head group of PI, which is composed of the core of the inositol ring of phosphoinositides, but lacks the phosphate groups at the same protein/ligand ratio (Figure 3.2C). Thus, this result serves as a control to identify specific chemical shift perturbations with phosphorylated inositol rings. To further confirm

whether the phosphoinositides share the same binding residues in the Tollip C2 domain, we performed a lipid-protein overlay competition assay. The protein (as a GST-fusion) was preincubated with Ins(1,4,5)P_3 and this mixture was then added to a membrane bound PtdIns3*P*. As shown in Figure 3.3(A), Ins(1,4,5)P_3 significantly reduced PI3*P* binding to the Tollip C2 domain.

Structural analysis of the Tollip C2 domain

Far-UV CD spectroscopy was used to characterize the secondary structure of the Tollip C2 domain. Figure 3.3(B) shows that the domain exhibits a typical spectrum of a β-sheet protein with a minimum at 218 nm. Prediction of the secondary structure revealed that the C2 domain presents ~34% β-sheet and negligible α-helical content (~4%). After addition of 16-fold of Ins(1,3)P_2, the PtdIns3*P* head group, did not induce any secondary structure change in the protein (Figure 3.3B and results not shown). Tryptophan, tyrosine and phenylalanine residues are the main chromophores in the CD of the near-UV region and, therefore, provide information about the tertiary structure of proteins [30]. The Tollip C2 near-UV spectrum exhibits a negative peak between 278 and 310 nm with a minimum at ~292 nm, which is likely due to the contribution of its tyrosine and tryptophan side chains in the tertiary structure (Figure 3.3C). The overall intensity of the Tollip C2 spectrum is shifted up somewhat by the addition of Ins(1,3)P_2 (Figure 3.3B). Although the cause of this intensity difference is not clear, the shape similarities of the two spectra indicate that the head group does not induce a conformational change in the tertiary structure of the protein upon

binding. Thus, most of the chemical shift changes observed in the Tollip C2 spectrum upon the addition of Ins(1,3)P_2 (Figure 3.2A) are likely a consequence of direct contact between the protein and the lipid head group. Recently we reported that the CUE domain forms dimers [16] and, therefore, it represents a contributor of Tollip oligomerization. Some C2 domains have been reported to mediate protein dimerization [31-33]. Therefore, we have also investigated the oligomeric state of the Tollip C2 domain by analytical size-exclusion chromatography. The protein eluted at a volume that corresponded to a 15.5 kDa globular protein (Figure 3.3D), a value close to its theoretical molecular mass (15.7 kDa). Mass spectral analysis of the protein revealed a prominent signal at 15 481 (Figure S3.1), confirming the monomeric nature of the protein. Thermal denaturation analysis indicated that the Tollip C2 domain showed two-state melting transitions, indicative of highly cooperative unfolding transition between 50°C and 60°C with an apparent melting temperature of 54°C. The fluorescence spectrum of the Tollip C2 domain exhibited a maximum at 340 nm and a further red shift of ~6 nm and reduced emission intensity after denaturation with guanidine hydrochloride (Figure 3.3F), indicative of a relatively buried average localization for the three tryptophans present in the native conformation of the protein domain.

The Tollip C2 domain binds Ca^{+2}, which is not required for phosphoinositide binding

Ca^{+2} is a physiological ligand for most of C2 domains, whose binding is necessary to increase the affinity of the protein to lipids for membrane

docking events. The Tollip C2 domain lacks two of the five aspartic acid residues involved in Ca^{+2} ligation found in other C2 domains [6]. Nonetheless, we experimentally investigated whether the Tollip C2 domain binds Ca^{+2} using CD and NMR spectroscopy. The CD spectrum of the Tollip C2 domain does not exhibit any conformational change upon addition of up to 30 mM $CaCl_2$ (data not shown). However, NMR spectroscopy analysis demonstrates that Ca^{+2} selectively induces chemical shift perturbations in the spectrum of the protein (Figure 3.4A). The binding also appears to be on a fast exchange regime indicating a low affinity for the ligand in solution. Many C2 domains have been shown to interact with lipids in a Ca^{+2}-dependent manner. Therefore, we investigated whether Ca^{+2} binding contributes to phosphoinositide recognition by the Tollip C2 domain. As shown in Figure 3.4B, the Tollip C2 domain did not exhibit Ca^{+2}-dependent binding to PtdIns3*P*, and that the binding was not further changed by the presence of EGTA, a Ca^{+2} chelator. PtdIns(4,5)P_2 binding by the Tollip C2 domain was also Ca^{+2}-independent (results not shown).

Kinetic analysis of Tollip C2 domain-phosphoinositide interactions

The interaction of the Tollip C2 domain with phosphoinositide-enriched liposomes was kinetically examined by surface plasmon resonance (SPR), utilizing tag-free Tollip C2 domain as an analyte and either PtdIns3*P*- or PtdIns(4,5)P_2-enriched liposomes immobilized on an L1 sensor chip as ligands. The Vam7p PX domain binds Ptdns3*P* [29] and was employed as a positive control. In all cases, proteins

exhibited fast association and dissociation rates. The Tollip C2 domain bound phosphoinositide-enriched liposomes following a two-state conformational change model and displayed reversible binding (Figures 3.5A and 3.5B). No fitting could be obtained when plots were analyzed using the 1:1 Langmuir model (results not shown). Binding affinity and kinetic properties of proteins and their phosphoinositide ligands are summarized in Table 3.1. The Tollip C2 domain bound with dissociation constants (K_D) of 4.6 and 11 μM for PtdIns(4,5)P_2 and PtdIns3*P* liposomes, respectively. These affinity values are comparable with that determined for PtdIns(4,5)P_2 binding by C2 domains of classical protein kinases C [34] but much lower than the affinities reported for the synaptotagmin C2b and PKC C2 domains for the same ligand [22,24]. On the other hand, the Vam7p PX domain, bound PtdIns3*P* following a 1:1 Langmuir model (Figure 3.5C). The affinity of the Vam7p PX domain for PtdIns3*P* liposomes was 1000-fold higher with a K_D value of 9.5 nM (Table S3.1), a phosphoinositides affinity value similar to those determined for other PX domains [35]. The affinity differences between the proteins for phosphoinositides are reflected by plotting the log of the maximum resonance units against protein concentration, in which the Tollip C2 domain exhibits a modest affinity when compared with the Vam7p PX domain (Figure 3.5D). However, in all titrations, phosphoinositide binding exhibited a saturable binding isotherm that is associated with specific binding (Figure 3.5D).

Conserved basic residues in the Tollip C2 domain play a critical role in phosphoinositide recognition

Since phosphoinositides are negatively charged, several conserved basic residues of the Tollip C2 domain (Figure S3.2) were mutated to alanine and analyzed for binding to PtdIns3*P*, one of the most preferred Tollip C2 domain ligands, using the lipid-protein overlay assay. As expected, Tollip bound to PtdIns3*P* in a lipid mass-dependent manner (Figure 3.6A). Mutation in the nonconserved Lys^{150} residue (Figure S3.2) to glutamic acid in Tollip has been shown to abrogate lipid binding [12]. However, we found that a mutation of the same residue to a neutral amino acid reduced but did not eliminate PtdIns3*P* binding and rather a mutation to the conserved Lys162 residue to alanine almost completely abolished PtdIns3*P* binding (Figure 3.6A). Curiously, the isolated C2 domain consistently showed higher binding signal when compared with the full-length Tollip protein (Figure 3.6A). This observation suggests that neighbour regions may modulate phosphoinositide recognition by the C2 domain. We further screened for PtdIns3*P*-binding residues by site-directed mutagenesis in the Tollip C2 domain. We found that alanine mutations at Arg^{78}, Arg^{123}, His^{135}, Arg^{157}, and Lys^{162} almost eliminated PtdIns3*P* binding, whereas mutations at Lys^{102} and Lys^{150} mirrored the strength of binding of the wild type Tollip C2 domain for the same phosphoinositide (Figure 3.6A). Overall, these data indicate that specific conserved basic residues in the Tollip C2 domain play a critical role in phosphoinositide recognition. We then functionally and structurally investigated the K162A mutant of the C2 domain for simplicity. Consistent

with our findings, the inability of the Tollip C2 K162A to bind PtdIns3*P* was evident using the liposome-binding assay (Figure 3.6B). Likewise, PtdIns3*P* binding by the Tollip C2 K162A mutant was also negligible using SPR (results not shown). Mutation at Lys^{162} did not alter the secondary structure, the tryptophan fluorescence emission, and the stability and compactness of the Tollip C2 domain (Figure S3.3) indicating that the mutation specifically disrupts PtdIns3*P* binding. Our studies also demonstrate that Tollip bound PtdIns(4,5)P_2 and that Tollip K162A exhibited a slightly reduced, but not abolished, binding to the phosphoinositide (Figure 3.6C). Mutation at Lys^{150} showed no major differences with Tollip for binding to PtdIns(4,5)P_2 (results not shown). Whereas residues Arg^{78}, Arg^{123} and His^{135} in the isolated C2 domain seemed to be critical for PtdIns(4,5)P_2 binding, the Lys^{162} mutation exhibited only a minor reduction in binding to the same lipid (Figure 3.6C). PtdIns(4,5)P_2 binding by K102A and R157A C2 domains were indistinguishable to that observed for the wild-type protein (Figure 3.6C). Thus, our findings indicate that unique Tollip C2 domain residues are able to discriminate the position of the phosphorylation(s) at the inositol ring in phosphoinositide ligands.

TABLES AND FIGURES

Table 3.1 **Liposome-binding parameters of the Tollip C2 domain determined from SPR analysis**

k_{a1}, association rate constant; k_{a2}, forward rate constant changing complex; k_{d1}, dissociation rate complex; k_{d2}, reverse dissociation rate constant changing complex

Binding Partner	k_{a1} (M^{-1} s^{-1})	k_{d1} (s^{-1})	k_{a2} (s^{-1})	k_{d2} (s^{-1})	k_D (M)	Fit (χ^2)
PI3P	$3.3 \pm 0.2 \times 10^{3}$	$3.9 \pm 0.07 \times 10^{-2}$	$5.6 \pm 0.2 \times 10^{-4}$	$1.6 \pm 0.02 \times 10^{-2}$	1.1×10^{-5}	9.6
$PI(4,5)P_2$	$6.8 \pm 0.3 \times 10^{4}$	$5.1 \pm 0.23 \times 10^{-1}$	$7.1 \pm 0.1 \times 10^{-4}$	$1.1 \pm 0.04 \times 10^{-3}$	4.6×10^{-6}	7.7

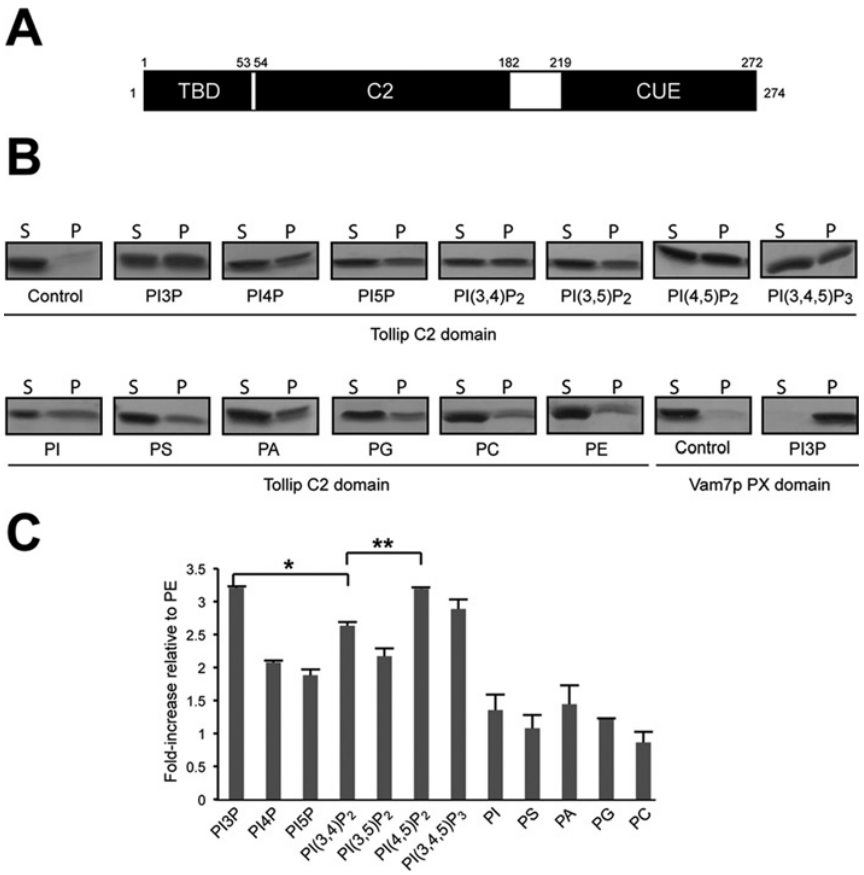

Figure 3.1 **Lipid ligand preference of the Tollip C2 domain.**

(**A**) Schematic representation of the Tollip primary structure with the boundaries of each of the domains indicated on top. (**B**) Phospholipid specificity of the Tollip C2 domain using liposomes containing 5% of various phospholipids and compared against control liposomes (PC/PE). The Vam7p PX domain was employed as a positive control. P and S indicate pellet and supernatant fractions, respectively, after centrifugation, SDS-PAGE, and Coomassie Blue staining. (**C**) Bands were quantified using Alpha-imager and normalized to the liposomes control. Both * and **, $P<0.05$. The ratios represent averages of three independent assays. Error bars represent standard deviations of the averages.

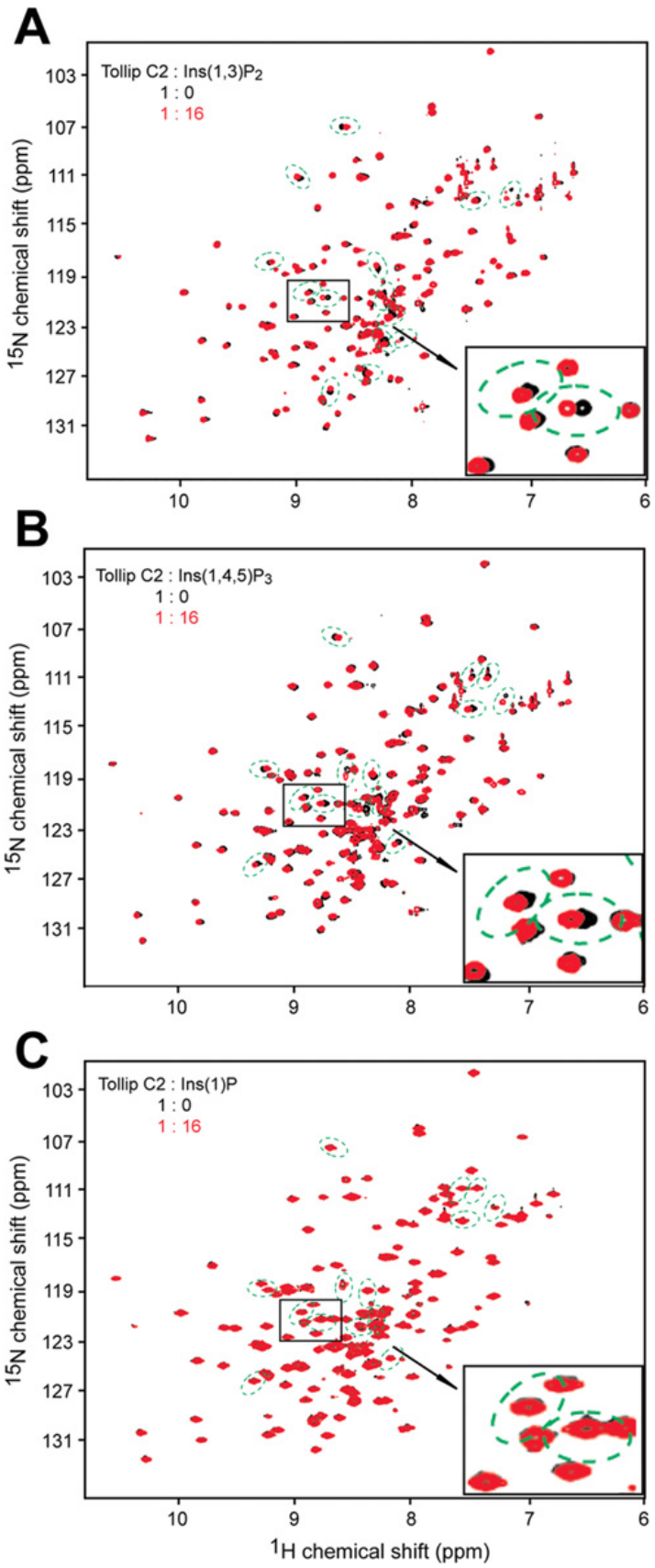

Figure 3.2 **The Tollip C2 domain interacts with phosphorylated inositol rings at positions 3, 4 and 5.**

The ^{15}N-labelled Tollip C2 domain (black) was subjected to ^{1}H-^{15}N HSQC analysis following titration with Ins(1,3)*P*$_2$ (**A**), Ins(1,4,5)*P*$_3$ (**B**) or Ins1*P* (**C**) at a protein/lipid head group molar ratio of 1:16. Tollip C2 domain residues that shift upon head-group titration in (**A**) and (**B**) are illustrated with green broken ovals. The location of these residues is also shown in (**C**). A representative section of the HSQC titration is magnified in each panel for clarification.

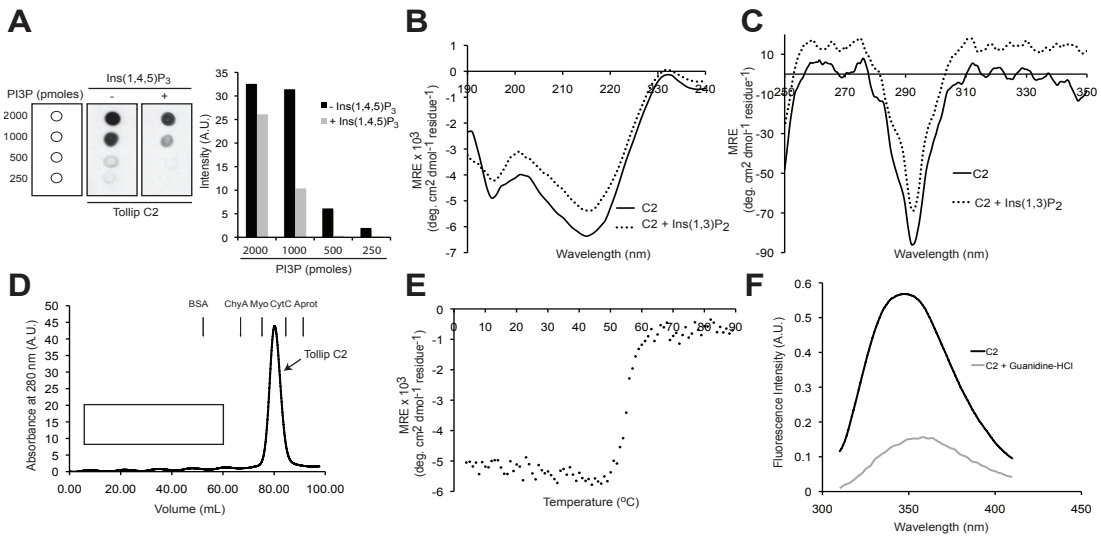

Figure 3.3 **Structural analysis of the free and head group-bound Tollip C2 domain.**

(**A**) PtdIns3*P* and PtdIns(4,5)P_2 compete with each other for binding to the Tollip C2 domain. The GST-Tollip C2 domain (10 µM) was preincubated with 50 µM Ins(1,4,5)P_3 for 30 min at room temperature and the mixture was further incubated with strips containing PtdIns3*P* at the indicated amounts and further processed as described in the Experimental section. (**B**) Far-UV CD spectra of the Tollip C2 domain in the absence and presence of 16-fold Ins(1,3)P_2. MRE, mean residue ellipticity. (**C**) Near-UV CD spectra of the Tollip C2 domain in the absence and presence of 16-fold of Ins(1,3)P_2. (**D**) Size-exclusion chromatography elution profile of the Tollip C2 domain monitored at 280 nm. Arrows denote the positions of the molecular weight standards. A.U., arbitrary units. (**E**) Thermal denaturation of the Tollip C2 domain at 218 nm. (**F**) Fluorescence emission spectra of the Tollip C2 domain in the absence (black line) and presence of 6 M guanidine hydrochloride (grey line).

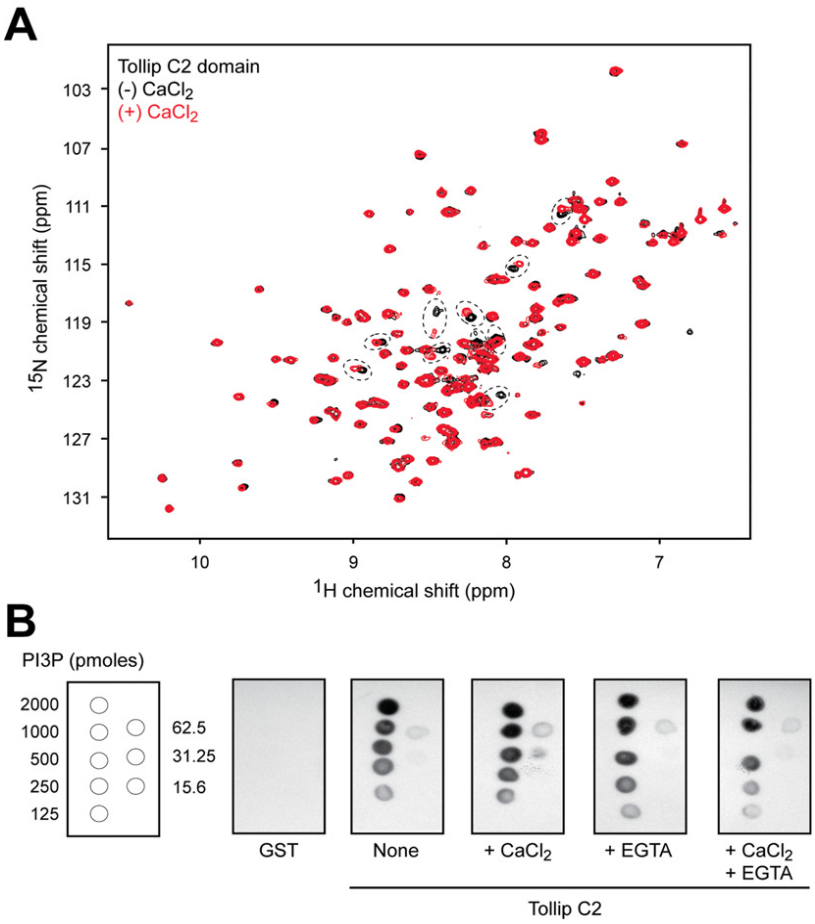

Figure 3.4 **Ca^{2+} binding by the Tollip C2 domain and role of Ca^{2+} in phosphoinositide interactions**

(A) Overlay of the ^{1}H-^{15}N HSQC spectra of the Tollip C2 domain in the absence (black) and presence (red) of 5 mM $CaCl_2$. Perturbed resonances are labelled with black broken ovals. (B) Ca^{2+} independent phosphoinostide binding of the Tollip C2 domain determined by the lipid-protein overlay assay. Each spot contains 15.6-2000 pmols of PtdIns3*P*. A GST-Tollip C2 domain fusion protein was incubated with lipid strips in the absence or presence of 1 mM $CaCl_2$, 1 mM EGTA, or both. GST was employed as a negative control.

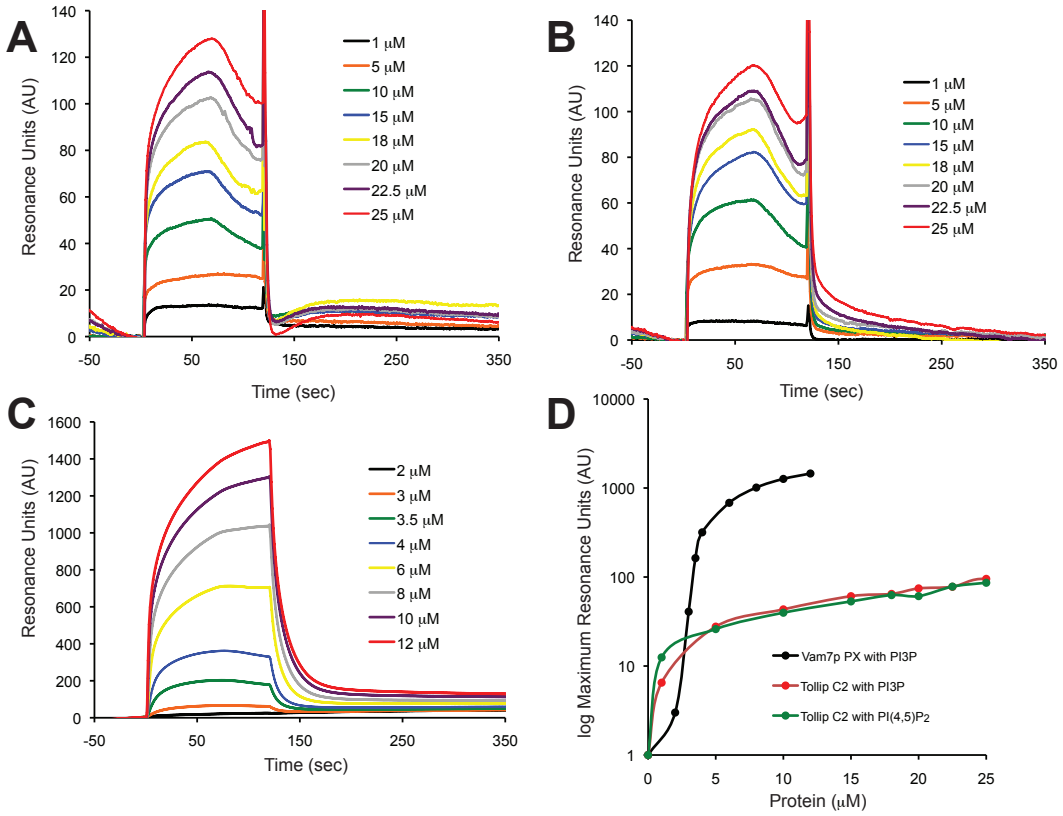

Figure 3.5 **Kinetic analysis of Tollip C2 domain interactions with phosphoinositides.**

SPR sensorgrams for the binding of the Tollip C2 domain with PtdIns(4,5)P_2-containing liposomes (**A**), and with PtdIs3*P* liposomes (**B**). As a control, the Vam7p PX domain was probed against PtdIns3*P* liposomes (**C**). Varying concentrations of each of the protein domains were flowed over the liposomes attached on an L1 sensorchip for 120 sec. (**D***)* Strength of the associations is represented in the plot in which the resonance units are on a logarithmic scale.

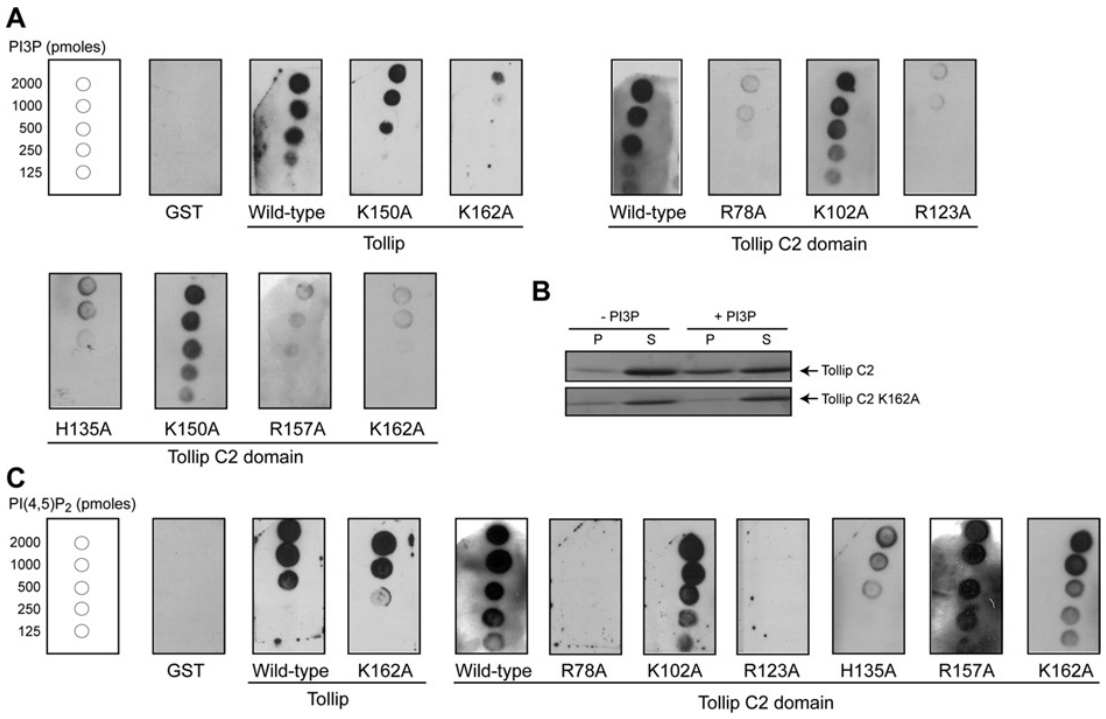

Figure 3.6 **Identification of the Tollip residues critical for PtdIns3*P* and PtdIns(4,5)P_2 binding.**

(**A**) Lipid-protein overlay assay of immobilized PtdIns3*P* at the indicated amounts and GST fusion Tollip, C2 domain, and mutants in basic residues within the C2 domain. GST was used as a negative control. (**B**) Liposome binding assay of wild-type Tollip C2 domain or its K162A mutant with liposomes without or with PtdIns3*P*. P and S represent pellet and supernatant fractions, respectively, after centrifugation, SDS-PAGE, and Coomassie Blue staining. (**C**) Lipid-protein overlay assay of immobilized PtdIns(4,5)P_2 at the indicated amounts and GST fusion Tollip, C2 domain, and mutants in conserved basic residues within the C2 domain.

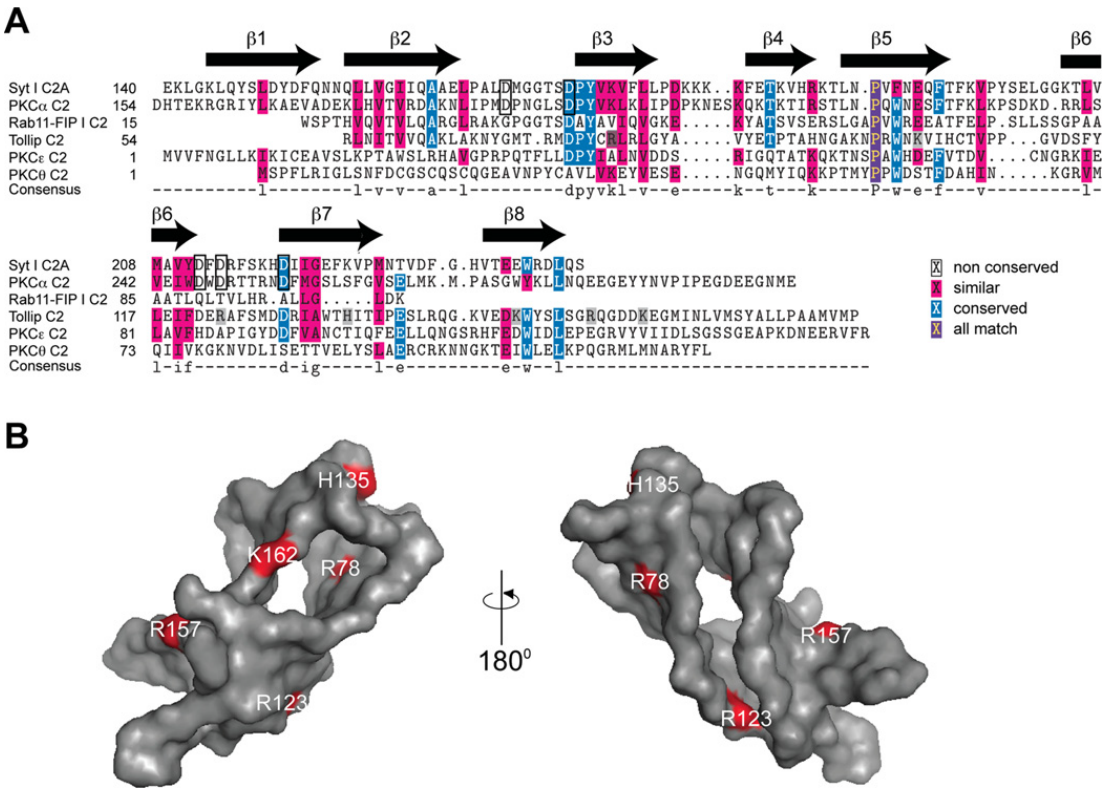

Figure 3.7 **Sequence alignment, structural properties and location of critical basic residues in the modeled structure of the Tollip C2 domain.**

(**A**) Sequence alignment of the C2A domain of human synaptotagmin I (Genbank accession number NP_005630), the C2 domain of the human PKCα (Genbank accession number NP_002728), the C2 domain of the human Rab11 family of interacting proteins (FIP) (Genbank accession number NP_079427), the C2 domain of human Tollip (Genbank accession number CAG38508), the C2 domain of the human PKCξ (Genbank accession number CAA46388), and the C2 domain of the human PKCθ (Genbank accession number NP_006248) constructed from the Biology WorkBench database (http://workbench.sdsc.edu). Boxes indicate the conserved aspartic acid residues engaged in Ca^{+2} ligation in both synaptotagmin I

and PKCα C2 domains. The secondary structure content determined for the synaptotagmin I C2 domain is depicted above the sequence alignment. Mutated Tollip C2 domain residues from this study are labelled in grey. (**B**) Two views of the predicted tertiary structure of the Tollip C2 domain constructed from the AL2TS database (http://proteinmodel.org/AS2TS/al2ts.html) using the C2A domain of synaptotagmin I as a template and depicted using Pymol (http://www.pymol.org). Experimentally determined PtdIns3*P*-binding residues are labelled in red on the predicted Tollip C2 domain tertiary structure.

DISCUSSION

Tollip is a key regulator of TLR-dependent signaling pathways [36]. To exert this function, Tollip binds to the tail of TLR proteins in association with adaptor proteins at the boundaries of the cytosolic face of the plasma membrane and endosomes to inhibit IRAK function. However, the determinants by which Tollip associates with these proteins at the membrane boundaries still remain unclear. In the present paper, we show for the first time that Tollip preferentially binds to phosphoinositides by its conserved C2 domain. Phosphatidylinositols represent less than 15% of the total phospholipids present in eukaryotes, with PtdIns4*P* and PtdIns(4,5)P_2 being the most abundant phosphoinositides in mammalian cells [37]. Each of the seven phosphoinositides found in these cells exhibit distinctive subcellular membrane localization. For example, PtdIns(4,5)P_2 and PtdIns(3,4,5)P_3 are enriched at the plasma membrane, whereas PtdIns3*P* is exclusively found in endosomes [37]. Remarkably, the subcellular localization of these phospholipids correlates with the reported subcellular localization of Tollip. Tollip is localized on early endosomes, multivesicular bodies [8], and the Golgi apparatus [12]. Thus, the subcellular localization of Tollip and its ability to bind phosphoinositides and ubiquitin suggest that it may be involved in the recognition and transport of ubiquitinated proteins in endocytic pathways. TLR proteins signal from both the plasma membranes and endosomes [2]. Thus, given the broad phosphoinositide specificity of its C2 domain, it is conceivable that Tollip is phosphoinositide-dependent partitioned in different subcellular

membrane pools to control TLR function via MyD88-dependent pathways. The broad specificity of the Tollip C2 domain to phosphoinositides may also increase the membrane affinity of Tollip or it may help to properly orient Tollip at the membrane.

Phospholipid-binding domains, including C2, PX, FYVE, PH, and ENTH domains, are modules engaged in membrane trafficking by recruiting signaling peripheral proteins to specific cell membrane surfaces. These domains exhibit diverse affinity and specificity to negatively charged phospholipids found at the membrane and present a strong positive potential on their surface that promote these associations. Of these, members of the PH and C2 domains are the most commonly found in eukaryotes. Despite its ubiquitous presence, the C2 domain, unlike other lipid-binding modules, does not exhibit a well-defined lipid binding site nor a conserved cationic patch [18]. Moreover, not all C2 domains can be easily identified by sequence homology. Another level of complexity is the fact that C2 domains are present in soluble and transmembrane proteins, they bind lipids either in a Ca^{+2}-dependent or independent fashion, and that they can either bind strongly or weakly to biological membranes [18]. Therefore, sequence homology is unlikely to predict the biological function of an uncharacterized C2 domain on the basis of studies performed with the same module found in unrelated proteins. From our statistical analysis, the Tollip C2 domain showed the highest preference of binding to liposomes enriched with the phosphoinositides PtdIns3*P*, PtdIns(4,5)P_2, and PtdIns(3,4,5)P_3

(Figures 3.1B and 3.1C). Therefore, we investigated further the Tollip binding properties of two of these ligands [PtdIns3*P* and PtdIns(4,5)P_2] given their strength of binding as well as the different location of the phosphate groups at their inositol rings. Titration of the Tollip C2 domain with the head groups of PtdIns3*P* and PtdIns(4,5)P_2 showed chemical shift deviations for restricted sets of NH signals (Figure 3.2). We were unable to assign the residues associated with these NMR chemical shifts due to the insolubility of the Tollip C2 domain at high concentration. However, comparison of chemical shift perturbations of the protein NMR spectrum by the addition of Ins(1,3)P_2 and Ins(1,4,5)P_3 suggest that phosphoinositide ligands share some residues in their binding sites. Competition analysis further confirmed this observation (Figure 3.3A). These results are not surprising given the intrinsic nature of C2 domains in recognizing a broad range of phospholipids [18]. Some C2 domains exhibit a dual lipid recognition mechanism, in which multiple lipid ligands must be present at the membrane to achieve high affinity and to properly localize intracellularly [17]. However, our experimental results suggest that two of the Tollip C2 domain lipid ligands, PtdIns3*P* and PtdIns(4,5)P_2, overlap their binding sites (Figures 3.2 and 3.3A).

Far-UV CD spectroscopy analysis of the Tollip C2 domain support the presence of β- sheet secondary structure and that the protein lacks any major conformational change upon Ins(1,3)P_2 binding (Figure 3.3B and results not shown). In addition, a cooperative unfolding transition is observed in the protein with a relatively

low temperature midpoint (~54ºC). Similar properties are displayed by the synaptotagmin I C2A domain [38]. The near-UV spectrum of the Tollip C2 domain is unaffected by the presence of the lipid head group, indicating that no major changes in the tertiary folding of the protein are induced upon ligand binding. This is agreement with the observation of selected NMR cross-peaks perturbed by the addition of phosphoinositide head groups (Figure 3.3).

A proposed Ca^{+2}-binding role has been shed by the observation that CBR regions are usually surrounded by positively charged residues [39,40], amino acids that are also found near the second aspartic acid-rich region in Tollip (see Figure 3.7A). However, the presence of only three of the five aspartic acid residues required for Ca^{+2} binding suggests that Tollip may not bind Ca^{+2} (Figure 3.7A). Nonetheless, we experimentally demonstrate that the Tollip C2 domain binds Ca^{+2} but the ion seems to be dispensable for phosphoinositide binding. This result is not surprising since similar observations were reported for the C2A domain of dysferlin, which contains four negatively charged residues of the five total required for Ca^{+2}-binding proteins [41]. Intriguingly, the synaptotagmin IV C2B domain contains all five aspartic residues but still is unable to bind Ca^{+2} [23]; therefore, Ca^{+2}-binding properties cannot be predicted from sequence analysis. As a Ca^{+2}-independent lipid-binding protein, basic residues at the surface of the Tollip C2 domain could make direct membrane contact as proposed for other C2 domains [18]. A distinct C2 family, related with the phosphoinositide 3-kinase C2 domain, has been recently been proposed to

interact with negatively charged lipids in a Ca^{+2}-independent manner through a patch of basic and hydrophobic residues located at the concave surface of the upper β-sheet that make a PtdIns(4,5)P_2–binding site and membrane penetration [42]. However, this region, located between β-strands 5 and 6 in C2 domains, does not exhibit a conserved basic and hydrophobic signature in Tollip (Figures 3.7A and S3.2). The CBR of Ca^{+2}-independent lipid binding C2 domains has been proposed to play a role in lipid binding and specificity [43-45]. Further investigation is required to determine the role of Ca^{+2}-binding by the Tollip C2 domain, which is beyond the scope of the present studies.

SPR experiments allowed us to characterize the kinetics of Tollip C2 domain binding to phosphoinositides. The protein bounds to PtdIns3*P* and PtdIns(4,5)P_2 with K_D values of 11 and 4.6 μM respectively, following a conformational change model. This may be the general mechanism by which Tollip binds to TLRs by a first association step with phosphoinositide-enriched membranes accompanied by a conformational change of the protein that further enhances binding to TLRs. For comparison purposes, we also measured the affinity of the Vam7p PX domain to PtdIns3*P* which resulted in a 1,000-fold higher affinity than the C2 domain and the mode of binding followed a one to one interaction model. Despite the fact that both Tollip and Vam7p proteins are found in endosomes, differences in affinity can be explained by the low phospholipid specificity exhibited by the Tollip C2 domain. Our investigation suggests that the isolated C2 domain binds phosphoinositides stronger than Tollip,

suggesting that other domains (*i.e.*, TBD, CUE) in the protein may exert a modulatory function. The C2 domain of the cytosolic phospholipase 2α binds more prominently than the full-length protein and a local effect on the C2 domain was proposed [22]. Likewise, the PtdIns(4,5)P_2-binding ubiquitin ligase Smurf2 protein exhibits autoinhibitory properties by intramolecular interaction between its C2 and HECT domains, leading to a reduction of its enzymatic activity and stabilizing the levels of the protein in the cell [46].

In the present work, we have identified for the first time conserved basic amino acids critical for Tollip C2 domain interactions with PtdIns3*P* and PtdIns(4,5)P_2. Many structures of Ca^{+2}-dependent C2 domains have been solved in detail and they exhibit a common fold with a well-defined cationic β-groove and with the CBR in the protein engaged in lipid-binding [18]. A phosphoinositide-binding site has also been mapped in the C2B domain of rabphilin-3A, which shows that its polar C-terminal region as well as its β-strands 3, 4, 6 and 7 to be critically involved in lipid recognition in a Ca^{+2}-independent manner [47]. Our mutational analysis indicates that the Tollip C2 domain could bind phosphoinositides in a similar fashion (Figures 3.7B). Mutation of Lys^{150} to glutamic acid has been shown to abolish phospholipid-binding by Tollip [12]. We have mutated this residue to alanine, since this amino acid will not cause a change in the overall charge of the protein. Both Tollip and C2 domain K150A mutants exhibited indistinguishable binding to phosphoinositides (Figure 3.6A and data not shown). This result is supported by the fact that the residue

is not conserved among Tollip proteins (Figure S3.2). Also, we found that some mutations in basic residues in the Tollip C2 domain abolished PtdIns3*P*, but not in PtdIns(4,5)P_2, binding. However, these lipids compete with each other for binding to the Tollip C2 domain. Therefore, it is conceivable that phosphoinositide binding sites overlap in Tollip but distinctive residues provide broad specificity of the protein for phosphoinositides. Binding between the Tollip C2 domain and the evaluated phosphoinositides is with moderated affinity, which can be explained from the proposed shallow, surface-exposed PtdIns3*P*-binding residues in the modeled structure of the protein (Figures 3.7B). Overall, we propose that, together with Ca^{+2}, a variety of hydrophobic and electrostatic forces can contribute to the Tollip-phosphoinositide interactions with biological membranes necessary for Tollip to modulate TLR signaling. Given the role of Tollip in recruiting adaptor proteins at the cytosolic tail of TLRs by its CUE domain, formation of such complexes may be further enhanced by initial Tollip interactions with phosphoinositides and membranes by its C2 domain. Further molecular studies are necessary to address how Tollip modulates TLR signaling. We are currently investigating the coordination between the C2, TBD, and CUE domains for their molecular interactions, which will provide new insights to understand the multimodular nature of Tollip.

AUTHOR CONTRIBUTION

Gayatri Ankem performed the purification of proteins and carried out liposome-binding assays, NMR titrations, CD measurements, and

protein-lipid overlay assays. Sharmistha Mitra carried out size-exclusion chromatography analysis, lipid-protein overlay assays and SPR experiments. Furong Sun and Anna Moreno purified proteins. Boonta Chutvirasakul designed constructs and purified proteins. Hugo Azurmendi carried out NMR experiments. Liwu Li provided reagents. Daniel Capelluto conceived the study, designed experiments, analyzed data, and wrote the manuscript.

ACKNOWLEDGMENTS

We are grateful to Dr. Kae-Jung Hwang and Rebecca Lehman for their contribution in the initial phase of this work. We thank Jeff Ellena for his assistance during the NMR titration experiments performed at the University of Virginia and to Dr. Carla Finkielstein and Dr. Janet Webster for her invaluable assistance during manuscript preparation.

FUNDING

This work was supported by the American Heart Association [grant number 086077E (to D.G.S.C.)].

REFERENCES

1 Kawai, T. and Akira, S. (2010) The role of pattern-recognition receptors in innate immunity: update on Toll-like receptors. Nat Immunol. **11**, 373-384

2 Barton, G. M. and Kagan, J. C. (2009) A cell biological view of Toll-like receptor function: regulation through compartmentalization. Nat Rev Immunol. **9**, 535-542

3 Bowie, A. and O'Neill, L. A. (2000) The interleukin-1 receptor/Toll-like receptor superfamily: signal

generators for pro-inflammatory interleukins and microbial products. J Leukoc Biol. **67**, 508-514

4 Frantz, S., Ertl, G. and Bauersachs, J. (2007) Mechanisms of disease: Toll-like receptors in cardiovascular disease. Nat Clin Pract. **4**, 444-454

5 Gan, L. and Li, L. (2006) Regulations and roles of the interleukin-1 receptor associated kinases (IRAKs) in innate and adaptive immunity. Immunol Res. **35**, 295-302

6 Burns, K., Clatworthy, J., Martin, L., Martinon, F., Plumpton, C., Maschera, B., Lewis, A., Ray, K., Tschopp, J. and Volpe, F. (2000) Tollip, a new component of the IL-1RI pathway, links IRAK to the IL-1 receptor. Nat Cell Biol. **2**, 346-351

7 Zhang, G. and Ghosh, S. (2002) Negative regulation of toll-like receptor-mediated signaling by Tollip. J Biol Chem. **277**, 7059-7065

8 Katoh, Y., Shiba, Y., Mitsuhashi, H., Yanagida, Y., Takatsu, H. and Nakayama, K. (2004) Tollip and Tom1 form a complex and recruit ubiquitin-conjugated proteins onto early endosomes. J Biol Chem. **279**, 24435-24443

9 Yamakami, M., Yoshimori, T. and Yokosawa, H. (2003) Tom1, a VHS domain-containing protein, interacts with tollip, ubiquitin, and clathrin. J Biol Chem. **278**, 52865-52872

10 Brissoni, B., Agostini, L., Kropf, M., Martinon, F., Swoboda, V., Lippens, S., Everett, H., Aebi, N., Janssens, S., Meylan, E., Felberbaum-Corti, M., Hirling, H., Gruenberg, J., Tschopp, J. and Burns, K. (2006) Intracellular trafficking of interleukin-1 receptor I requires Tollip. Curr Biol. **16**, 2265-2270

11 Ciarrocchi, A., D'Angelo, R., Cordiglieri, C., Rispoli, A., Santi, S.,

Riccio, M., Carone, S., Mancia, A. L., Paci, S., Cipollini, E., Ambrosetti, D. and Melli, M. (2009) Tollip is a mediator of protein sumoylation. PLoS One. **4**, e4404

12 Li, T., Hu, J. and Li, L. (2004) Characterization of Tollip protein upon Lipopolysaccharide challenge. Mol Immunol. **41**, 85-92

13 Shih, S. C., Prag, G., Francis, S. A., Sutanto, M. A., Hurley, J. H. and Hicke, L. (2003) A ubiquitin-binding motif required for intramolecular monoubiquitylation, the CUE domain. EMBO J. **22**, 1273-1281

14 Prag, G., Misra, S., Jones, E. A., Ghirlando, R., Davies, B. A., Horazdovsky, B. F. and Hurley, J. H. (2003) Mechanism of ubiquitin recognition by the CUE domain of Vps9p. Cell. **113**, 609-620

15 Kang, R. S., Daniels, C. M., Francis, S. A., Shih, S. C., Salerno, W. J., Hicke, L. and Radhakrishnan, I. (2003) Solution structure of a CUE-ubiquitin complex reveals a conserved mode of ubiquitin binding. Cell. **113**, 621-630

16 Azurmendi, H., Mitra, S., Ayala, I., Li, L., Finkielstein, C. V. and Capelluto, D. G. S. (2010) 1H, 15N, and 13C resonance assignments and secondary structure and of the Tollip CUE domain. Mol Cells. **30**, 581-585

17 Stahelin, R. V. (2009) Lipid binding domains: more than simple lipid effectors. J Lipid Res. **50**, S299-S304

18 Cho, W. and Stahelin, R. V. (2006) Membrane binding and subcellular targeting of C2 domains. Biochim Biophys Acta. **1761**, 838-849

19 Nalefski, E. A., Wisner, M. A., Chen, J. Z., Sprang, S. R., Fukuda, M., Mikoshiba, K. and Falke, J. J. (2001) C2 domains from different Ca2+ signaling pathways display functional

and mechanistic diversity. Biochemistry. **40**, 3089-3100

20 Ochoa, W. F., Garcia-Garcia, J., Fita, I., Corbalan-Garcia, S., Verdaguer, N. and Gomez-Fernandez, J. C. (2001) Structure of the C2 domain from novel protein kinase Cepsilon. A membrane binding model for Ca(2+)-independent C2 domains. J Mol Biol. **311**, 837-849

21 Lindsay, A. J. and McCaffrey, M. W. (2004) The C2 domains of the class I Rab11 family of interacting proteins target recycling vesicles to the plasma membrane. J Cell Sci. **117**, 4365-4375

22 Melowic, H. R., Stahelin, R. V., Blatner, N. R., Tian, W., Hayashi, K., Altman, A. and Cho, W. (2007) Mechanism of diacylglycerol-induced membrane targeting and activation of protein kinase Ctheta. J Biol Chem. **282**, 21467-21476

23 Dai, H., Shin, O. H., Machius, M., Tomchick, D. R., Sudhof, T. C. and Rizo, J. (2004) Structural basis for the evolutionary inactivation of Ca2+ binding to synaptotagmin 4. Nat Struct Mol Biol. **11**, 844-849

24 Fukuda, M., Kojima, T., Aruga, J., Niinobe, M. and Mikoshiba, K. (1995) Functional diversity of C2 domains of synaptotagmin family. Mutational analysis of inositol high polyphosphate binding domain. J Biol Chem. **270**, 26523-26527

25 Delaglio, F., Grzesiek, S., Vuister, G. W., Zhu, G., Pfeifer, J. and Bax, A. (1995) Nmrpipe - a Multidimensional Spectral Processing System Based on Unix Pipes. J Biomol NMR. **6**, 277-293

26 Garrett, D. S., Powers, R., Gronenborn, A. M. and Clore, G. M. (1991) A Common-Sense Approach to Peak Picking in 2-Dimensional, 3-Dimensional, and 4-Dimensional

Spectra Using Automatic Computer-Analysis of Contour Diagrams. J Magn Res. **95**, 214-220

27 Whitmore, L. and Wallace, B. A. (2004) DICHROWEB, an online server for protein secondary structure analyses from circular dichroism spectroscopic data. Nucleic Acids Res. **32**, W668-W673

28 Sreerama, N. and Woody, R. W. (2004) Computation and analysis of protein circular dichroism spectra. Methods Enzymol. **383**, 318-351

29 Cheever, M. L., Sato, T. K., de Beer, T., Kutateladze, T. G., Emr, S. D. and Overduin, M. (2001) Phox domain interaction with PtdIns(3)P targets the Vam7 t-SNARE to vacuole membranes. Nat Cell Biol. **3**, 613-618

30 Kelly, S. M., Jess, T. J. and Price, N. C. (2005) How to study proteins by circular dichroism. Biochim Biophys Acta. **1751**, 119-139

31 Guan, R., Dai, H., Tomchick, D. R., Dulubova, I., Machius, M., Sudhof, T. C. and Rizo, J. (2007) Crystal structure of the RIM1$ C2B domain at 1.7A° resolution. Biochemistry **46**, 8988–8998

32 Gerber, S. H., Garcia, J., Rizo, J. and Sudhof, T. C. (2001) An unusual C2-domain in the active-zone protein piccolo: implications for Ca2+ regulation of neurotransmitter release. EMBO J. **20**, 1605–1619

33 Liu, L., Song, X., He, D., Komma, C., Kita, A., Virbasius, J. V., Huang, G., Bellamy, H. D., Miki, K., Czech, M. P. and Zhou, G. W. (2006) Crystal structure of the C2 domain of class II phosphatidylinositide 3-kinase C2$. J. Biol. Chem. **281**, 4254–4260

34 Guerrero-Valero, M., Marin-Vicente, C., Gomez-Fernandez, J. C. and Corbalan-Garcia, S. (2007) The C2 domains of classical PKCs are specific PtdIns(4,5)P 2-sensing domains with

different affinities for membrane binding. J. Mol. Biol. **371**, 608–621

35 Stahelin, R. V., Karathanassis, D., Bruzik, K. S., Waterfield, M. D., Bravo, J., Williams, R. L. and Cho, W. (2006) Structural and membrane binding analysis of the Phox homology domain of phosphoinositide 3-kinase-C2alpha. J Biol Chem. **281**, 39396-39406

36 Abreu, M. T. (2010) Toll-like receptor signalling in the intestinal epithelium: how bacterial recognition shapes intestinal function. Nat Rev Immunol. **10**, 131-144

37 Di Paolo, G. and De Camilli, P. (2006) Phosphoinositides in cell regulation and membrane dynamics. Nature. **443**, 651-657

38 Shao, X., Li, C., Fernandez, I., Zhang, X., Sudhof, T. C. and Rizo, J. (1997) Synaptotagmin-syntaxin interaction: the C2 domain as a Ca2+-dependent electrostatic switch. Neuron. **18**, 133-142

39 Sutton, R. B., Davletov, B. A., Berghuis, A. M., Sudhof, T. C. and Sprang, S. R. (1995) Structure of the first C2 domain of synaptotagmin I: a novel Ca2+/phospholipid-binding fold. Cell. **80**, 929-938

40 Verdaguer, N., Corbalan-Garcia, S., Ochoa, W. F., Fita, I. and Gomez-Fernandez, J. C. (1999) Ca(2+) bridges the C2 membrane-binding domain of protein kinase Calpha directly to phosphatidylserine. EMBO J. **18**, 6329-6338

41 Therrien, C., Di Fulvio, S., Pickles, S. and Sinnreich, M. (2009) Characterization of lipid binding specificities of dysferlin C2 domains reveals novel interactions with phosphoinositides. Biochemistry. **48**, 2377-2384

42 Zhang, D. and Aravind, L. (2010) Identification of novel families

and classification of the C2 domain superfamily elucidate the origin and evolution of membrane targeting activities in eukaryotes. Gene. **469**, 18-30

43 Ananthanarayanan, B., Das, S., Rhee, S. G., Murray, D. and Cho, W. (2002) Membrane targeting of C2 domains of phospholipase C-delta isoforms. J Biol Chem. **277**, 3568-3575

44 Das, S., Dixon, J. E. and Cho, W. (2003) Membrane-binding and activation mechanism of PTEN. Proc Natl Acad Sci U S A. **100**, 7491-7496

45 Dunn, R., Klos, D. A., Adler, A. S. and Hicke, L. (2004) The C2 domain of the Rsp5 ubiquitin ligase binds membrane phosphoinositides and directs ubiquitination of endosomal cargo. J Cell Biol. **165**, 135-144

46 Wiesner, S., Ogunjimi, A. A., Wang, H. R., Rotin, D., Sicheri, F., Wrana, J. L. and Forman-Kay, J. D. (2007) Autoinhibition of the HECT-type ubiquitin ligase Smurf2 through its C2 domain. Cell. **130**, 651-662

47 Montaville, P., Coudevylle, N., Radhakrishnan, A., Leonov, A., Zweckstetter, M. and Becker, S. (2008) The PIP2 binding mode of the C2 domains of rabphilin-3A. Protein Sci. **17**, 1025-1034

SUPPLEMENTARY MATERIALS

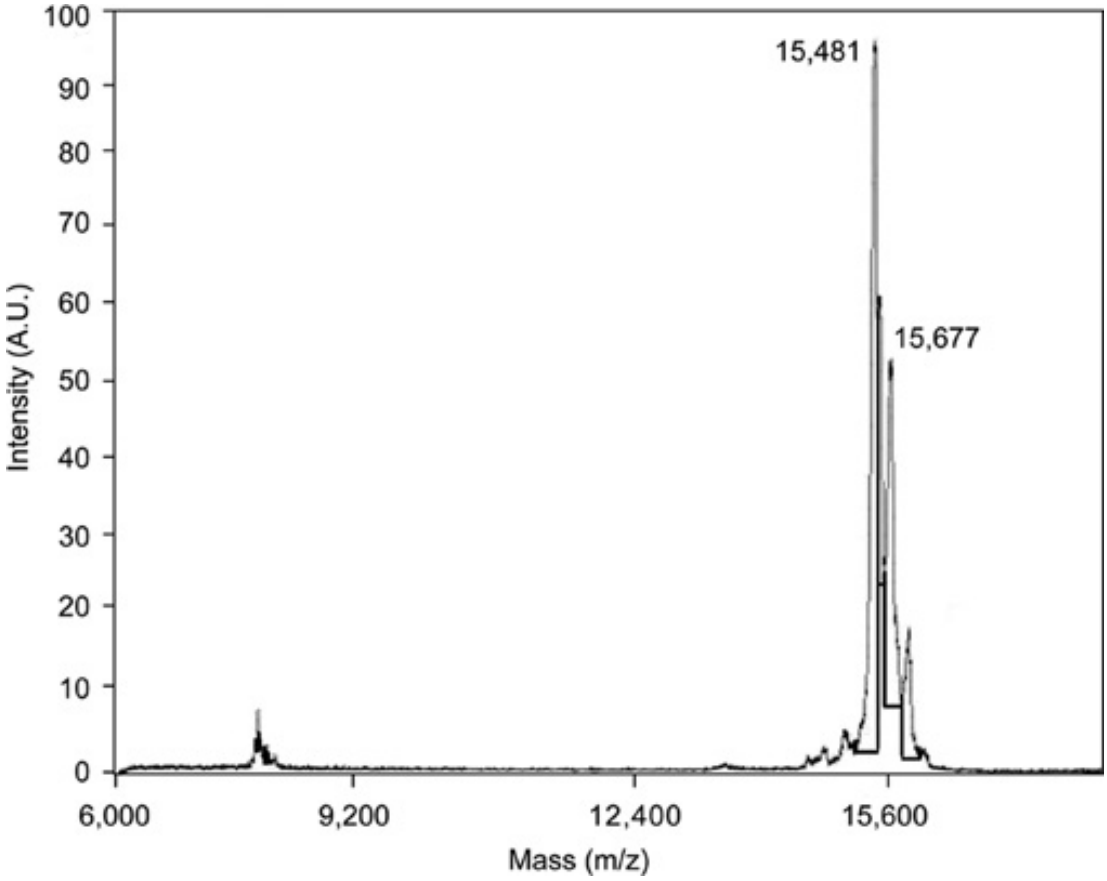

Figure S3.1 **MS analysis of the Tollip C2 domain.**

A.U., arbitrary units

Figure S3.2 **Sequence alignment of the Tollip C2 domains**

Sequences are from *Homo sapiens* (Genebank accession number CAG38508), *Mus musculus* (Genebank accession number CAB58121), *Xenopus levis* (Genebank accession number NP_001085420) and *Caenorhabditis elegans* (Genebank accession number NP_492757). The engineered mutations on the human Tollip C2 domain are indicated with red arrowheads above the sequences.

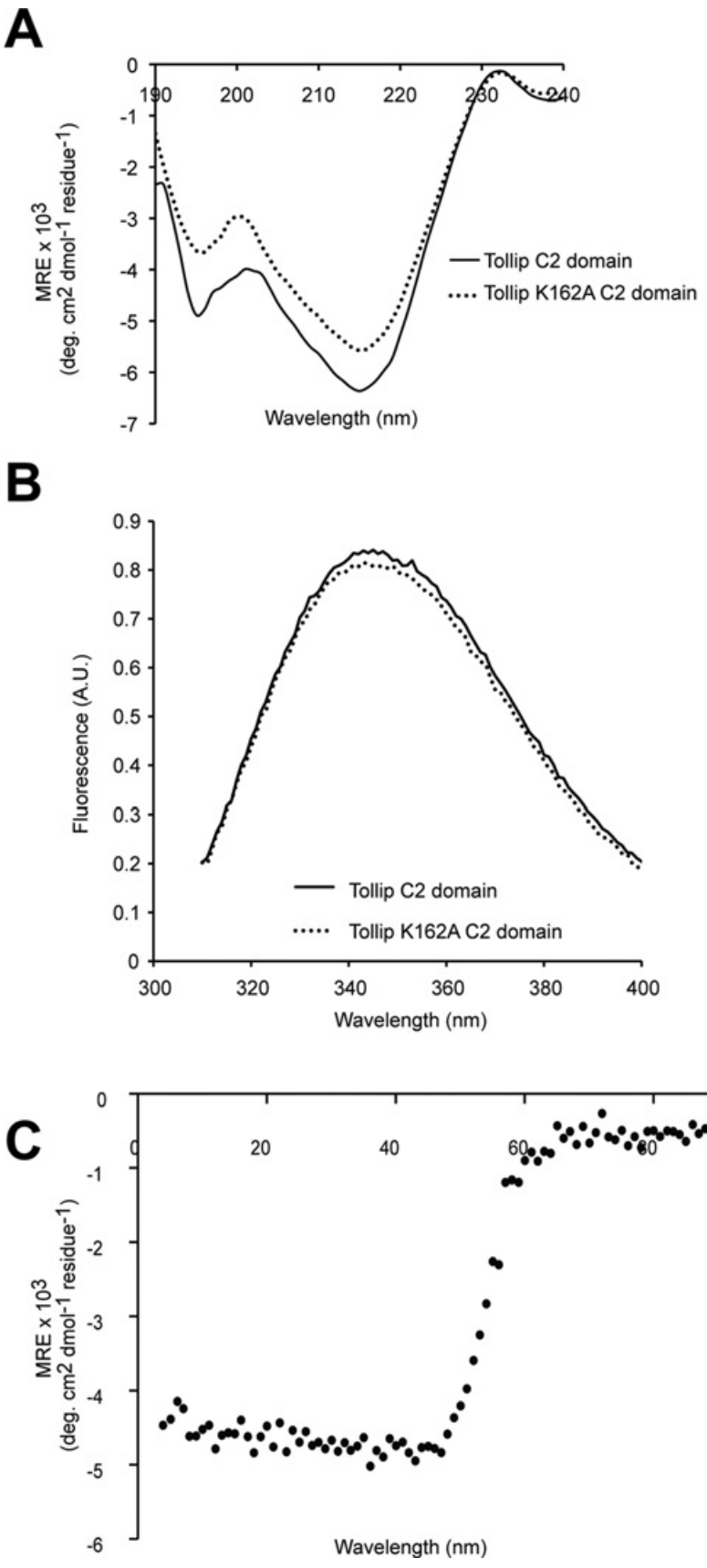
A
0
-1
-2
-3
-4
-5
-6
-7
190
200
210
220
230
240
MRE x 10^3
(deg. cm2 dmol-1 residue-1)
Wavelength (nm)
Tollip C2 domain
Tollip K162A C2 domain
B
0.9
0.8
0.7
0.6
0.5
0.4
0.3
0.2
0.1
0
300
320
340
360
380
400
Fluorescence (A.U.)
Wavelength (nm)
Tollip C2 domain
Tollip K162A C2 domain
C
0
-1
-2
-3
-4
-5
-6
0
20
40
60
80
MRE x 10^3
(deg. cm2 dmol-1 residue-1)
Wavelength (nm)

Figure S3.3 **Structural analysis of the effects of a lipid-binding mutation on the Tollip C2 domain**

(A) Far-UV CD spectra of the Tollip C2 domain (solid line) and K162A mutant (broken line). (B) Tryptophan fluorescence spectra of the Tollip C2 domain (solid line) and K162A mutant (broken line). (C) Thermal denaturation of the Tollip C2 K162A mutant. MRE, mean residue ellipticity

Table S3.1 **Apparent kinetic constants of the binding of the Vam7p PX domain to PtdIns3*P* liposomes using SPR detection**

The constants and error values of the fitting were obtained from a single titration experiment of the representative data set. K_a, association rate constant; k_d, dissociation rate constant.

Binding Partner	k_a (M^{-1} s^{-1})	k_d (s^{-1})	k_D (M)	Fit (χ^2)
PI3P	$2.4 \pm 0.8 \times 10^{5}$	$2.7 \pm 1.3 \times 10^{-2}$	1.1×10^{-7}	12.8

CHAPTER IV: Secondary structure and ^{1}H, ^{13}C, ^{15}N resonance assignments of the Tollip CUE domain

Hugo F. Azurmendi [1], Sharmistha Mitra [2], Iriscilla Ayala [2]

Liwu Li [3], Carla V. Finkielstein [4] and Daniel G.S. Capelluto [2,*]

[1] Department of Chemistry, [2] Protein Signaling Domains Laboratory, Department of Biological Sciences, [3] Laboratory of innate immunity and inflammation and [4]Integrated Cellular Responses Laboratory, Department of Biological Sciences, Virginia Polytechnic Institute and State University,

Blacksburg, VA 24061, USA

Running Title: Structural studies of the Tollip CUE domain

[*] To whom correspondence should be addressed.

Tel: + (540) 231-0974; Fax: (540) 231-3414

E-mail: capellut@vt.edu

The paper was published in *Mol Cells* in the year 2010 and reproduced with permission from author(s), 2011, *Mol Cells* 30, 581-585.

CONTRIBUTON TO THE PROJECT

In this short project we identified the resonance assignments of the Tollip CUE domain, which later was used, in my thesis to structurally characterize the binding between CUE domain and ubiquitin. I prepared the construct of Tollip CUE domain, purified protein, performed SEC and CD study of the protein and provided guidance to Iriscilla Ayala to perform the cross-linking experiment.

ABSTRACT

The Toll-interacting protein (Tollip) is a negative regulator of the Toll-like receptor (TLR)-mediated inflammation response. Tollip is a modular protein that contains an N-terminal Tom1-binding domain, a central conserved domain 2 (C2) and a C-terminal coupling of ubiquitin binding to endoplasmic reticulum degradation (CUE) domain. Here, we report the sequence-specific backbone ^{1}H , ^{15}N, and ^{13}C assignments of the human Tollip CUE domain. The CUE domain was found to be a stable dimer as determined by size-exclusion chromatography and molecular cross-linking studies. Analysis of the backbone chemical shift data indicated that the Tollip CUE domain exhibits three helical elements corresponding to 52% of the protein backbone. Circular dichroism spectrum analysis confirmed the helical nature of this domain. Comparison of the location of these helical regions with those reported for yeast CUE domains suggest differences in length for all helical elements. We expect the structural analysis presented here will be the foundation for future studies on the biological significance of the Tollip CUE domain, its molecular interactions and the mechanisms that modulate its function during the inflammatory response.

INTRODUCTION

Microbial sensing pathways are used by the vertebrate immune system to activate microbial defense mechanisms. There are two categories of immunity in vertebrates, innate and adaptive, which protect the host from infections. Whereas innate immunity detects invariant forms of microorganisms, the adaptive immunity is specific and is mediated by antigen receptors found at the surface of T and B lymphocytes (Iwasaki and Medzhitov, 2010). The Toll-like receptor (TLR) are the best-studied group of innate immunity receptors in detecting invading pathogens by what is referred to as pathogen-associated molecular patterns (PAMPs) (Iwasaki and Medzhitov, 2010). There are at least ten human TLR family members, each specific to a particular PAMP. These TLRs are localized in different subcellular compartments including the plasma membrane, endosomes, lysosomes and endolysosomes (Barton and Kagan, 2009). All members share the same modular architecture; i) an extracellular leucine-rich repeats-containing ectodomain region, which mediates the contact with PAMPs, ii) a transmembrane region and iii) a cytosolic tail that contains tandems of intracellular Toll-interleukin 1 (IL-1) receptor domains required for downstream signaling (Barton and Kagan, 2009). Although the mechanisms that triggers that TLR signaling is unknown, subsequent events results in the recruitment of one or more adaptor proteins, a process mediated by the cytosolic tail of TLRs. Downstream events promotes the activation of kinases including IL-1

receptor-associated kinases (IRAKs) 1, 2, M, and 4 that act upon their transcription targets to influence the expression of genes involved in the innate immune response (Gan and Li, 2006).

The Toll-interacting protein (Tollip) negatively regulates TLR signaling by interacting directly with IRAK proteins (Zhang and Ghosh, 2002). The current model proposes that, in resting cells Tollip associates to and prevents IRAK activation by autophosphorylation. After TLR activation, IRAK autophosphorylates and phosphorylates Tollip (Zhang and Ghosh, 2002), thus, releasing IRAK for signaling (Burns et al., 2000).

Tollip is modular in nature containing an N-terminal Tom1-binding domain (TBD), a central conserved domain 2 (C2) and a C-terminal coupling of ubiquitin binding to endoplasmic reticulum degradation (CUE) domain (Burns et al., 2000). Tollip has been shown to selectively bind to phosphatidylinositol-3-phosphate and phosphatidylinositol-3,4,5-triphosphate (Li et al., 2004), most likely through its C2 domain. The CUE domain is a mono-ubiquitin-binding domain (Shih et al., 2003), which is found in proteins of trafficking pathways. Interestingly, the Tollip CUE domain is phosphorylated by activated IRAK proteins (Zhang and Ghosh, 2002). Homologous CUE domains exhibit distinct features that establish the oligomerization state of relevance for ubiquitin binding. The tertiary structure of the yeast Vps9p CUE domain reveals a dimeric helical structure enclosed around ubiquitin (Prag et al., 2003). Unlike Vps9p CUE, the CUE2-1 domain

of the yeast Cue2 protein exhibits a monomeric structure and forms tights heterodimers with ubiquitin (Kang et al., 2003).

Here we report the first structural analysis of a mammalian CUE domain, including its oligomeric state, sequence-specific backbone resonance assignments, secondary structure prediction, and homology modeling of the human Tollip CUE domain. Finding from our work will help to elucidate the regulatory role of Tollip domains in modulating intracellular signaling.

MATERIAL AND METHODS

Cloning, expression and purification of the Tollip CUE domain

The human Tollip CUE domain cDNA (residues 219-272) was cloned into a pGEX6P1 vector (GE Healthcare) and expressed in *E. coli* (Rosetta; Stratagene). Cells were grown in Luria-Bertani media at 37ºC until they reached an optical density of ~0.8. Induction of the glutathione S-transferase (GST)-Tollip CUE domain fusion protein resulted from the addition of 1 mM isopropyl thio-β-D-thiogalactopyranoside followed by 4 h incubation at 25ºC. Cell pellets were suspended in cold buffer containing 50 mM Tris-HCl (pH 7.3), 500 mM NaCl, 500 mM benzamidine, 0.1 mg/mL lysozyme, 5 mM DTT and 0.1% Triton-X-100. Pellets were further processed by sonication, centrifuged and the supernatants were loaded onto a Glutathione Sepharose 4B (GE Healthcare) column. The GST tag was removed by incubation of the fusion protein with prescission protease (GE Healthcare; 0.04 U/µg protein) overnight

at 4°C. The CUE domain was collected in a buffer containing 20 mM Tris-HCl (pH 8), 500 mM NaCl, concentrated using a 3 kDa cut-off concentrator device (Millipore) and further purified by FPLC using a size-exclusion chromatography column (Superdex 75; GE Healthcare) equilibrated with 50 mM Tris-HCl (pH 8), 1 M NaCl and 1 mM DTT. Protein peak fractions were pooled, exchanged in 20 mM sodium phosphate buffer (pH 7) and further concentrated for structural analysis.

Chemical cross-linking

Chemical cross-linking of the Tollip CUE domain was performed in the presence of bis(sulfosuccinimidyl) suberate (BS^3) as described (Capelluto et al., 2002). Briefly, protein (10 μM) was incubated with fresh BS^3 (1 mM) in 100 mM HEPES (pH 7.5) for 1 h at room temperature. Reactions were stopped by the addition of Laemmli buffer. Samples were resolved by SDS-PAGE and visualized using Coomassie Blue staining.

NMR spectroscopy

NMR samples containing 1 mM of uniformly ^{15}N,^{13}C-labeled Tollip CUE domain were prepared in 90%H_2O/10% ^2H_2O, and 20 mM sodium phosphate (pH 7). Triple-resonance experiments were acquired at 25°C using a Bruker Avance III 600 MHz spectrometer (Virginia Polytechnic Institute and State University) equipped with an inverse detected TXI probe with z-axis pulse field gradients. ^1H chemical shifts were referenced using sodium 4,4-dimethyl-4-silapentane-1-sulfonate (500 mM) as an internal reference. Sequential assignments of the backbone ^1H, ^{13}C,

and ^{15}N resonances were made from ^{1}H, ^{15}N-HSQC, CBCA(CO)NNH, HNCACB and HNCO experiments (Grzesiek et al., 1993; Kay et al., 1993; Muhandiram and Kay, 1994). All spectra were processed in NMRpipe (Delaglio et al., 1995), and ^{1}H, ^{13}C, ^{15}N resonance assignments were determined using the CCPNMR package (Vranken et al., 2005). The secondary structure of the protein was derived from the backbone dihedral angles Φ and Ψ predicted using the DANGLE algorithm (Cheung et al., 2010).

Circular dichroism spectroscopy

Far-UV CD spectra were recorded on a Jasco J-720 spectropolarimeter. Experiments were carried out in a 1 mm path length quartz cell at 20°C. The Tollip CUE domain (5 μM) was in 20 mM sodium phosphate (pH 7). Spectra were obtained from five accumulated scans from 190 to 260 nm using a bandwidth of 1 nm and a response of 4 sec at a scan speed of 20 nm/min. Spectra were deconvoluted to estimate secondary structure content with the online server DICHROWEB (Whitmore and Wallace, 2004) using the CDSSTR algorithm (Sreerama and Woody, 2004).

RESULTS AND DISCUSSION

The C-terminal Tollip CUE domain (Fig. 4.1A) exhibits an excellent resonance dispersion in the ^{15}N,^{1}H heteronuclear single quantum coherence (HSQC) spectrum (Fig. 4.1B), which indicates that protein is folded at the NMR scale. The number of resonances in the HSQC spectrum are expected for a single conformation of the protein. Size-exclusion chromatography analysis

suggests that the human Tollip CUE domain is a stable dimer with a calculated molecular mass of 15.5 kDa (Fig. 4.2A). We also estimated the hydrodynamic dimensions of the Tollip CUE domain as a probe for elucidating compactness of its tertiary structure (Uversky, 1993). The corresponding calculated Stokes radius for an apparent mass of 15.5 kDa is 19.6 ± 0.1 Å. This value is close for the predicted Stokes radius of a globular CUE domain (13.2 kDa) that is calculated to be 18.5 ± 0.2 Å. The dimeric state of the Tollip CUE domain was further confirmed by cross-linking of the monomers of the protein with BS^3 (Fig. 4.2B), a chemical cross-linker that covalently interacts with primary amines that are 11 Å apart. The stable dimeric conformation of the Tollip CUE domain is contrast to the observed monomer-dimer equilibrium of the yeast Vps9p CUE domain (Prag et al., 2003). The appearance of Vps9p dimer organization, which can be applied to the human Tollip CUE domain, is suggested to be as a result of domain swapping (Liu and Eisenberg, 2002), in which the helix 3 of the dimeric CUE domains are exchanged between monomers (Prag et al., 2003). Findings show that the dimeric form of Vps9p CUE domain exhibits a 1,000-fold increase in binding affinity to ubiquitin when compared to the monomeric conformation. This event likely results from the direct interaction of the ligand with helix 2 of the Vpsp9 CUE domain, a structural feature that only arises as a result of dimer formation. Accordingly, mutation within helix 2, i.e., Leu427, results in a protein that is incapable of binding to ubiquitin and, thus, establishes the relevance of the oligomeric state for Vps9p activity (Prag

et al., 2003). The Vps9p/ubiquitin complex is required for efficient transport of the α-factor receptor (Ste3p) from the plasma membrane to the vacuolar compartments, where it is degraded (Davies et al., 2003). Likewise, the Tollip CUE domain is necessary for endosomal IL-1 receptor degradation (Brissoni et al., 2006), although the requirement of ubiquitin for this process remains to be investigated.

One hundred percent of ^{1}HN and ^{15}N of the backbone amide resonances of the protein (excluding the five Pro residues) were assigned (Fig. 4.1B and Table 4.1). In addition, 87% of carbonyls, 97% of Cα and 97% of Cβ resonances were assigned. On the basis of resonance assignments, three helical regions were defined in the Tollip CUE domain (Fig. 4.3A). The helices correspond to residues Glu231-Asp239 (helix 1), Gln246-Ala255 (helix 2) and Lys260-Gln269 (helix 3). Comparison among CUE domains found in yeast Vps9p and Cue2 proteins (Kang et al., 2003; Prag et al., 2003) indicate that helix 1 is shorter in the human Tollip CUE domain. Furthermore, the Tollip CUE domain exhibits a larger helix 2 and a shorter helix 3 when specifically compared with the Vps9p CUE domain secondary structure (Figs. 4.3A and 4.4A). From our analysis, the Met-Phe-Pro and Leu-Leu hydrophobic motifs, responsible for ubiquitin binding, are expected to be located in a loop after helix 1 and at the end of helix 3 respectively (Fig 4.3A). The far-UV circular dichroism spectrum of the Tollip CUE domain exhibits two minima at 208 and 222 nm and a positive signal at ~190 nm (Fig. 4.3B), indicative of helical structure. Prediction of the secondary structure composition shows

that the Tollip CUE domain contains 59% helical structure, in close agreement with the NMR data (52 %; Fig. 4.3A). The presence of three helix bundles in CUE domains suggest that they share structural similarities with a 40-amino acid length ubiquitin-binding ubiquitin associated (UBA) domain (Prag et al., 2003), which also binds monoubiquitin but exhibits a greater affinity for polyubiquitins (Bertolaet et al., 2001; Wilkinson et al., 2001). Remarkably, Vps9p CUE domain also binds polyubiquitin *in vitro* (Shih et al., 2003).

An attempt to define the three dimensional structure of the Tollip CUE domain led to the structural determination of a domain fragment (PDB: 1WGL), albeit backbone resonance assignments of the protein were not reported. Despite the lack of information, there is a strong agreement with respect to the position of the secondary structure elements in the Tollip CUE domain and those predicted based on our NMR chemical shift data. An in depth analysis of the 1WGL tertiary structure reveals unstructured regions located at the N- and C-termini, which we believe result from the presence of seven and six additional residues translated from the vector, respectively, and that represent more than 20% of the protein domain. Instead we have performed homology modeling of the Tollip CUE using the Vps9p CUE domain as a template, a decision based on the sequence homology (23% identity) and functional similarities found in there two proteins. The homology modeling rendered an easy superimposition of the backbones of both proteins, with helices 2 and 3 antiparallel to helix 1 (Fig. 4.4B). Superimposed structures aid the

visualization of areas of sequence conservation, such as the Met-Phe-Pro and Leu-Leu motifs located at the end of helix 1 and helix 3, respectively (Fig. 4.4B) and, thus, help to infer possible configurations of the protein-ligand complexes.

We envision using the collective data from NMR resonance assignments and homology modeling to precisely define the Tollip CUE domain molecular interactions and kinetic properties with other binding partners, *i.e.,* IRAK (Burns et al., 2000), to further understand how these associations modulate TLR responses. An advantage of two-dimensional NMR chemical shift mapping over other well characterized approaches relies in its utmost importance for the identification of yet uncharacterized ligand binding regions while depicting molecular interactions (Pellecchia, 2005). As we show here, this technique relies on ligand binding to an ^{15}N- or ^{13}C-labeled protein, an event that leads to shifting or broadening in some cases, of specific backbone resonances of protein. Thus identifying the NMR chemical shift fingerprint of the Tollip CUE domain opens the possibility of mapping the binding site, and determining the stoichiometry and the kinetic and affinity values for even weak and transient ligand-binding events.

TABLES AND FIGURES

Table 4.1 Chemical shifts of $^{1}H_{N}$, ^{15}N, ^{13}CO, $^{13}C\alpha$ and $^{13}C\beta$ of the Tollip CUE domain. All chemical shifts were referenced relative to the frequency of the methyl proton resonance of DSS. ND: not detected

Residue	^{1}HN	^{15}N	^{13}CO	$^{13}C\alpha$	$^{13}C\beta$
219Pro			ND	ND	ND
220Pro			ND	63.01	31.95
221Ala	8.33	124.10	177.32	52.39	19.40
222Ala	8.26	123.37	177.65	52.21	19.42
223Val	8.08	119.13	175.79	62.55	32.71
224Asn	8.43	121.92	174.45	53.16	38.96
225Ala	8.18	124.47	177.09	52.39	19.50
226Gln	8.29	120.72	ND	53.88	29.02
227Pro			176.52	63.04	32.16
228Arg	8.58	121.69	175.86	56.15	31.43
229Cys	8.37	118.79	173.84	57.84	28.65
230Ser	9.08	119.85	175.45	57.54	64.19
231Glu	9.05	126.29	178.62	59.59	29.37
232Glu	8.55	119.15	179.05	59.68	28.54
233Asp	7.75	121.55	177.46	57.49	40.47
234Leu	7.86	120.28	178.46	58.63	41.55
235Lys	7.94	118.61	177.88	59.14	32.24
236Ala	7.77	120.17	180.91	55.02	18.28
237Ile	8.09	117.74	178.11	65.42	37.64
238Gln	8.63	121.07	178.29	59.42	28.90
239Asp	8.07	116.32	177.82	56.62	40.54
240Met	7.36	118.05	175.26	57.60	34.11
241Phe	7.57	116.90	ND	55.47	39.72
242Pro			ND	64.99	32.20
243Asn	8.75	114.74	175.11	53.15	38.65
244Met	7.69	120.64	175.13	54.99	34.10
245Asp	8.60	124.09	177.34	54.41	42.63
246Gln	8.96	125.79	177.61	59.84	28.83
247Glu	8.91	118.84	179.58	59.12	28.92
248Val	7.43	121.94	177.84	65.99	31.64
249Ile	7.40	119.90	177.01	66.08	37.52
250Arg	8.26	118.02	177.91	60.20	30.00
251Ser	7.96	114.04	177.41	61.65	62.90
252Val	8.27	124.16	177.54	66.57	31.59
253Leu	8.46	121.28	179.27	58.80	41.80
254Glu	8.45	118.39	180.66	59.66	29.46
255Ala	8.31	125.02	179.51	55.14	18.18
256Gln	7.78	113.59	175.73	53.95	26.74
257Arg	8.16	117.32	176.41	56.85	27.00
258Gly	8.69	104.00	173.24	45.75	
259Asn	7.38	118.85	173.94	53.13	38.98
260Lys	8.64	128.99	176.72	60.39	32.70
261Asp	8.17	118.44	178.55	57.89	40.35
262Ala	7.95	122.51	180.68	54.49	18.44
263Ala	8.30	121.45	178.34	55.37	18.57
264Ile	8.56	118.96	177.09	66.91	38.35
265Asn	7.86	116.27	177.78	57.02	38.41
266Ser	7.96	115.31	176.96	62.18	63.35
267Leu	8.25	123.21	179.66	57.99	41.05
268Leu	8.40	119.98	179.40	57.64	42.31
269Gln	7.57	116.78	177.17	57.24	28.77
270Met	7.62	118.75	176.74	57.45	33.25
271Gly	7.97	107.64	173.76	45.42	
272Glu	7.97	120.00	176.11	56.27	30.72
273Glu	8.33	123.36	ND	54.36	29.73
274Pro			ND	ND	ND

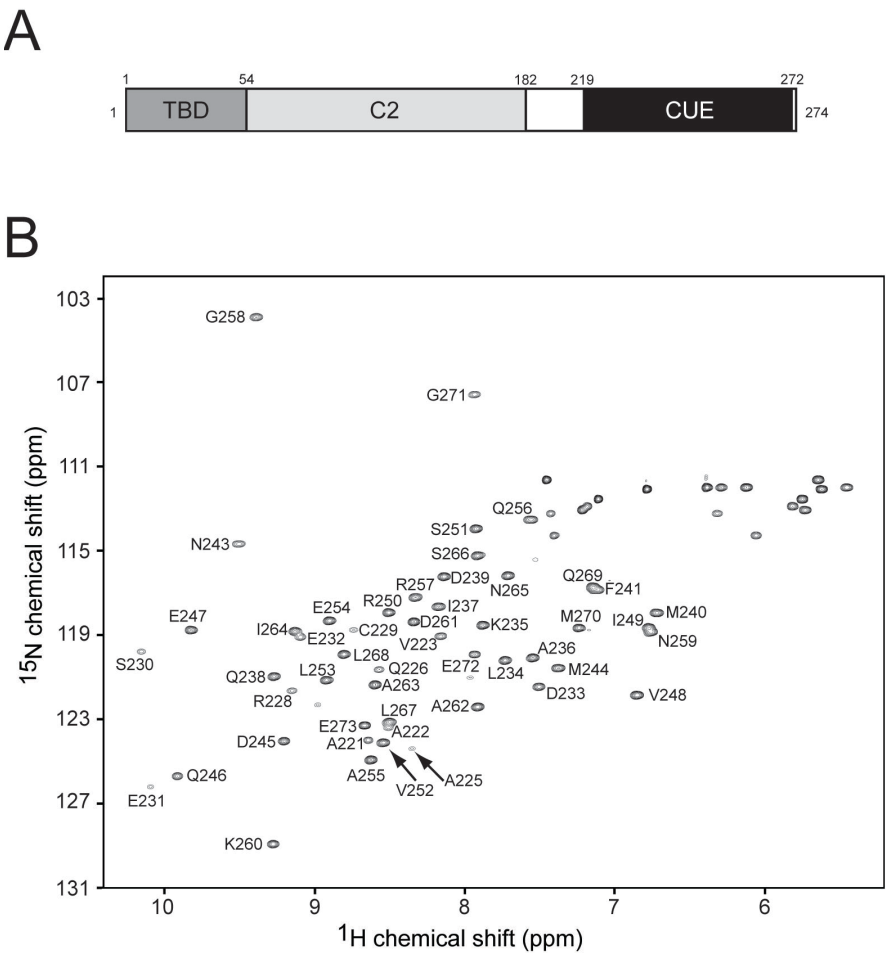

Fig 4.1 (A) Schematic representation of Tollip primary structure showing the location of the Tom-binding domain (TBD), C2 and CUE domains in the protein. (B) Two-dimensional ^{15}N, ^{1}H HSQC spectrum of the human Tollip CUE domain. Selected resonances are labeled with the corresponding residue numbers found in Tollip

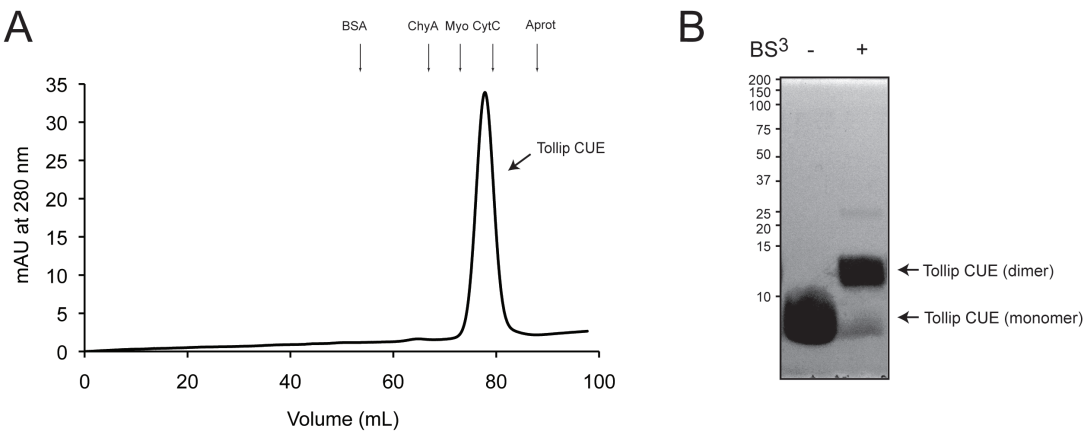

Fig 4.2 Oligomeric state of the Tollip CUE domain. (A) Size-exclusion chromatography (Superdex 75) of the purified Tollip CUE domain. Protein standards were as follows: bovine serum albumin (BSA, 67 kDa), chymotrypsinogen A (ChyA, 25 kDa), myoglobin (Myo, 17 kDa), cytochrome C (CytC, 12.5 kDa), and aprotinin (Aprot, 6.5 kDa). Arrows indicate the elution volume of each molecular mass marker. (B) Molecular cross-linking with BS^3 of the purified CUE domain. Samples were resolved by SDS-PAGE and visualized using Coomassie Blue staining

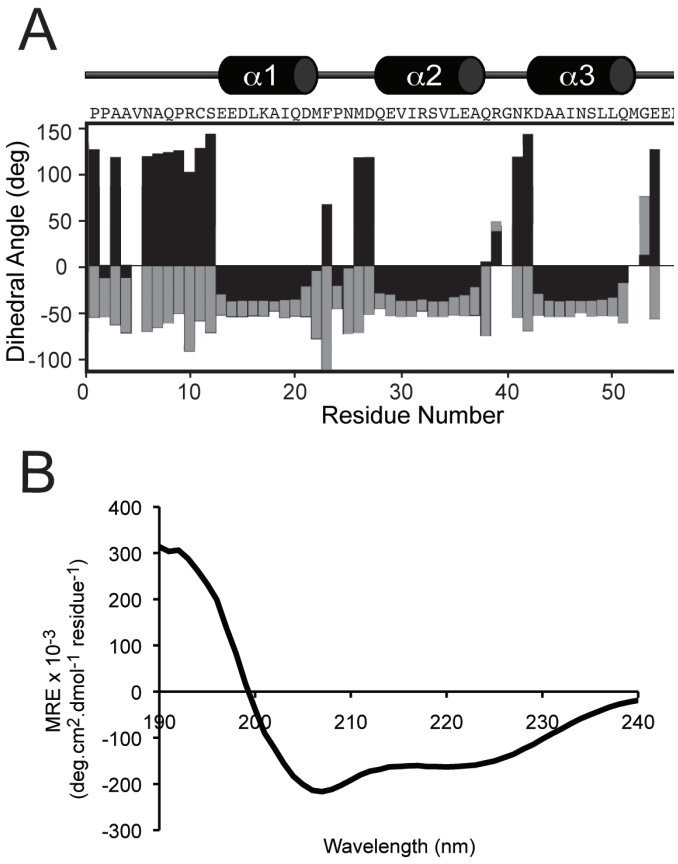

Fig 4.3 Secondary structure analysis of the Tollip CUE domain. (A) Prediction of the secondary structural elements of the protein based on the backbone dihedral angles as a function of the Tollip residue number. Gray bars represent prediction of ϕ angles, whereas black bars represent ψ angles. Predicted secondary structural elements of the Tollip CUE domain are depicted on top. (B) Far-UV circular dichroism spectrum of the Tollip CUE domain

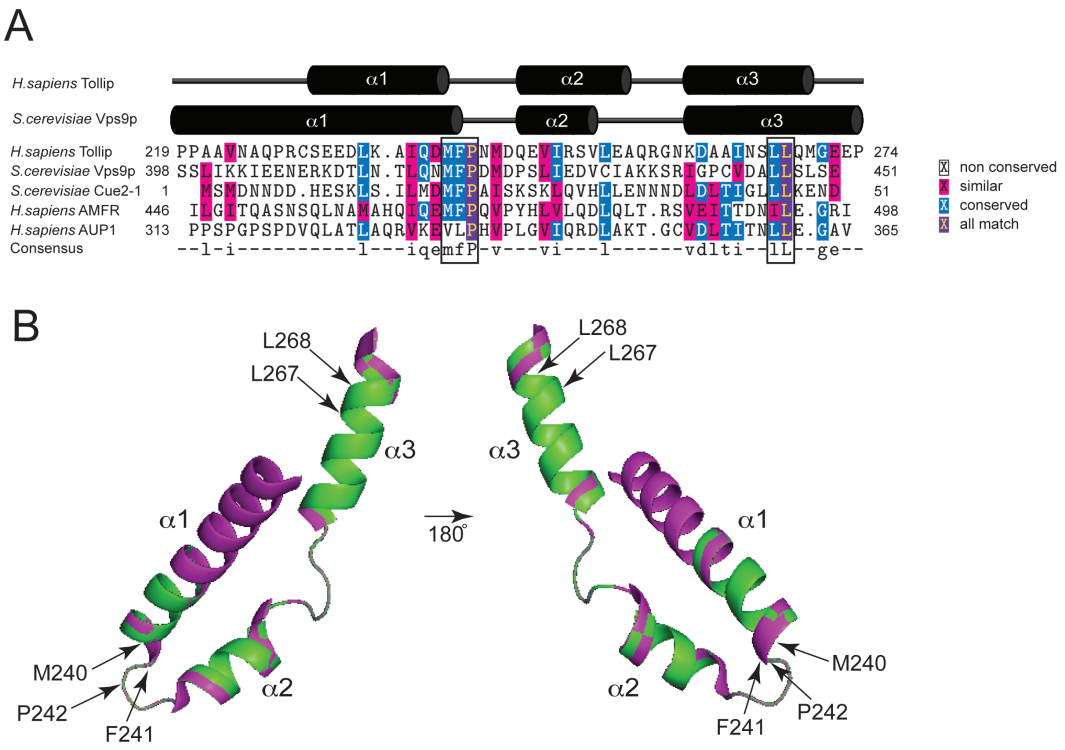

Figure 4.4 Sequence conservation and structural properties of CUE domains. (A) Sequence alignment of CUE domains of human Tollip (GenBank: CAG38508), yeast Vps9p (GenBank: AAC49314), yeas Cue-2-1 (GenBank: P36075), human autocrine motility factor receptor (AMFR; GenBank: NP_001135), and human ancient ubiquitous protein 1 (AUP1; GenBank: AAH33646) reproduced from the Biology WorkBench database (http://workbench.sdsc.edu). Boxes indicate the conserved ubiquitin binding motifs found in yeast CUE domains. Secondary structures of Tollip CUE domain, determined from chemical shifts, and Saccharomyces cerevisiae Vps9p CUE domain are depicted above sequences. (B) Two views of the super-imposed structures of Tollip CUE domain (green) and Vps9p (magenta). Human Tollip CUE domain structure was modeled based on

sequence homology to Vps9p using AL2TS (http://proteinmodel.org/AL2TS/al2ts.html) and depicted using Pymol. Ubiquitin binding residues, determined in yeast Vps9p CUE domain, are indicated on the structures

ACKNOWLEDGEMENT

This work was supported by the National Science Foundation CAREER Award (844491) (C.V.F.) and the American Heart Association grant (086077E) (D.G.S.C.). We are thankful to Dr. Janet Webster for her invaluable assistance during manuscript preparation.

REFERENCES

Barton, G.M., and Kagan, J.C. (2009). A cell biological view of Toll-like receptor function: regulation through compartmentalization. Nat Rev Immunol *9*, 535-542.

Bertolaet, B.L., Clarke, D.J., Wolff, M., Watson, M.H., Henze, M., Divita, G., and Reed, S.I. (2001). UBA domains of DNA damageinducible proteins interact with ubiquitin. Nat. Struct. Biol. **8**, 417-422.

Brissoni, B., Agostini, L., Kropf, M., Martinon, F., Swoboda, V., Lippens, S., Everett, H., Aebi, N., Janssens, S., Meylan, E., et al. (2006). Intracellular trafficking of interleukin-1 receptor I requires Tollip. Curr. Biol. 16, 2265-2270.

Burns, K., Clatworthy, J., Martin, L., Martinon, F., Plumpton, C., Maschera, B., Lewis, A., Ray, K., Tschopp, J., and Volpe, F. (2000). Tollip, a new component of the IL-1RI pathway, links IRAK to the IL-1 receptor. Nat Cell Biol *2*, 346-351.

Capelluto, D.G., Kutateladze, T.G., Habas, R., Finkielstein, C.V., He, X., and Overduin, M. (2002). The DIX domain targets dishevelled to actin stress fibres and vesicular membranes. Nature *419*, 726-729.

Cheung, M.S., Maguire, M.L., Stevens, T.J., and Broadhurst, R.W. (2010). DANGLE: A Bayesian inferential method for predicting protein backbone dihedral angles and secondary structure. J Magn Reson Ser B *202*, 223-233.

Davies, B.A., Topp, J.D., Sfeir, A.J., Katzmann, D.J., Carney, D.S., Tall, G.G., Friedberg, A.S., Deng, L., Chen, Z., and Horazdovsky, B.F. (2003). Vps9p CUE domain ubiquitin binding is required for efficient endocytic protein traffic. J. Biol. Chem. 278, 19826-19833.

Delaglio, F., Grzesiek, S., Vuister, G.W., Zhu, G., Pfeifer, J., and Bax, A. (1995). NMRpipe - a multidimensional spectral processing system based on Unix pipes. J Biomol NMR *6*, 277-293.

Gan, L., and Li, L. (2006). Regulations and roles of the interleukin-1 receptor associated kinases (IRAKs) in innate and adaptive immunity. Immunol Res *35*, 295-302.

Grzesiek, S., Anglister, J., and Bax, A. (1993). Correlation of Backbone Amide and Aliphatic Side-Chain Resonances in C-13/N-15-Enriched Proteins by Isotropic Mixing of C-13 Magnetization. Journal of Magnetic Resonance Series B *101*, 114-119.

Iwasaki, A., and Medzhitov, R. (2010). Regulation of adaptive immunity by the innate immune system. Science 327, 291-295.

Kang, R.S., Daniels, C.M., Francis, S.A., Shih, S.C., Salerno, W.J., Hicke, L., and Radhakrishnan, I. (2003). Solution structure of a CUE-ubiquitin complex reveals a conserved mode of ubiquitin binding. Cell *113*, 621-630.

Li, T., Hu, J., and Li, L. (2004). Characterization of Tollip protein upon

Lipopolysaccharide challenge. Mol Immunol *41*, 85-92.

Liu, Y., and Eisenberg, D. (2002). 3D domain swapping: as domains continue to swap. Protein Sci *11*, 1285-1299.

Muhandiram, D.R., and Kay, L.E. (1994). Gradient-Enhanced Triple-Resonance 3-Dimensional Nmr Experiments with Improved Sensitivity. Journal of Magnetic Resonance Series B *103*, 203-216.

Pellecchia, M. (2005). Solution nuclear magnetic resonance spectroscopy

techniques for probing intermolecular interactions. Chem. Biol. 12, 961-971.

Prag, G., Misra, S., Jones, E.A., Ghirlando, R., Davies, B.A., Horazdovsky, B.F., and Hurley, J.H. (2003). Mechanism of ubiquitin recognition by the CUE domain of Vps9p. Cell *113*, 609-620.

Shih, S.C., Prag, G., Francis, S.A., Sutanto, M.A., Hurley, J.H., and Hicke, L. (2003). A ubiquitin-binding motif required for intramolecular monoubiquitylation, the CUE domain. EMBO J *22*, 1273-1281.

Sreerama, N., and Woody, R.W. (2004). Computation and analysis of protein circular dichroism spectra. Methods Enzymol *383*, 318-351.

Uversky, V.N. (1993). Use of fast protein size-exclusion liquid chromatography to study the unfolding of proteins which denature through the molten globule. Biochemistry *32*, 13288-13298.

Vranken, W.F., Boucher, W., Stevens, T.J., Fogh, R.H., Pajon, A., Llinas, M., Ulrich, E.L., Markley, J.L., Ionides, J., and Laue, E.D. (2005). The CCPN data

model for NMR spectroscopy: development of a software pipeline. Proteins *59*, 687-696.

Whitmore, L., and Wallace, B.A. (2004). DICHROWEB, an online server for protein secondary structure analyses from circular dichroism spectroscopic data. Nucleic Acids Res *32*, W668-673.

Wilkinson, C.R., Seeger, M., Hartmann-Petersen, R., Stone, M., Wallace, M., Semple, C., and Gordon, C. (2001). Proteins containing the UBA domain are able to bind to multi-ubiquitin chains. Nat. Cell Biol. **3**, 939-943.

Zhang, G., and Ghosh, S. (2002). Negative regulation of toll-like receptor-mediated signaling by Tollip. J Biol Chem *277*, 7059-7065.

CHAPTER V: Ubiquitin Interacts with the Tollip C2 and CUE Domains and Inhibits Tollip's Phosphoinositide Binding

Sharmistha Mitra, C. Alicia Traughber, Stephanie Gomez, and Daniel G. S. Capelluto

Keywords: Tollip; ubiquitin; C2 domain; CUE domain; phosphoinositides; endosome; membrane trafficking; nuclear magnetic resonance

The paper has been submitted to *J. Biol. Chem* and is under review

CONTRIBUTION TO THE PROJECT

This is the main project pertaining to my thesis that established the role of ubiquitin as a modulator of Tollip's function. Here, I identified Tollip C2 domain as a novel UBD, biophysically characterized the ubiquitin binding properties of the protein and established the role of ubiquitin in controlling the oligomeric state of Tollip C-terminal domain. I performed all the work pertaining to this project including preparing of the DNA constructs, purifying the proteins, the experiments and analysis of NMR, SPR, CD, LPOA study, analysis of AUC data and provided guidance to Alicia Traughber and Stephanie Gomez to perform LPOA and SEC experiments respectively.

ABSTRACT

A large number of cellular signaling processes are directed through internalization of polyubiquitinated cargo proteins via endocytosis. Tollip is an adaptor protein that facilitates endosomal cargo sorting for lysosomal degradation. Tollip preferentially binds phosphatidylinositol 3-phosphate (PtdIns(3)P) via its C2 domain, an association that may be required for endosomal membrane targeting. Here we show that Tollip binds ubiquitin through its C2 and CUE domains and that the association to the C2 domain inhibits PtdIns(3)P binding. NMR analysis demonstrates that the C2 and CUE domains bind to overlapping binding sites on ubiquitin, suggesting that two ubiquitin molecules associate with Tollip simultaneously. Hydrodynamic studies reveal that ubiquitin forms heterodimers with the CUE domain, indicating that the association disrupts CUE's dimeric state. We propose that, in the absence of polyubiquitinated cargo, ubiquitin's dual binding partitions Tollip into membrane-bound and membrane-free states, a function that contributes to Tollip's engagement in both membrane trafficking and cytosolic pathways.

INTRODUCTION

Post-translational modification of proteins, including phosphorylation, glycosylation, lipidation, acetylation, and methylation, represents key mechanisms that cells use to respond to environmental changes and to modulate protein function. An additional layer of protein regulation is the covalent attachment of ubiquitin to proteins, a process called ubiquitination. Although ubiquitination commonly signals for protein degradation by the proteasome machinery, it can also lead to other nondegradative pathways, including DNA repair, cellular trafficking, chromatin remodeling, and immune responses (1). Ubiquitin is a 76-amino acid globular protein that can be attached as a single unit (monoubiquitination), conjugated to multiple sites in the target protein (multi-monoubiquitination), or attached as a polyubiquitin chain. Monoubiquitination leads to the conjugation of a single ubiquitin molecule onto one or more lysine residues on the target protein' surface. Polymerization of ubiquitin occurs by conjugation of any of the ξ-amino groups on the seven surface lysine residues or the N-terminal methionine to the C-terminal glycine (2). In addition, ubiquitin is recognized by ubiquitin-binding domains (also known as ubiquitin receptors), which translate ubiquitinated target signals into cell signaling cascades. Over twenty distinct ubiquitin-binding domains associate noncovalently with ubiquitin moieties with affinities in the micromolar range (1), which can be explained by the fact that intracellular ubiquitin concentration can be as high as 85 μM (3). The majority of the ubiquitin-binding domains bind to ubiquitin through a hydrophobic patch in which ubiquitin's Leu8, Ile44, and Val70 residues play critical roles (4). Ubiquitin-binding domains are structurally classified in α-helical, zinc-fingers,

pleckstrin-homology folds, and ubiquitin-conjugating-like domains (1). The coupling of ubiquitin conjugation to endosomal reticulum degradation (CUE), GGA and Tom1 (GAT), and Vps27/Hrs/Stam (VHS) domains belong to the helical subfamily of ubiquitin-binding domains (1). Despite the fact that the ubiquitin backbone is rigid (with the exception of its C-terminus), association of ubiquitin-binding domains lead to conformational changes in ubiquitin (5). Ubiquitin-binding domains display more selectivity and bind more tightly to certain types of polyubiquitinated chains, in which these polymers can adopt packed or extended conformations depending on what lysine residues link ubiquitin chains (reviewed in (1)). Several ubiquitin-binding domains have been shown to mediate intramolecularubiquitination, leading to a ubiquitin-binding domain-containing protein conformation that exhibits altered function and localization and likely alters its interactions with ubiquitinated cargo during endosomal trafficking (reviewed in (6)).

To control cellular processes, cells dampen signaling through a broad range of mechanisms including cargo internalization. The mechanism of cargo removal includes its internalization by endocytosis, followed by ubiquitin-mediated delivery to early endosomes, where cargo sorting takes place (7). Cargo is further sorted into intralumenal vesicles of late endosomes/multivesicular bodies (MVBs). Alternatively, some cargo is retrieved from this pathway. Once all the retrieved molecules have been removed, late endosomes/MVBs fuse with lysosomes leading to cargo degradation in the vesicular lumen (8). Adaptor proteins regulate protein sorting by interacting with

different macromolecules at the surface of endosomal membranes. The function of many adaptor proteins is associated with their ubiquitin-binding domains, ensuring the precise sorting of ubiquitinated cargo proteins inside the intralumenal endosomal vesicles. One of these adaptor proteins is Tollip, which is involved in protein sorting by association with Tom1, ubiquitin, and clathrin (9). Tollip is primary localized on early endosomes where it is required for degradation of ubiquitin-conjugated cargo (10), including sorting of the interleukin-1 receptor (IL-1R) (11) and the transforming growth factor receptor-β type I receptor (12) for their degradation. Tollip also controls innate immune responses by regulating IL-1R-associated kinase-1 (IRAK-1) function in both the Toll-like receptor (TLR) and the IL-1R signaling pathways (10,13,14). By binding to IRAK proteins, Tollip indirectly regulates the function of transcription factors, such as nuclear factor (NF)-kB, to influence the expression of innate immune-related genes, such as those that codify for cytokines and interferons (15). Moreover, Tollip has been shown to be sumoylated and mediates IL-1R sumoylation (16), placing Tollip as a modulator of nuclear and cytoplasmic protein trafficking. Tollip is modular with a Tom1-binding domain (TBD), conserved 2 (C2), and CUE domains (17). The Tollip TBD associates with the Tom1 GAT domain to facilitate membrane trafficking (10). We have recently demonstrated that the C2 domain of Tollip preferentially binds phosphoinositides, particularly PtdIns(3)P and PtdIns(4,5)P_2 (18). Thus, Tollip likely acts in the recruitment of several proteins on the endosomes via PtdIns(3)P (for membrane trafficking) and the plasma membrane via PtdIns(4,5)P_2 (for TLR signaling regulation). The Tollip CUE domain is a ubiquitin-binding module (19) that has been shown to bind

to and be phosphorylated by IRAK proteins (14). As observed for the yeast Vps9p CUE domain (20), the human Tollip CUE domain forms tight dimers (21), which can contribute to Tollip oligomerization and ligand recognition. Most of the ubiquitin-binding domains mediate intramolecular interactions; however, it has not yet been demonstrated whether CUE domains exert such regulatory functions (6).

Here, we provide detailed structural insights into Tollip-ubiquitin complex formation. We demonstrate that ubiquitin binding to Tollip disrupts Tollip-phosphoinositide interactions. In addition to the Tollip CUE domain, we identify the Tollip C2 domain as a novel ubiquitin-binding domain. By comparison, Tollip C2 and CUE domains bind ubiquitin in partially overlapped sites with moderate affinity, with the Tollip C2 domain showing an extensive contact surface whereas the corresponding site for the CUE domain is mapped on an exposed hydrophobic patch around Ile44. Remarkably, we demonstrate that the dimeric Tollip CUE domain dissociates when bound to ubiquitin. Based on our findings, we propose that ubiquitin binds to two independent sites in Tollip, an association that leads to conformational change, dissociation of the Tollip CUE domain dimers, and direct inhibition of PtdIns(3)P ligation, leading to membrane release of adaptor protein complexes in the absence of polyubiquitinated cargo.

MATERIALS AND METHODS

Chemicals—1,2-dioleyl-sn-glycero-3 phosphocholine (PtdCho), 1,2-dipalmitoyl-sn-glycero-3-phosphoethanolamine (PtdEth), and phosphatidylinositol (PtdIns) were from Avanti Polar Lipids; PtdIns(3)P and PtdIns(4,5)P_2 were from Echelon Biosciences. All other chemicals were analytical reagent grade.

Cloning, Expression, and Purification of Tollip and Ubiquitin Constructs—The cloning, expression, and purification of human Tollip and the isolated C2 (residues 54-182) and CUE (residues 223-278) domains as GST-fusions and untagged proteins were carried out as we previously reported (18,21). The cDNA of human ubiquitin, cloned into the pET24d vector, was a generous gift from Dr. Julie Forman-Kay (University of Toronto). Site directed mutagenesis of Tollip CUE domain was performed using QuikChange (Stratagene). Ubiquitin constructs were expressed in *E. coli* Rosetta strain (Stratagene). Unlabeled proteins were generated in Luria-Bertani media, whereas ^{15}N-labeled proteins were produced in minimal media supplemented with $^{15}NH_4Cl$ (Cambridge Isotope Laboratory Inc.) as the source of nitrogen. Induction of the His-tagged fusion ubiquitin was performed by the addition of 1 mM IPTG to the bacterial cell culture at an OD of ~0.8 followed by a 2 h-incubation at 25°C. Cell pellets were suspended in ice-cold equilibrium buffer containing 50 mM sodium phosphate (pH 8), 300 mM NaCl, 0.1 mg/ml lysozyme, 1 mM β-mercaptoethanol, 1 mM leupeptin, 1 mM pepstatin, 8.6 μg/ml TPCK, 4.3 μg/ml TLCK, 0.15 μg/ml aprotinin, 0.1 % Triton X-100, 0.1 % Tween-20, and 0.1 % NP-40. Suspension was further processed by sonication and centrifugation and the

resulting supernatant was incubated with Talon metal affinity resin (Clontech). In some cases, fusion proteins were eluted off the beads by the addition of a buffer containing 50 mM sodium phosphate (pH 8), 1 M NaCl, and 200 mM imidazole. For untagged protein purifications, His-tag was removed by incubation of the fusion protein with TEV protease in buffer containing 50 mM sodium phosphate (pH 8), 100 mM NaCl, 10 % glycerol, 1 mM DTT, and 0.5 mM EDTA at room temperature for three days. Proteins were recovered in a buffer containing 50 mM sodium phosphate (pH 8), 300 mM NaCl, and 1 mM DTT, and concentrated using a 3-kDa-cut-off concentrator device (Millipore) and further purified by an AKTA FPLC system using a Superdex 30 column (GE Healthcare), previously equilibrated with 50 mM Tris-HCl (pH 8), 200 mM NaCl, and 1 mM DTT. Protein concentrations were calculated using the BCA method. Purity of proteins was over 95% as judged by SDS-PAGE and MALDI-TOF mass spectrometry analyses and by their identity using N-terminal sequencing (Tufts University, MA).

Liposome Preparation—Stocks of PtdIns(3)P, PtdCho, and PtdEth, were prepared in organic solvents using chloroform:methanol:water (65:35:8). PtdIns(3)P liposomes were prepared by weight ratio of 1:1 of PtdCho:PtdEth and 10% PtdIns(3)P. Control liposomes contained 1:1 of PtdCho:PtdEth. Lipid films were generated under a dessicator overnight and hydrated in 20 mM Tris-HCl (pH 6.8) and 100 mM NaCl to 1 mg/mL at 60ºC for 1h. Liposomes were sonicated, pelleted, and suspended at 2.5 mg/mL in the same buffer and then subjected to extrusion at 60ºC using 400 nm-membranes and immediately used for SPR experiments.

Lipid-protein Overlay Assay—Lipid strips were prepared by spotting 1 µl of the indicated amount of PtdIns(3)P dissolved in chloroform/methanol/water (65:35:8) onto Hybond-C extra membranes (GE Healthcare). Membrane strips containing the immobilized PtdIns(3)P were blocked with 3% (w/v) fatty-acid-free BSA (Sigma) in 20 mM Tris-HCl (pH 8.0), 1500 mM NaCl, and 0.1 % Tween-20 for 1 h at room temperature. In some cases, GST-fusion proteins were preincubated with two- to four-fold excess molar ratios of ubiquitin. Then, membranes were incubated with ubiquitin-free or protein-ubiquitin mixtures in the same buffer overnight at 4°C. Following four washes with the same buffer, bound proteins were probed with rabbit anti-GST antibody (Santa Cruz Biotechnology) and donkey anti-rabbit-horseradish peroxidase antibody (GE Healthcare). Protein binding was detected using Supersignal West Pico chemiluminescent reagent (Pierce).

SPR Analysis—The kinetics and affinity of protein-protein and protein-lipid interactions were determined using a BIAcore X100 instrument. For ubiquitin interactions, 200 nM of His-tagged ubiquitin (ligand) was immobilized using a $NiCl_2$-activated NTA sensor chip (GE Healthcare) surface and used as a ligand, whereas untagged Tollip CUE or C2 domains, or GST-Tollip were flown as analyte. The first flow cell of the sensor chip was used as a control surface (no protein), whereas the second flow cell was employed as the active surface. His-tagged ubiquitin, in a buffer containing 10 mM HEPES (pH 8.3), 150 mM NaCl, 0.005% Tween-20, 50 µM EDTA, and 1 mM NaN_3, was immobilized on

the surface of one flow cell of the sensor chip. A range of concentrations of protein analytes prepared in the same buffer was injected on both flow cell surfaces at a flow rate of 30 μl/min. Association and dissociation times for each protein injection were set at 120 and 600 s, respectively. The remaining bound protein was washed away by the injection of 30 μl of 10 mM HEPES (pH 8.3), 150 mM NaCl, 0.005% Tween-20, 350 mM EDTA, and 1 mM NaN_3. Tollip-PtdIns(3)P interactions were followed using PtdIns(3)P-free and -enriched liposomes as ligands and GST-Tollip as an analyte similar to what we previously described (18). In all cases, sensorgrams were obtained from eight different concentrations of each of the tested proteins. For the competition experiments, GST-Tollip (900 nM) was preincubated with increasing molar concentrations of untagged ubiquitin for 1 h at room temperature. Free and ubiquitin-bound GST-Tollip was then flown over PtdIns(3)P-free and PtdIns(3)P-enriched liposomes, which were immobilized on the L1 sensor chip surface. To estimate the kinetic parameters, sensorgrams best fitted to the two-state (conformational change) and bivalent analyte binding models using BIAcore X100 evaluation software (version 2.0). The χ^2 values were lesser than 10% of the maximal binding response (R_{max}) for each data set.

NMR Spectroscopy—NMR data were acquired at 25°C using a Bruker Avance III 600 MHz spectrometer (Virginia Tech) equipped with an inverse TBI probe with z-axis pulsed-field gradients. Two-dimensional ^{1}H, ^{15}N-HSQC experiments were used to track backbone amide resonance changes in ^{15}N-labeled proteins due to interaction with the unlabeled protein partner. For ubiquitin-Tollip C2 domain interactions, 30 uM of ubiquitin

was prepared in 20 mM d_{11}-Tris-HCl (pH 7.5), 350 mM NaCl, 1 mM NaN_3, and 1 mM d_{18}-DTT and unlabeled Tollip C2 domain was added at 8-fold excess to visualize resonance perturbations. In the case of ubiquitin-Tollip CUE domain interactions, 50 μM of ^{15}N-Tollip CUE domain was prepared in 20 mM phosphate buffer (pH 7) and unlabeled ubiquitin was added at 2-fold excess. Reciprocally, 50 μM ^{15}N-ubiquitin was prepared in the same buffer and unlabeled Tollip CUE domain was added at 2-fold excess. Spectra were processed with NMRPipe (22) and analyzed using nmrDraw (23). Chemical shift perturbations were calculated according to the following formula (24):

$$\Delta\delta(^1H,^{15}N)=[(\Delta\delta^1H)^2 + (\Delta\delta^{15}N)^2/6]^{0.5}$$

Circular Dichroism Spectroscopy—Far-UV (190-240 nm) circular dichroism (CD) experiments were performed on a JASCO J-815 spectropolarimeter equipped with a Jasco PFD-425 S temperature control unit. Five accumulated untagged protein (10 μM) CD spectra was recorded in 5 mM Tris-HCl (pH 7.0) and 100 mM KF at 25°C using a 1 mm-path-length quartz cell, a bandwidth of 4 nm, a response time of 1 s and a scan rate of 20 nm/min. Buffer backgrounds were subtracted from the protein spectra.

Analytical Gel Filtration—Various concentrations of free protein and complex were incubated in 50 mM Tris-HCl (pH 8), 200 mM NaCl, and 1mM DTT for 30 min at 25°C. Protein samples (1.5 ml) were applied to a Superdex 75 column (GE Healthcare), equilibrated with the same buffer, and run at 1 ml/min at 4 °C using an AKTA 900 Purifier FPLC system (GE Healthcare). Proteins were detected by their absorption at

280 nm. Fractions were collected and analyzed by 10% SDS-PAGE and Coomassie blue staining. The column was calibrated with protein standards (blue dextran, BSA, ovoalbumin, chymotrypsinogen A, myoglobin, ribonuclease A, and aprotinin). Stokes radii of the proteins were determined by logarithmic interpolation.

Analytical Ultracentrifugation—Sedimentation velocity experiments with Tollip CUE (605 μM), ubiquitin (900 μM), and a 1:1 molar ratio of the Tollip CUE-ubiquitin complex (350 μM each) were carried out using a Beckman Optima XL-I ultracentrifuge equipped with a 50Ti eight-hole rotor and using a 12-mm path length cell (Biophysics Core, University of Colorado Denver). Absorbance profiles at 273 nm were collected every 30 sec at 45,000 rpm and 25°C. Sedimentation coefficient continuous c(S) distributions were determined using SEDFIT software (25). The resulting apparent sedimentation coefficients were corrected to standard conditions as reported (26). The calculated molecular weight of the protein was estimated using the Siegel-Monty analysis (27).

RESULTS

Ubiquitin Inhibits Tollip's Phosphoinositide Binding—Tollip localizes to endosomal membranes and the subcellular localization of the protein is likely associated to its ability to preferentially bind PtdIns(3)P through its central C2 domain (18). Since Tollip binds ubiquitin through its CUE domain (19), we then asked whether ubiquitin regulates phosphoinositide recognition. Whereas Tollip binds PtdIns(3)P and ubiquitin

does not, pre-incubation of Tollip with ubiquitin led to inhibition of Tollip's PtdIns(3)P binding in a dose-dependent manner (Fig. 5.1*A*). Likewise, ubiquitin also inhibited PtdIns(4,5)P_2 binding of Tollip (Fig. S5.1*A*), but not on PtdIns(3)P binding of the Vam7p PX domain (Fig. S5.1*B*), suggesting that ubiquitin specifically blocks Tollip's phosphoinositide binding. Tollip reversibly bound PtdIns(3)P-containing liposomes with a dissociation constant (K_D) of 46 nM (Fig. 5.1*B* and Table 5.1). To quantify the effect of ubiquitin on Tollip-PtdIns(3)P association, we performed a competition experiment using SPR analysis. Pre-incubation of Tollip with ubiquitin reduced PtdIns(3)P in a ubiquitin dose-dependent manner (Fig. 5.1*C*) with an estimated IC_{50} of 3.8 μM.

The Tollip C2 Domain is an Ubiquitin-binding Domain—To make sure that the effects we observed in Fig. 5.1 are due to the Tollip CUE domain's ability to bind to ubiquitin, we performed a control experiment using the Tollip C2 domain. To our surprise, ubiquitin inhibited Tollip C2 domain's PtdIns(3)P-binding (Fig. 5.2*A*). Next, SPR was used to determine whether the Tollip C2 domain binds ubiquitin. His-tagged ubiquitin was immobilized on the surface of an NTA sensor chip, and untagged Tollip C2 domain was employed as an analyte. When the Tollip C2 domain was flown over the sensor chip, binding to ubiquitin was observed in a concentration-dependent manner and exhibited rapid association and dissociation rates (Fig. 5.2*B*). The binding event best fit with the two-state conformational change model, consistent with the large number of ubiquitin NMR resonances perturbed by the Tollip C2 domain (Fig. 5.2*C*). The Tollip C2 domain bound ubiquitin with a K_D of 10.8 μM (Table 5.1), which was determined from

the kinetic rate constants. This value is within the range of the affinities reported for other ubiquitin-binding domains (28). Binding of the Tollip C2 domain to ubiquitin exhibited a saturable binding trace that is indicative of specific binding. To map the Tollip C2 domain's binding site in ubiquitin, we collected ^{1}H, ^{15}N-heteronuclear single quantum coherence (HSQC) spectra of ^{15}N-labeled ubiquitin. Changes in the position of the HSQC chemical shifts can be induced by ligand binding or by changes in structure and/or dynamics of the protein. Addition of unlabeled Tollip C2 domain to the ^{15}N-labeled ubiquitin led to a large number of perturbations in chemical shifts in the HSQC spectrum of ubiquitin (Fig. 5.2*C*), suggesting that Tollip C2 domain binding is accompanied by a conformational change in ubiquitin. Large chemical shift changes were observed in ubiquitin residues Asp32 and Lys33 at the end of the first helix, residues Gly47 and Glu51 located around the fourth β-strand element, and Gln62 and Leu71 found around the fifth β-strand element (Fig. 5.2*D*). Minor perturbations were also detected in residues around Gly47 and Leu71 such as Lys6, Gly10, Lys11, Leu43, Ile44, Leu69, Val70, and Leu73, which form a relatively hydrophobic patch binding site characteristic for ubiquitin's protein interactions (Fig. 5.2*E*). Thus, these results suggest that a large region of ubiquitin' surface is compromised to associate to the Tollip C2 domain. To identify key Tollip C2-ubiquitin-interacting residues, we performed alanine mutagenesis on ubiquitin residues, whose resonances were perturbed by the presence of the Tollip C2 domain, and evaluated using SPR detection. Mutations in residues located in and around the hydrophobic patch (Leu43) and in residues located at the C-terminal flexible region of ubiquitin (*i.e.*, Leu71) reduced Tollip C2 domain affinity about

2 to 3-fold (Table S5.1). Mutations in Leu71 neighbor residues, such as Lys6 and Leu73, did not affect Tollip C2 domain binding (Table S5.1). Identification of the ubiquitin-binding residues in the Tollip C2 domain using NMR spectroscopy was not possible since we were unable to obtain a stable Tollip C2 domain sample at the concentration required to assign its NMR resonances. Nonetheless, alanine mutation in a Tollip C2 domain basic residue important for PtdIns(3)P binding (Lys162) reduced the affinity for ubiquitin 2-fold, but mutations in other PtdIns(3)P-binding residues (His135, Arg157) did not affect ubiquitin binding (Table S5.1). Using the predicted structure of the Tollip C2 domain (18), we found that the conserved residue Leu142 is close to Lys162. Alanine mutation in both Leu142 and Lys162 reduced the affinity for ubiquitin 6-fold, without altering the overall structure of the protein (Table S5.1 and Fig. S5.2). Taken together, these results suggest that PtdIns(3)P and ubiquitin binding sites in the Tollip C2 domain partially overlap.

The Tollip C2 and CUE Domain Binding Sites in Ubiquitin Partially Overlap— The data indicated that both the Tollip CUE and C2 domains bind to ubiquitin, suggesting that ubiquitin binds at two sites on Tollip with distinct affinities. Alternatively, it is also possible that one molecule of ubiquitin binds both domains at different interfaces leaving Tollip in a closed conformation. To address this, we identified the ubiquitin residues that associate to the Tollip CUE domain using HSQC chemical shift-based analysis. Ubiquitin bound the Tollip CUE domain triggering a large number of chemical shift changes in the ubiquitin spectrum (Fig. 5.3*A*), suggesting that Tollip CUE domain

binding is accompanied by a conformational change in ubiquitin. Drastically perturbed ubiquitin residues include the N-terminal Leu8 and Ile13 residues, the surface hydrophobic protein-interacting residues Leu43, Ile44, and Gly47, and the C-terminal residues Gln62, Leu67, His68, Leu69, and Val70 (Fig. 5.3*B*). Most of these residues form a relatively hydrophobic binding site on the ubiquitin surface (Fig. 5.3*C*). Several ubiquitin resonances that are perturbed by the Tollip CUE domain, such as those corresponding to Ile13, Leu43, Ile44, Gly47, and Gln62, to mention a few, were also perturbed by the presence of the Tollip C2 domain (Fig. 5.2 and 5.3), suggesting that their binding sites partially overlap in ubiquitin. Unlike the Tollip C2 and CUE domains, the N-terminal Tollip TBD region did not bind ubiquitin (data not shown). Interestingly, full-length Tollip bound ubiquitin with higher affinity than its individual domains, with a K_D of 423 nM (Table 5.1 and Fig. S5.3), suggesting that cooperativity of the individual domains and oligomerization contribute for ubiquitin avidity. Taken together, we propose that two individual ubiquitin molecules can simultaneously bind Tollip through their C2 and CUE domains with both oligomerization and cooperativity of these domains playing a role on ubiquitin avidity.

Tollip CUE Domain Binds Ubiquitin Using its Conserved MPF Motif—To define the structural basis of the Tollip CUE domain-ubiquitin interaction and given the availability of the NMR resonance assignments of the Tollip CUE domain (21), we carried out HSQC measurements of ^{15}N-labeled Tollip CUE domain alone and with unlabeled ubiquitin (Fig. 5.4). Several Tollip CUE domain resonances were perturbed by the

presence of ubiquitin, which likely indicates that binding is accompanied by conformational changes in the CUE domain as we observed with the reverse experiment (Fig. 5.3*A*). Two ubiquitin-interacting regions are evident from the normalized chemical shift perturbation calculations (Fig. 5.4*B*). One region involves Ile237, Asp239, Met240, Phe241, and Asn243 residues located between helices 1 and 2 in the Tollip CUE domain (Fig. 5.4*B*). Two of these residues, Met240 and Phe241, belong to the Met-Phe-Pro motif responsible for ubiquitin recognition in yeast CUE domains (20,29). The second region includes C-terminal CUE domain residues, such as Met270, Gly271, and Asp272. In contrast to the role of the Leu-Leu motif in ubiquitin interaction in yeast CUE domains (20,29), the Tollip CUE domain Leu-Leu motif (amino acids 267-268) was not significantly perturbed by the presence of ubiquitin. To identify the binding surface, we generated a homology model of the Tollip CUE domain based on the structure of the Vps9p CUE domain, a protein that exhibits 23% identity with the Tollip CUE domain. The two ubiquitin-interacting regions are located at opposite ends of the CUE domain structure, inferring that it is possible that the Tollip CUE domain wraps around ubiquitin. We further quantitatively characterized the association of the Tollip CUE domain to ubiquitin using SPR analysis. Binding exhibited rapid association and dissociation rates and best fitted the conformational change model, in agreement with the HSQC titration results (Fig. 5.4*A*) with a resultant K_D of 1.35 μM (Table 5.1). Thus, this result suggests that Tollip is able to simultaneously bind two ubiquitin molecules with affinities in the low micromolar range. Based on chemical shift perturbations induced by the Tollip CUE domain and using SPR analysis, we screened ubiquitin key-

interacting residues for Tollip CUE association. We found that ubiquitin Ile44 mutation to alanine reduced Tollip CUE domain binding by about 43-fold, whereas mutation in Leu69, close to Ile44, reduced 3-fold the affinity for the protein (Table S5.2). Mutagenesis of neighbor residues in the tertiary structure of the protein (e.g., His68) as well as in other NMR-perturbed residues (e.g., Leu8) did not significantly alter Tollip CUE domain binding (Table S5.2). The structural integrity of ubiquitin upon mutation in Ile44 was preserved based on a strong overlap on the CD traces (Fig. S5.2), indicating that mutation in ubiquitin affected Tollip CUE domain binding. Reciprocally, we introduced mutations in residues of the Tollip CUE domain that were perturbed by ubiquitin in HSQC titrations. Thus, replacement of Gly271 with a valine residue decreased the affinity 53-fold and alanine mutations in residues Asp239, Met240, and Asn243 reduced ubiquitin association 19-, 69-, and 9-fold, respectively, whereas mutation in Phe241 did not affect ubiquitin binding (Table S5.2). Accordingly, a triple mutant (D239A/M240A/N243A) of the Tollip CUE domain reduced its association to ubiquitin 78-fold (Table S5.3). Furthermore, mutations in ubiquitin-interacting residues did not alter the secondary structure of the Tollip CUE domain (Fig. S5.2). Consequently, the CUE domain conserved region that includes Met240 and neighbor residues as well as the C-terminal region, including Gly271, are compromised to ubiquitin ligation.

Ubiquitin dissociates the Tollip CUE domain into Monomers—We previously reported that the Tollip CUE domain is a dimer (21), in agreement with the reported oligomeric

state of the yeast Vps9 CUE domain (20). Results from sedimentation velocity ultracentrifugation and analytical gel filtration are consistent with Tollip CUE and ubiquitin existing in dimeric and monomeric states, respectively (Fig. 5.5*A* and 5.5*B*). Whereas the Vps9p CUE domain binds ubiquitin in a dimeric conformation (20), the yeast Cue2 CUE domain predominantly interacts with ubiquitin as a monomer (29), thus, raising the questions of whether the Tollip CUE domain retains the dimeric state or whether binding to ubiquitin alters its oligomeric state. The sedimentation coefficient and gel filtration distribution revealed the presence of a single peak for this protein complex with a $S_{20,w}$ of 1.91 S and a Stokes radius of 1.56 nm (Fig. 5.5*C*). Combining these parameters (27) allowed us to calculate the molecular mass of 12.5 kDa consistent with a heterodimeric complex. Taken together, the 1:1 stoichiometry established for the interaction indicates that ubiquitin triggers Tollip CUE dissociation into monomers.

TABLES AND FIGURES

Table 5.1 **Dissociation constants (K_D) and association (k_a) and dissociation (k_d) rate constants of Tollip interactions.**

Following a two-state conformational change model

Complex	k_{a1} (M^{-1} s^{-1})	k_{d1} (s^{-1})	k_{a2} (s^{-1})	k_{d2} (s^{-1})	K_D (M)	Fit (χ^2)
Tollip-PtdIns(3)P	8.8 ± 0.3x10^{2}	7.4 ± 1.3x10^{-4}	1.4 ± 0.1x10^{-3}	3.9 ± 1.5x10^{-4}	4.60 x 10^{-8}	0.28
Tollip C2-ubiquitin	8.3 ± 0.1x10^{3}	3.8 ± 0.1x10^{-2}	8.4 ± 0.1x10^{-4}	9.6 ± 0.1x10^{-3}	1.08 x 10^{-5}	0.83
Tollip CUE-ubiquitin	3.0 ± 0.3x10^{4}	2.4 ± 0.1x10^{-1}	2.1 ± 0.1x10^{-3}	1.2 ± 0.1x10^{-4}	1.35 x 10^{-6}	3.06

Following a bivalent analyte model

Complex	k_{a1} (M^{-1} s^{-1})	k_d (s^{-1})	K_{D1} (M)	Fit (χ^2)	k_{a2} (1/RU)	k_{d2} (s^{-1})
Tollip-ubiquitin	2.3 ± 0.1x10^{3}	9.5 ± 0.3x10^{-4}	4.23 x 10^{-7}	14.67	3 ± 1.0x10^{-6}	9.6 ± 0.5x10^{-}

Data represent the average of three independent experiments.

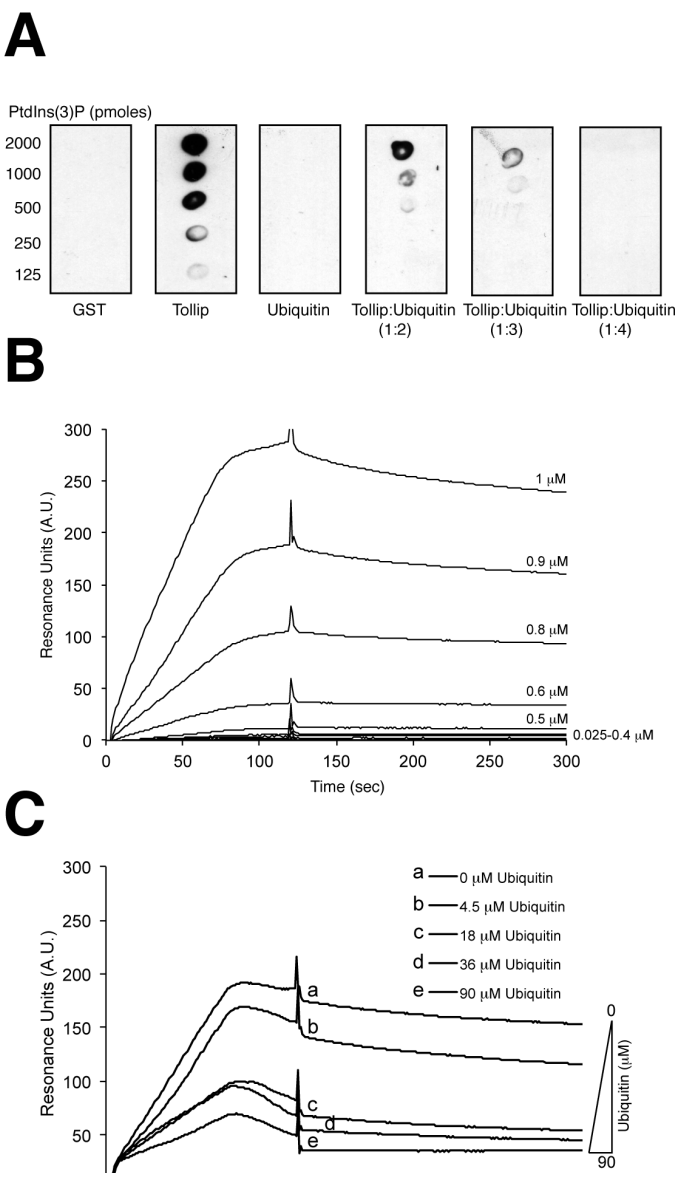

Figure 5.1 **Ubiquitin inhibits Tollip's PtdIns(3)P binding.**

(A) Lipid-protein overlay assay of the indicated proteins with immobilized PtdIns(3)P. To test ubiquitin function, GST-Tollip was pre-incubated with ubiquitin at the indicated molar ratios for 1 h at room temperature. GST and GST-ubiquitin were employed as negative controls.

(B) Representative SPR sensorgram for the binding of GST-Tollip to PtdIns(3)P-containing liposomes. Various indicated concentrations of GST-Tollip were flown over immobilized PtdIns(3)P liposomes.

(C) Kinetics of ubiquitin-mediated inhibition of Tollip-PtdIns(3)P association. Tollip was pre-incubated with ubiquitin at the indicated concentrations and association of Tollip to immobilized PtdIns(3)P liposomes was followed using SPR.

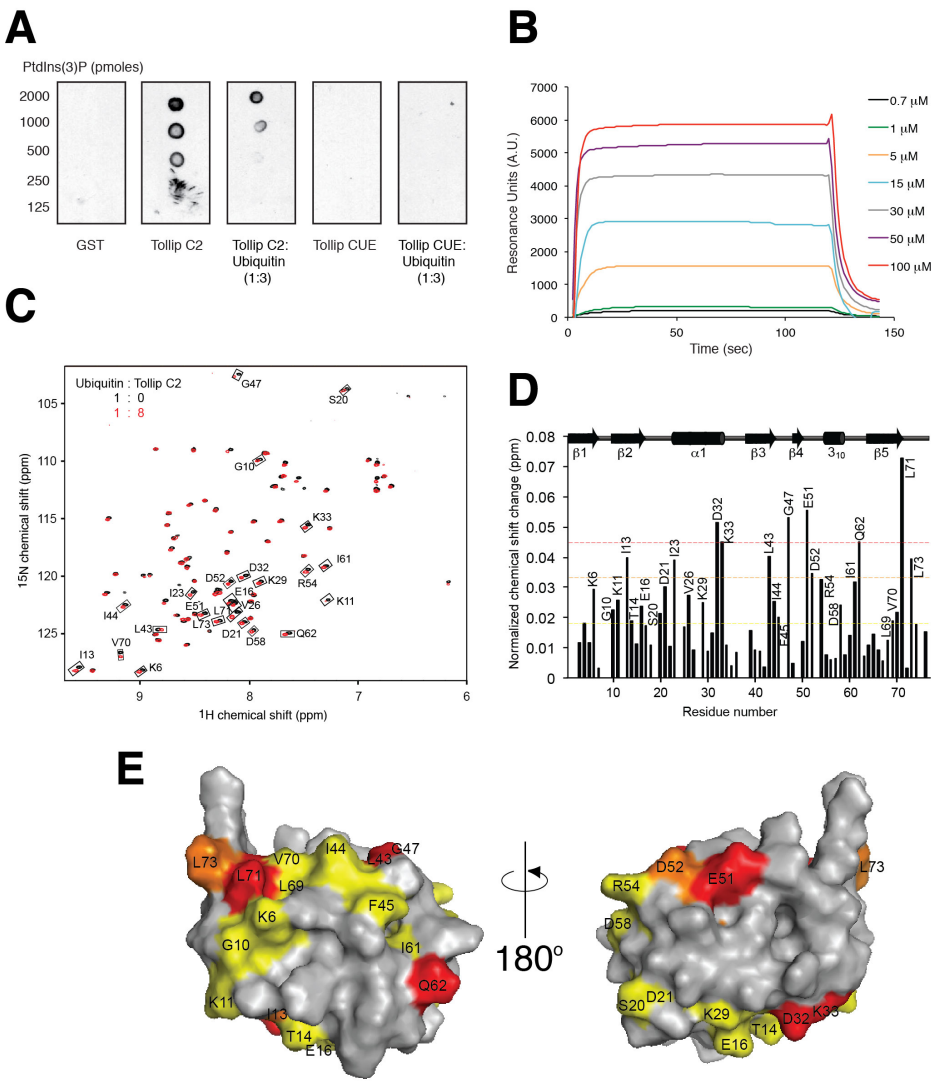

Figure 5.2 **The Tollip C2 domain is an ubiquitin-binding domain.**

(A) Lipid-protein overlay assay of the indicated proteins with immobilized PtdIns(3)P. To test ubiquitin function, the Tollip C2 and CUE domains were pre-incubated with ubiquitin at the indicated molar ratio for 1 h at room temperature.

(B) Representative SPR sensorgram for the binding of Tollip C2 domain to immobilized ubiquitin. Various concentrations of the Tollip C2 were flown over His-tagged ubiquitin attached on an NTA sensor chip.

(C) Identification of the ubiquitin residues involved in Tollip C2 domain binding. ^{15}N-labeled ubiquitin was subjected to HSQC analysis in the absence (black) and presence of the Tollip C2 domain (red). Perturbed ubiquitin resonances are boxed.

(D) Histogram identifying ubiquitin critical residues for Tollip C2 domain recognition. The colored dashed lines represent significant changes, based on the magnitude of their associated chemical shifts changes: red ($\Delta\delta_{average}$ + 1.5 x standard deviation) > orange ($\Delta\delta_{average}$ + 1 x standard deviation) > yellow ($\Delta\delta_{average}$).

(E) Two different views of ubiquitin showing the residues involved in Tollip C2 domain binding and color-coded according to the scales defined in (D).

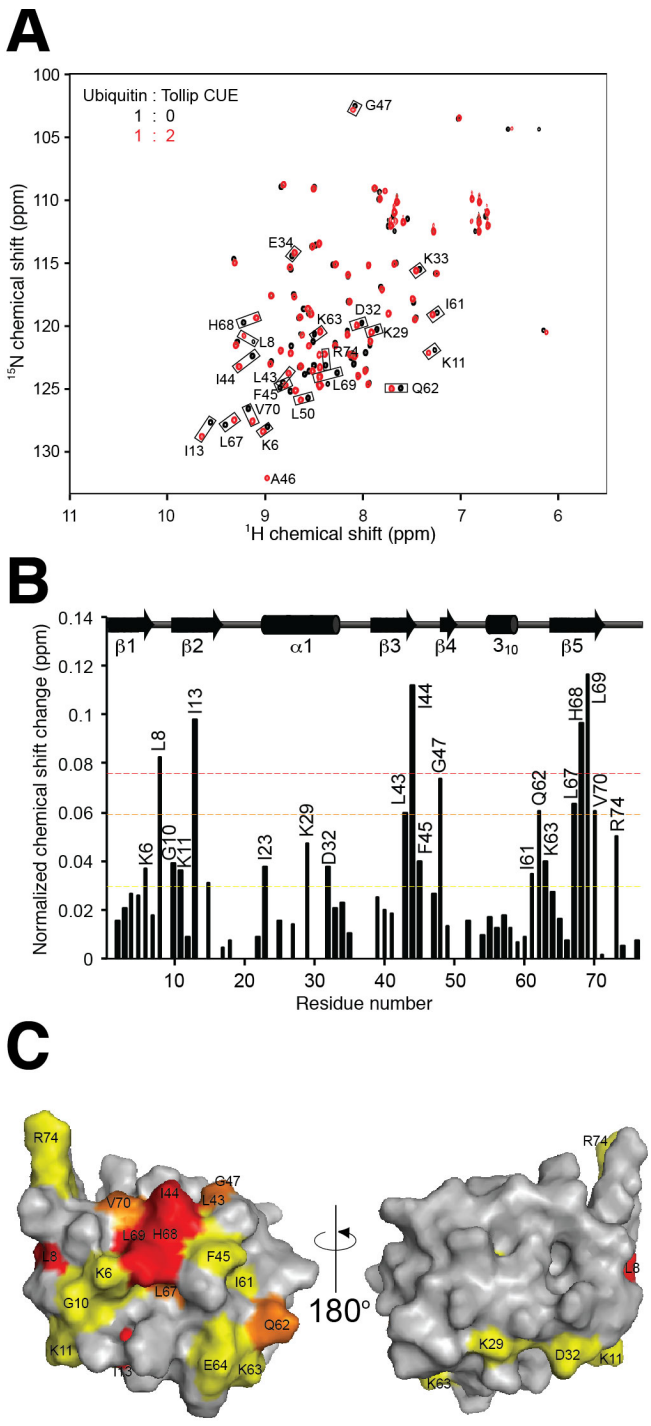

Figure 5.3 **Identification of ubiquitin residues involved in Tollip CUE domain binding.**

(A) ^{15}N-labeled ubiquitin was subjected to HSQC analysis in the absence (black) and presence of the Tollip CUE domain (red). Perturbed ubiquitin resonances are boxed.

(B) Histogram identifying ubiquitin critical residues in Tollip CUE domain recognition. Chemical shift perturbations are classified as indicated in Figure 2.

(C) Two different views of ubiquitin showing the residues involved in Tollip CUE domain binding and color-coded according to the scales defined in (B).

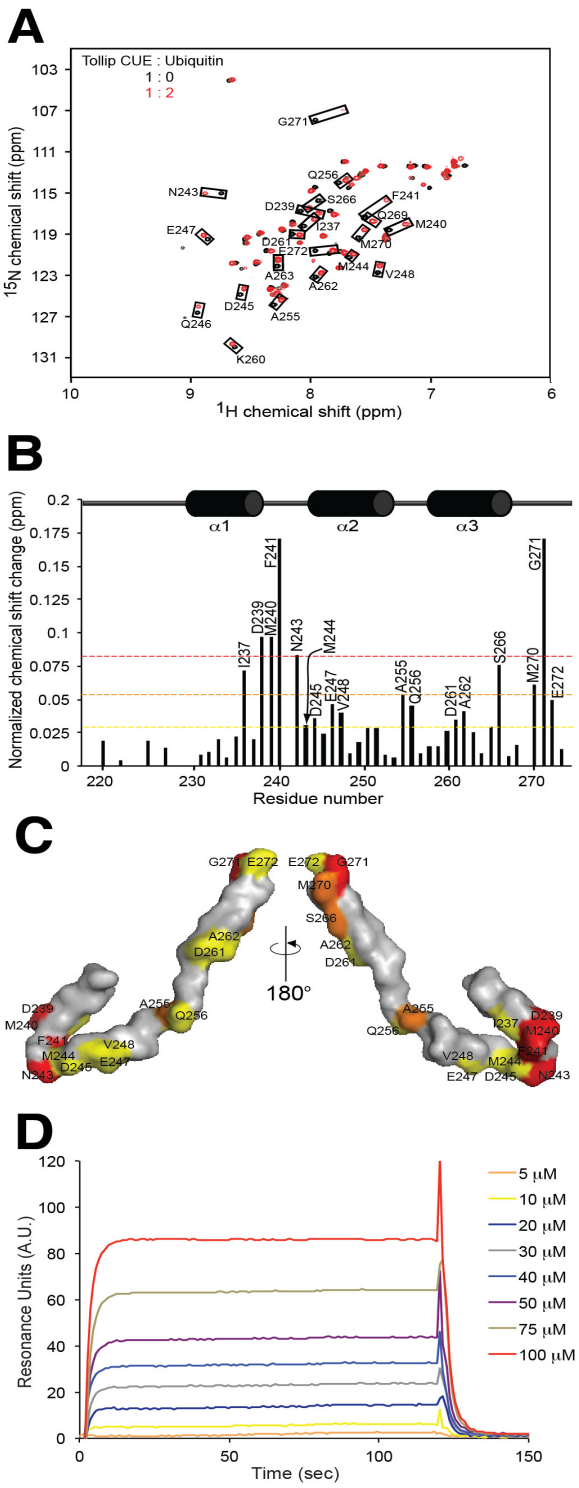
A
Tollip CUE : Ubiquitin
1 : 0
1 : 2
^{15}N chemical shift (ppm)
^{1}H chemical shift (ppm)
B
Normalized chemical shift change (ppm)
Residue number
α1
α2
α3
C
180°
D
Resonance Units (A.U.)
Time (sec)
5 μM
10 μM
20 μM
30 μM
40 μM
50 μM
75 μM
100 μM

Figure 5.4 **Identification of Tollip CUE domain residues involved in ubiquitin binding.**

(A) ^{15}N-labeled Tollip CUE domain was subjected to HSQC analysis in the absence (black) and presence of ubiquitin (red). Perturbed resonances of the Tollip CUE domain are boxed.

(B) The histogram shows normalized chemical shift perturbations in the backbone amides of the CUE domain induced by ubiquitin. Chemical shift perturbations are classified as indicated in Figure 2.

(C) Residues that exhibit significant chemical shift perturbations in (A) are labeled on the modeled Tollip CUE domain surface and color-coded according to the scales defined in (B).

(D) Representative SPR sensogram for the binding of Tollip CUE domain to immobilized ubiquitin. Various concentrations of the Tollip CUE were flown over His-tagged ubiquitin attached on an NTA sensor chip.

A

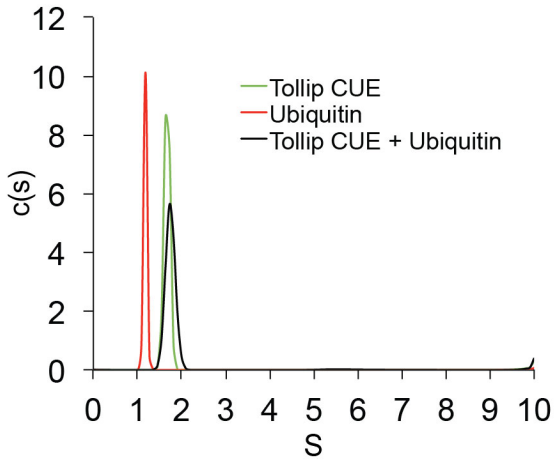

B

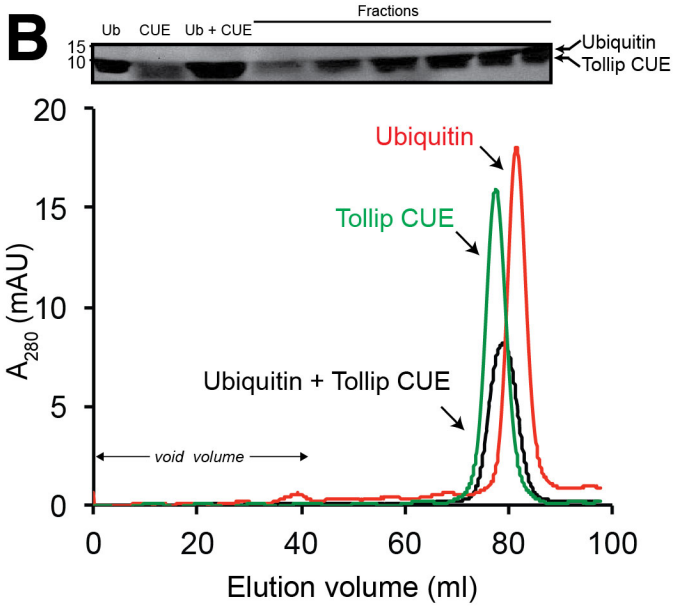

C

Protein	$s_{20,w}$ (S)	Stokes radius (nm)	Calculated MW (kDa)	Theoretical MW (kDa)	Ratio
Tollip CUE	1.72	1.62	11.73	6.58	1.8
Ubiquitin	1.35	1.47	8.33	8.84	0.9
Tollip CUE + Ubiquitin	1.91	1.56	12.50	15.42*	0.8

Figure 5.5 **Hydrodynamic properties of the Tollip CUE-ubiquitin complex.**

(A) Representative sedimentation velocity analysis of the Tollip CUE-ubiquitin complex. Sedimentation coefficient distribution of free Tollip CUE (S_{app}= 1.64; green line), free ubiquitin (S_{app}= 1.18; red line), and Tollip CUE-ubiquitin complex (S_{app}= 1.73; black line).

(B) Representative gel filtration analysis of ubiquitin (red), Tollip CUE domain (green), and ubiquitin:Tollip CUE domain (1:1 molar ratio; black) using a Superdex 75 column. Fractions of each of the peaks were analyzed using SDS-PAGE (top).

(C) Summary of the results obtained from the sedimentation velocity ultracentrifugation and analytical gel filtration analyses.

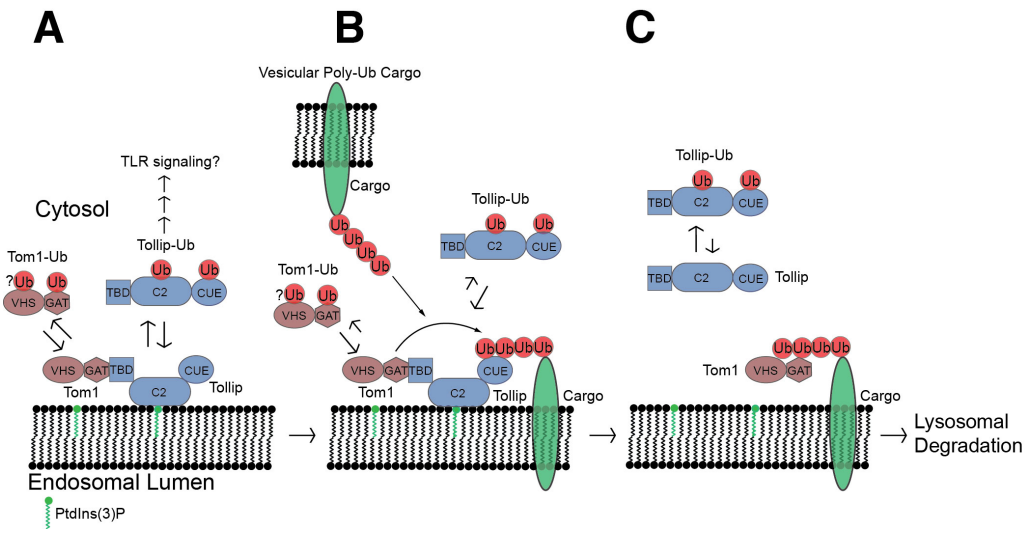

Figure 5.6 **A proposed model for the regulation of the endosomal membrane-associated- Tollip.**

(A) Tollip cycles between ubiquitin-free and bound states in the absence of cargo proteins. Membrane binding is mediated by the interaction of the Tollip C2 domain with PtdIns(3)P and the protein trafficking role of Tollip is associated with Tom1, which interacts with Tollip TBD and ubiquitin in a mutually exclusive fashion. Tollip also binds to ubiquitin making this complex available in the cytosol for other molecular interactions. Of note, it has not yet demonstrated whether the Tom1 VHS domain binds ubiquitin.

(B) Tollip exhibits higher affinity for polyubiquitinated cargo (*i.e.*, IL-1R) via its CUE domain (and perhaps via its C2 domain) as demonstrated in yeast CUE and UBA domains. Therefore, the protein complex is stabilized at the endosomal membranes. It is also possible that polyubiquitinated cargo directly binds to Tom1, leading to Tollip release from the membrane. Cargo sequestration at the endosomal membrane favors Tom1 interactions, which exhibit higher affinity for polyubiquitinated cargo.

(C) Consequently, Tollip interaction to the endosomal membrane becomes weaker; the protein is released to the cytosol and binds to free ubiquitin. Tom1 and subsequently the ESCRT complex (not shown) mediate cargo sorting for lysosomal degradation (or cargo recycling).

DISCUSSION

The results presented in this study demonstrate that phosphoinositide binding of Tollip is negatively modulated by ubiquitin and that this occurs by ubiquitin association to both Tollip C2 and CUE domains. This suggests the presence of a dual mode of recognition for ubiquitin by Tollip. Whereas ubiquitin directly competes with PtdIns(3)P binding to the Tollip C2 domain, the action of ubiquitin on the CUE domain may reside in promoting Tollip's monomerization, at least by dissociation of the dimer at its C-terminus, which may reduce the affinity of Tollip for the phosphoinositide. On the basis of our findings, we propose that recruitment of Tollip to endosomal membranes, and formation of protein complexes with other adaptor proteins depend on its central C2 domain and the presence of PtdIns(3)P in endosomal membranes (Fig. 5.6). In the absence of polyubiquitinated cargo, Tollip could be partitioned in membrane-bound and membrane-free states, which depend on both the presence of PtdIns(3)P-rich domains and ubiquitin. The affinity of Tollip for PtdIns(3)P is 46 nM, which is ~240-fold higher than its isolated C2 domain (18). This increment is not due to additional interactions of the protein via either TBD or CUE domains with PtdIns(3)P (data not shown); thus, oligomerization of Tollip provides high affinity and sensitivity to PtdIns(3)P levels at endosomal membranes. Since ubiquitin inhibits PtdIns(3)P binding, the Tollip-ubiquitin complex would remain membrane-free. Likewise, Tom1 is also an adaptor protein that associates to and acts downstream of Tollip and is also required to traffic ubiquitinated cargo, such as the IL-1R, to late endosomes (11). Tom1 contains two-ubiquitin binding domains, namely the VHS and GAT domains, and association of ubiquitin to the GAT

domain prevents Tollip binding (10). Since Tom1 shares common ubiquitin binding properties with Tollip, we speculate that ubiquitin binding also prevents Tom1 recruitment to endosomal membranes via Tollip interactions and this may occur in the absence of polyubiquitinated cargo (Fig. 5.6).

The question remains, what is the role of the Tollip-ubiquitin complex? Ubiquitin binds noncovalently to a variety of ubiquitin-binding domains, the majority of which associate to the hydrophobic patch around ubiquitin Ile44 (1). Ubiquitin-binding domains cannot only interact with ubiquitin, but they also can associate with ubiquitinated proteins and be regulated by ubiquitination. Polyubiquitination of a protein can be a signal for its degradation by the proteosomal pathway; however, ubiquitin conjugation can also be a signal for changing protein localization or for regulation of a protein function (30). For example, the canonical activation of the transcription factor NF-kB through myeloid differentiation primary-response protein 88-dependent TLR signaling requires activation of IRAK-4, which activates IRAK-1 by phosphorylation. Activated IRAK-1 associates with TRAF6, which in turn, activates its E3 ubiquitin ligase activity, that together with Ubc13 and Uev1A, catalyzes the Lys63-linked polyubiquitination of IRAK1, NEMO, and TRAF6 itself (31). Thus, these chains act as a scaffold by helping the recruitment of ubiquitin-binding proteins including NEMO and TAB2/3. These associations facilitate the accumulation of NF-kB, required for the expression of pro-inflammatory proteins. We currently do not know whether the Tollip C2 and CUE domains bind polyubiquitin chains and, if so, whether they exhibit higher affinity than

ubiquitin as demonstrated for the yeast CUE and UBA domains *in vitro* (19,32). However, in this context, it is also possible that Tollip can be intracellularly partitioned and sequestered by interactions with polyubiquitin chains of IRAK-1 via its C2 and CUE domains. This could be important as Tollip would be placed in proximity with IRAK-1 to modulate its activity in the absence of microbial products.

PtdIns(3)P is highly enriched in the cytosolic leaflet of the early endosomal membranes (33) and its function in these compartments is to recruit PtdIns(3)P-binding proteins. Formation of such protein-PtdIns(3)P complexes control membrane transport and dynamics such as intralumenal vesicle formation, receptor downregulation, docking, fusion, and motility (34). Phosphoinositides are characterized for their rapid interconversion through the action of specific kinases and phosphatases. In mammals and yeast, PtdIns(3)P is produced from phosphatidylinositol by the class III PI 3-kinase. PtdIns(3)P synthesis is controlled by the small GTPase Rab5 since the class III PI 3-kinase acts as a Rab5 effector (34). In addition, PtdIns(3)P is dephosphorylated by lipid phosphatases (35). Thus, specific lipid kinases and phosphatases play a key role in the spatial and temporal regulation of PtdIns(3)P, which are crucial for tethering of adaptor protein complexes at endosomal membranes. From this study, we propose that ubiquitin binding to the Tollip C2 domain could represent a novel regulation of PtdIns(3)P-dependent Tollip's recruitment to cell membranes. Likewise, the endosomal ELL-associated protein of 45 kDa (Eap45) GRAM-like ubiquitin-binding in Eap45 (GLUE) domain binds ubiquitin and 3-phosphoinositides (36). Ubiquitin and phosphoinositide-

binding sites in the GLUE domain may not overlap and are likely independent-binding events (37). However, ubiquitin- and phosphoinositide-binding to the Eap45 GLUE domain have been proposed to be mutually exclusive to avoid ESCRT-II complex association to endosomal membranes in the absence of polyubiquitinated cargo (36). Despite the fact that the Tollip C2 domain shares the same set of ligands with the Eap45 GLUE domain, GLUE domain-ubiquitin interactions resemble the Tollip CUE domain-ubiquitin association. For example, the canonical Ile44 hydrophobic surface of ubiquitin represented by the residues Leu8, Ile44, Gly47, and Val70, which are perturbed by the presence of the Tollip CUE domain, form hydrophobic and van der Waals interactions with the Eap45 GLUE domain (37). We were unable to see significant changes in the resonances represented by most of the residues of this region in excess of the Tollip C2 domain. Instead, resonances that involve Leu71 and neighbor residues seemed to be compromised in Tollip C2 domain recognition. Indeed, Hicke and colleagues demonstrate that ubiquitin residues Gly47, Val70, and Leu71, whose resonances are perturbed by the Tollip C2 domain, are functionally relevant in yeast (38). It is well known that the tertiary structure of ubiquitin is quite rigid, with the exception of the C-terminal region. Work reported by de Groot and colleagues showed that association of a ubiquitin-binding domain to ubiquitin triggers conformational changes in ubiquitin (5). This model was later supported by Wlodarski and Zagrovic, who demonstrated that the conformational change in ubiquitin upon ligand binding is favored by an induced fit mechanism close to the binding site, which adds specificity for the interaction (39). Since we see Tollip C2 domain-induced perturbations in a large

number of ubiquitin residues, we speculate that the Tollip C2 domain-ubiquitin interface is consequently more extended than that for the Tollip CUE domain and is accompanied by a conformational change in ubiquitin. Despite the impossibility of having the resonance assignments of the Tollip C2 domain, we reasoned that competition of ubiquitin and PtdIns(3)P would be built based on common Tollip C2 domain interacting residues. We previously reported that conserved basic residues, such as Lys162, are relevant for PtdIns(3)P recognition (18). Using site-directed mutagenesis on the Tollip C2 domain, we found that a conserved Tollip region comprising residues Leu142 and Lys162 reduced the affinity for ubiquitin. Curiously, this region, which is predicted to be surface exposed, is not present in other C2 domain proteins (18), which explains the uniqueness of the Tollip C2 domain for ubiquitin binding. Indeed, surface exposed residues Lys143 and Lys162 have been also implicated as potential sites for Tollip sumoylation (16) emphasizing the role of this region in multiple cellular functions. Collectively, we experimentally demonstrated that the Tollip C2 domain cannot bind to both ubiquitin and phosphoinositides simultaneously, and we hypothesize that this property helps Tollip to be intracellularly partitioned for engagement in both endosomal trafficking and other cytosolic commitments in the absence of cargo (Fig. 5.6).

The CUE domain is a helical module that belongs to the family of ubiquitin-binding domains (1). Whereas the Vps9p CUE domain binds ubiquitin in a dimeric conformation (20), the yeast Cue2 CUE domain predominantly interacts with ubiquitin as a monomer (29). Our oligomeric state analysis indicated that the dimeric Tollip CUE

domain dissociated in the presence of ubiquitin suggesting that could reduce its avidity for PtdIns(3)P leading to its release from endosomal membranes in the absence of cargo. Whereas the CUE domain mediates dimerization of Tollip (21) and Tollip itself forms homodimers (data not shown), we cannot exclude the possibility that additional regions in Tollip (*i.e.*, TBD, but not the C2 domain) mediate oligomerization of the protein as reported from pull-down experiments (14). We found that Tollip binds to ubiquitin with a K_D of 423 nM; this is expected since, whereas ubiquitin-binding domains bind ubiquitin with low to moderate affinity as we see for both the individual C2 and CUE domains, the presence of multiple ubiquitin-binding domains cooperatively contribute to ubiquitin ligation (1). Cooperativity of neighbor ubiquitin-binding domains has recently been observed in the signal transducing adaptor molecule 2 (STAM2), one of the ESCRT-0 subunits that coordinate the proper function of the ESCRT protein complex responsible for committing ubiquitinated cargo to the MVB pathway (40). STAM2 possesses two ubiquitin-binding domains, the VHS domain and the ubiquitin-interacting motif, which are separated from each other by a linker of twenty amino acids (41). Also, we observed that the affinity of Tollip for PtdIns(3)P is about 10-fold higher than that for ubiquitin. We reasoned that the relatively high intracellular concentration of free ubiquitin would compensate that difference and favor an equilibrium of free and membrane-bound Tollip states. In summary, our observations are in agreement with the general behavior of ubiquitin-binding proteins, which exhibit relatively moderate affinity for ubiquitin. However, this property is compensated by the presence of multiple ubiquitin-binding domains and, in some cases, by protein oligomerization (1). All together, our

results place free ubiquitin as a novel modulator of Tollip's membrane targeting, by triggering inhibition of PtdIns(3)P ligation and dissociation of the CUE domain dimers. Since ubiquitin-binding domains generally exhibit higher affinity for polyubiquitin chains, the inhibitory function of ubiquitin should be balanced by an increment of polyubiquitinated cargo traffic, which in turn, will favor the commitment of Tollip, and other adaptor proteins, to sort cargo proteins through the endosomal pathway.

FUNDING

This work was supported by the American Heart Association and by the Thomas F. Jeffress and Kate Miller Jeffress Memorial Trust (to D.G.S.C.). I was supported by an American Heart Association pre-doctoral fellowship, Fralin Fellowship, Graduate student research and development grant (GRDP) and College of Science Roundtable Scholarship. C. Alicia Traughber was supported by the MAOP undergraduate scholarship. Stephanie Gomez was supported by both the McNair summer undergraduate and Virginia Tech-AMP scholarships.

REFERENCES

1. Husnjak, K., and Dikic, I. (2012) Ubiquitin-binding proteins: decoders of ubiquitin-mediated cellular functions. *Ann Rev Biochem* **81**, 291-322
2. Ikeda, F., Crosetto, N., and Dikic, I. (2010) What determines the specificity and outcomes of ubiquitin signaling? *Cell* **143**, 677-681
3. Kaiser, S. E., Riley, B. E., Shaler, T. A., Trevino, R. S., Becker, C. H., Schulman, H., and Kopito, R. R. (2011) Protein standard absolute quantification (PSAQ) method for the measurement of cellular ubiquitin pools. *Nat Methods* **8**, 691-696
4. Dikic, I., Wakatsuki, S., and Walters, K. J. (2009) Ubiquitin-binding domains - from structures to functions. *Nat Rev Mol Cell Biol* **10**, 659-671
5. Lange, O. F., Lakomek, N. A., Fares, C., Schroder, G. F., Walter, K. F., Becker, S., Meiler, J., Grubmuller, H., Griesinger, C., and de Groot, B. L. (2008) Recognition dynamics up to microseconds revealed from an RDC-derived ubiquitin ensemble in solution. *Science* **320**, 1471-1475
6. Haglund, K., and Dikic, I. (2012) The role of ubiquitylation in receptor endocytosis and endosomal sorting. *J Cell Sci* **125**, 265-275
7. Cullen, P. J. (2008) Endosomal sorting and signalling: an emerging role for sorting nexins. *Nat Rev Mol Cell Biol* **9**, 574-582
8. Saftig, P., and Klumperman, J. (2009) Lysosome biogenesis and lysosomal membrane proteins: trafficking meets function. *Nat Rev Mol Cell Biol* **10**, 623-635

9. Yamakami, M., Yoshimori, T., and Yokosawa, H. (2003) Tom1, a VHS domain-containing protein, interacts with tollip, ubiquitin, and clathrin. *J Biol Chem* **278**, 52865-52872

10. Katoh, Y., Shiba, Y., Mitsuhashi, H., Yanagida, Y., Takatsu, H., and Nakayama, K. (2004) Tollip and Tom1 form a complex and recruit ubiquitin-conjugated proteins onto early endosomes. *J Biol Chem* **279**, 24435-24443

11. Brissoni, B., Agostini, L., Kropf, M., Martinon, F., Swoboda, V., Lippens, S., Everett, H., Aebi, N., Janssens, S., Meylan, E., Felberbaum-Corti, M., Hirling, H., Gruenberg, J., Tschopp, J., and Burns, K. (2006) Intracellular trafficking of interleukin-1 receptor I requires Tollip. *Curr Biol* **16**, 2265-2270

12. Zhu, L., Wang, L., Luo, X., Zhang, Y., Ding, Q., Jiang, X., Wang, X., Pan, Y., and Chen, Y. (2012) Tollip, an intracellular trafficking protein, is a novel modulator of the transforming growth factor-beta signaling pathway. *J Biol Chem* **287**, 39653-39663

13. Burns, K., Clatworthy, J., Martin, L., Martinon, F., Plumpton, C., Maschera, B., Lewis, A., Ray, K., Tschopp, J., and Volpe, F. (2000) Tollip, a new component of the IL-1RI pathway, links IRAK to the IL-1 receptor. *Nat Cell Biol* **2**, 346-351

14. Zhang, G., and Ghosh, S. (2002) Negative regulation of toll-like receptor-mediated signaling by Tollip. *J Biol Chem* **277**, 7059-7065

15. Kawai, T., and Akira, S. (2010) The role of pattern-recognition receptors in innate immunity: update on Toll-like receptors. *Nat Immunol* **11**, 373-384

16. Ciarrocchi, A., D'Angelo, R., Cordiglieri, C., Rispoli, A., Santi, S., Riccio, M., Carone, S., Mancia, A. L., Paci, S., Cipollini, E., Ambrosetti, D., and Melli, M. (2009) Tollip is a mediator of protein sumoylation. *PLoS One* **4**, e4404

17. Capelluto, D. G. (2012) Tollip: a multitasking protein in innate immunity and protein trafficking. *Microbes Infect* **14**, 140-147

18. Ankem, G., Mitra, S., Sun, F., Moreno, A. C., Chutvirasakul, B., Azurmendi, H. F., Li, L., and Capelluto, D. G. (2011) The C2 domain of Tollip, a Toll-like receptor signalling regulator, exhibits broad preference for phosphoinositides. *Biochem J* **435**, 597-608

19. Shih, S. C., Prag, G., Francis, S. A., Sutanto, M. A., Hurley, J. H., and Hicke, L. (2003) A ubiquitin-binding motif required for intramolecular monoubiquitylation, the CUE domain. *EMBO J* **22**, 1273-1281

20. Prag, G., Misra, S., Jones, E. A., Ghirlando, R., Davies, B. A., Horazdovsky, B. F., and Hurley, J. H. (2003) Mechanism of ubiquitin recognition by the CUE domain of Vps9p. *Cell* **113**, 609-620

21. Azurmendi, H. F., Mitra, S., Ayala, I., Li, L., Finkielstein, C. V., and Capelluto, D. G. (2010) Backbone (1)H, (15)N, and (13)C resonance assignments and secondary structure of the Tollip CUE domain. *Mol Cells* **30**, 581-585

22. Delaglio, F., Grzesiek, S., Vuister, G. W., Zhu, G., Pfeifer, J., and Bax, A. (1995) NMRpipe - a multidimensional spectral processing system based on Unix pipes. *J Biomol NMR* **6**, 277-293

23. Garrett, D. S., Powers, R., Gronenborn, A. M., and Clore, G. M. (1991) A common-sense approach to peak picking in 2-dimensional, 3-dimensional, and 4-dimensional spectra using automatic computer-analysis of contour diagrams. *J Magn Reson Ser B* **95**, 214-220

24. Gautier, A., Mott, H. R., Bostock, M. J., Kirkpatrick, J. P., and Nietlispach, D. (2010) Structure determination of the seven-helix transmembrane receptor sensory rhodopsin II by solution NMR spectroscopy. *Nat Struct Biol Biol* **17**, 768-774

25. Schuck, P., and Rossmanith, P. (2000) Determination of the sedimentation coefficient distribution by least-squares boundary modeling. *Biopolymers* **54**, 328-341

26. Lebowitz, J., Lewis, M. S., and Schuck, P. (2002) Modern analytical ultracentrifugation in protein science: a tutorial review. *Protein Sci* **11**, 2067-2079

27. Siegel, L. M., and Monty, K. J. (1966) Determination of molecular weights and frictional ratios of proteins in impure systems by use of gel filtration and density gradient centrifugation. Application to crude preparations of sulfite and hydroxylamine reductases. *Biochim Biophys Acta* **112**, 346-362

28. Hicke, L., Schubert, H. L., and Hill, C. P. (2005) Ubiquitin-binding domains. *Nat Rev Mol Cell Biol* **6**, 610-621

29. Kang, R. S., Daniels, C. M., Francis, S. A., Shih, S. C., Salerno, W. J., Hicke, L., and Radhakrishnan, I. (2003) Solution structure of a CUE-ubiquitin complex reveals a conserved mode of ubiquitin binding. *Cell* **113**, 621-630

30. Petroski, M. D. (2008) The ubiquitin system, disease, and drug discovery. *BMC Biochem* **9 Suppl 1**, S7

31. Bhoj, V. G., and Chen, Z. J. (2009) Ubiquitylation in innate and adaptive immunity. *Nature* **458**, 430-437

32. Wilkinson, C. R., Seeger, M., Hartmann-Petersen, R., Stone, M., Wallace, M., Semple, C., and Gordon, C. (2001) Proteins containing the UBA domain are able to bind to multi-ubiquitin chains. *Nat Cell Biol* **3**, 939-943

33. Gillooly, D. J., Morrow, I. C., Lindsay, M., Gould, R., Bryant, N. J., Gaullier, J. M., Parton, R. G., and Stenmark, H. (2000) Localization of phosphatidylinositol 3-phosphate in yeast and mammalian cells. *EMBO J* **19**, 4577-4588

34. Bissig, C., Johnson, S., and Gruenberg, J. (2012) Studying lipids involved in the endosomal pathway. *Methods Cell Biol* **108**, 19-46

35. Mayinger, P. (2012) Phosphoinositides and vesicular membrane traffic. *Biochim Biophys Acta* **1821**, 1104-1113

36. Slagsvold, T., Aasland, R., Hirano, S., Bache, K. G., Raiborg, C., Trambaiolo, D., Wakatsuki, S., and Stenmark, H. (2005) Eap45 in mammalian ESCRT-II binds ubiquitin via a phosphoinositide-interacting GLUE domain. *J Biol Chem* **280**, 19600-19606

37. Hirano, S., Suzuki, N., Slagsvold, T., Kawasaki, M., Trambaiolo, D., Kato, R., Stenmark, H., and Wakatsuki, S. (2006) Structural basis of ubiquitin recognition by mammalian Eap45 GLUE domain. *Nat Struct Mol Biol* **13**, 1031-1032

38. Sloper-Mould, K. E., Jemc, J. C., Pickart, C. M., and Hicke, L. (2001) Distinct functional surface regions on ubiquitin. *J Biol Chem* **276**, 30483-30489

39. Wlodarski, T., and Zagrovic, B. (2009) Conformational selection and induced fit mechanism underlie specificity in noncovalent interactions with ubiquitin. *Proc Natl Acad Sci U S A* **106**, 19346-19351

40. Lange, A., Castaneda, C., Hoeller, D., Lancelin, J. M., Fushman, D., and Walker, O. (2012) Evidence for cooperative and domain-specific binding of the signal transducing adaptor molecule 2 (STAM2) to Lys63-linked diubiquitin. *J Biol Chem* **287**, 18687-18699

41. Mizuno, E., Kawahata, K., Kato, M., Kitamura, N., and Komada, M. (2003) STAM proteins bind ubiquitinated proteins on the early endosome via the VHS domain and ubiquitin-interacting motif. *Mol Biol Cell* **14**, 3675-3689

SUPPLEMENTARY MATERIALS

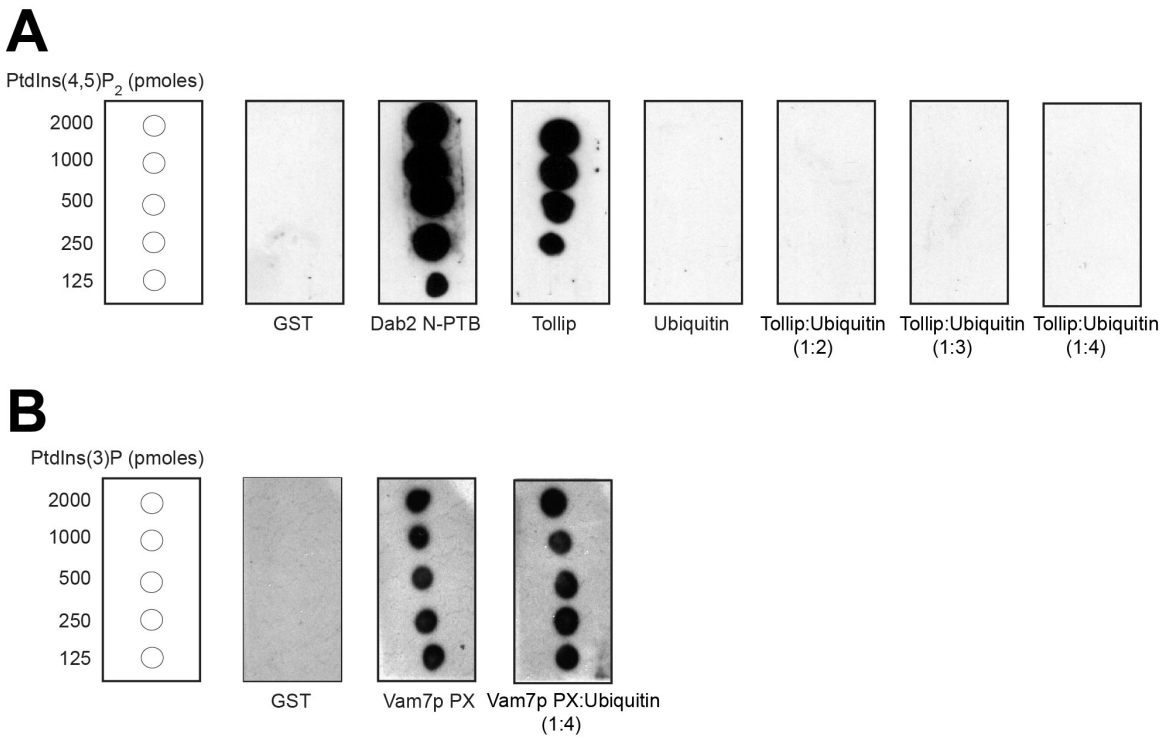

Figure S5.1, related to Figure 1**. Ubiquitin's effect on phosphoinositide binding.**

(A). Lipid-protein overlay assay showing the interaction of Tollip with PtdIns(4,5)P_2 in the absence and presence of 1-, 2-, and 4-fold ubiquitin. GST and Disabled-2 (Dab2) N-terminal region containing the PTB domain (N-PTB) were employed as negative and positive controls, respectively.

(B) Lipid-protein overlay assay showing the interaction of the Vam7p PX domain with PtdIns(3)P in the absence and presence of 4-fold ubiquitin. GST was used as a negative control

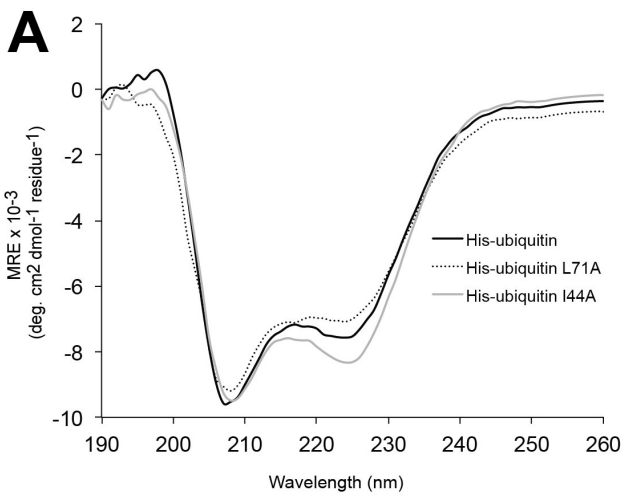
A
MRE x 10-3
(deg. cm2 dmol-1 residue-1)
2
0
-2
-4
-6
-8
-10
190
200
210
220
230
240
250
260
Wavelength (nm)
His-ubiquitin
His-ubiquitin L71A
His-ubiquitin I44A

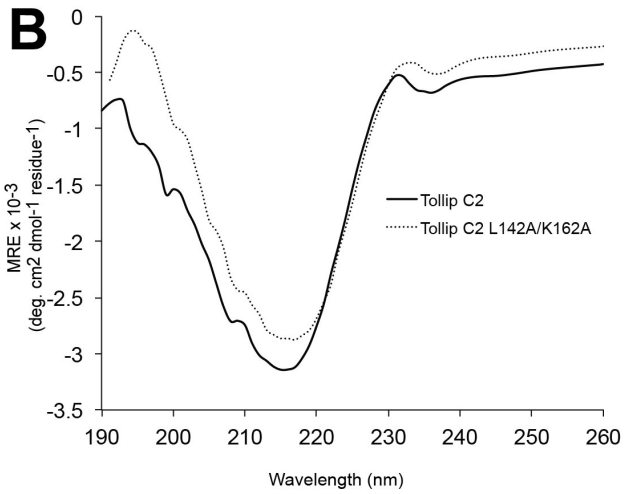
B
MRE x 10-3
(deg. cm2 dmol-1 residue-1)
0
-0.5
-1
-1.5
-2
-2.5
-3
-3.5
190
200
210
220
230
240
250
260
Wavelength (nm)
Tollip C2
Tollip C2 L142A/K162A

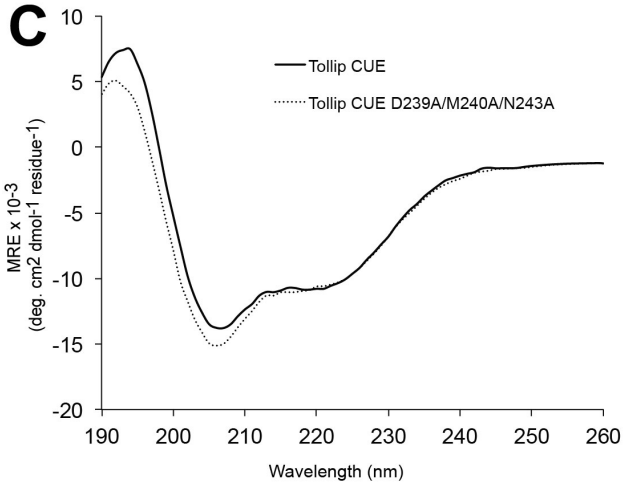
C
MRE x 10-3
(deg. cm2 dmol-1 residue-1)
10
5
0
-5
-10
-15
-20
190
200
210
220
230
240
250
260
Wavelength (nm)
Tollip CUE
Tollip CUE D239A/M240A/N243A

Figure S5.2, related with Figures 2, 3, and 4. **Mutations in ubiquitin and Tollip C2 and CUE domains do not alter their overall secondary structure.** Protein samples were analyzed at a concentration of 10 μM. Data were collected from 190–250 nm. Comparison of the far-UV CD spectra of his-ubiquitin and its L71A and I44A mutants (A), Tollip C2 domain and its L142A/K162A mutant (B), and the Tollip CUE domain and its D239A/M240A/N243A mutant.

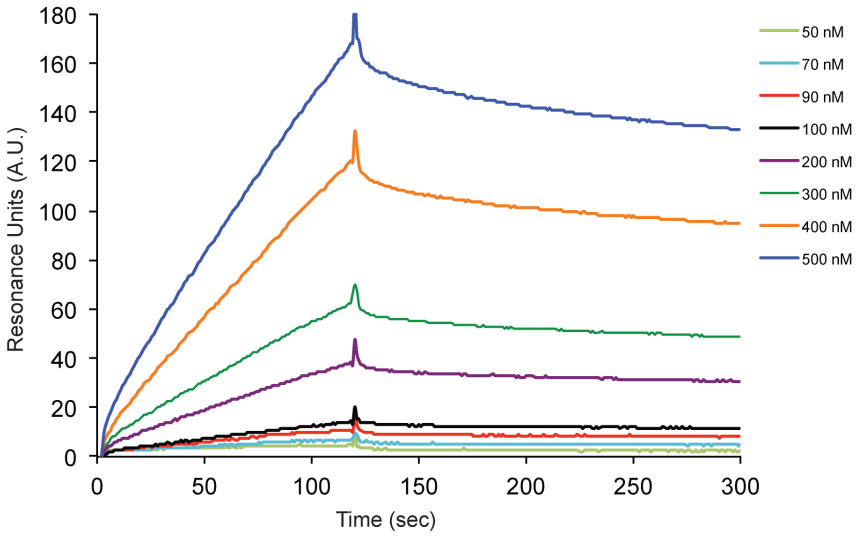

Figure S5.3, related to Figures 1, 2, and 3. **SPR traces of Tollip-ubiquitin association.** Binding traces of immobilized his-ubiquitin with increasing concentrations of GST-Tollip (color-coded at the inset). Association (k_{on}) and dissociation (k_{off}) rates and dissociation constant (K_D) were measured and calculated using Biacore X100 software 2.0. Binding curves best fit the bivalent analyte model in agreement with the presence of two ubiquitin-binding sites in the dimeric Tollip protein

Table S5.1, related to Figure 2. **Identification of critical residues for the Tollip C2 domain-ubiquitin interaction.** SPR-derived binding affinities of Tollip C2 domain for ubiquitin and their corresponding mutants designed based on HSQC titration analyses.

Protein	Construct	K_D (M)	Fit (χ^2)	Fold
Ubiquitin	Wild-type	1.08×10^{-5}	0.83	1
Ubiquitin	L43A	1.81×10^{-5}	0.81	2
Ubiquitin	I44A	1.25×10^{-5}	1.61	1
Ubiquitin	E51A	1.12×10^{-5}	1.76	1
Ubiquitin	L71A	2.83×10^{-5}	2.30	3
Ubiquitin	K6A/L71A	2.76×10^{-5}	1.67	3
Ubiquitin	L71A/L73A	2.76×10^{-5}	2.54	3
Tollip C2	H135A	3.54×10^{-6}	2.07	<1
Tollip C2	R157A	2.57×10^{-6}	1.55	<1
Tollip C2	K162A	1.83×10^{-5}	0.82	2
Tollip C2	L142A/K162A	5.98×10^{-5}	0.44	6

Table S5.2, related to Figures 3 and 4. **Identification of critical residues for the Tollip CUE domain-ubiquitin interaction.** SPR-derived binding affinities of Tollip CUE domain for ubiquitin and their corresponding mutants designed based on HSQC titration analyses.

Protein	Construct	K_D (M)	Fit (χ^2)	Fold
Ubiquitin	Wild-type	1.35×10^{-6}	3.06	1
Ubiquitin	L8A	2.00×10^{-6}	4.53	1
Ubiquitin	I44A	5.80×10^{-5}	1.33	43
Ubiquitin	K63A	3.10×10^{-6}	1.07	2
Ubiquitin	H68A	2.00×10^{-6}	2.00	1
Ubiquitin	L69A	3.80×10^{-6}	0.62	3
Tollip CUE	D239A	2.52×10^{-5}	0.24	19
Tollip CUE	M240A	9.33×10^{-5}	0.09	69
Tollip CUE	F241A	1.05×10^{-6}	3.60	<1
Tollip CUE	N243A	1.16×10^{-5}	0.12	9
Tollip CUE	G271V	7.11×10^{-5}	0.56	53
Tollip CUE	D239A/ M240A/ N243A	1.05×10^{-4}	2.06	78

CHAPTER VII: CONCLUSIONS AND FUTURE PERSPECTIVES

Tollip is a unique protein which participates in both innate immune signaling and endocytosis. However the biophysical basis of Tollip's role in these pathways remain unclear. Therefore, we seek to understand ligand binding properties of Tollip and how this modulates Tollip's function. The biophysical basis of lipid binding by Tollip will contribute to understand Tollip's subcellular localization in different cellular compartments. The detail molecular mechanisms of Tollip modulation by ubiquitin presented in this thesis will contribute to further understandings of Tollip's role as an adaptor protein in endosomal trafficking.

In this study, we identified PtdIns3*P* as the main target for Tollip C2 domain and described the ubiquitin binding property of this domain for the first time. C2 domains are the second most abundant lipid-binding modules and mostly found in membrane trafficking proteins. In order to exert proper membrane trafficking function, C2 domains uniquely associate with both lipid and protein binding partners. Hence, it is not surprising that in our study we found ubiquitin, perhaps the most important moiety of endosomal trafficking binds to the Tollip C2 domain. Further, we have biophysically characterized this binding with the canonical ubiquitin binding property of the Tollip CUE domain. In contrast to the Tollip C2 domain, which interacts with ubiquitin to its C-terminal residues, the CUE domain interaction surfaces are mapped around the well-known hydrophobic patch consisting of residues Leu43, Ile44, His68, and Val70. Nevertheless, in both cases a large surface area on ubiquitin was compromised, which

is indicative of conformational changes in the protein structures followed by binding events. Interestingly, the affinity of the full-length protein for ubiquitin is higher than individual C2 or CUE domain affinity values, which is indicative of the additive effect imparted by the presence of two individual UBDs. Remarkably, when we measured the full-length protein affinity to PtdIns3*P*, the affinity was much higher than the individual C2 domain or the protein binding to ubiquitin. As C2 domain is the only lipid-binding module in Tollip, we speculate that the affinity for lipid in Tollip is enhanced by the oligomeric state of the protein. The lower affinity of Tollip to ubiquitin can be explained by the fact that intracellular ubiquitin concentration is very high and thus would compensate for this. Another interesting aspect of our research was to see that the binding of ubiquitin to Tollip CUE domain dissociates its dimeric state. We speculate that the conformational changes and the dissociation of CUE dimer to monomer reduce the affinity for membrane PtdIns3*P*, which pulls off Tollip from the endosomal membrane and now the protein is prepared for cytosolic commitments. The overall summary of the work is depicted in Figure 6.1.

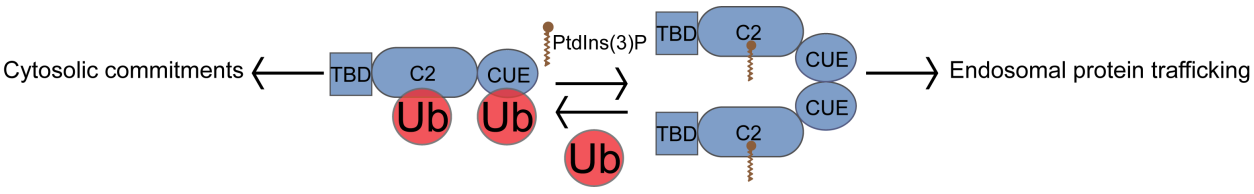

Fig 6.1. A cartoon representing ubiquitin modulated PtdIns3*P* binding in Tollip. When Tollip binds to cellular ubiquitin via its C2 and CUE domains, these associations disrupts Tollip's dimeric state and inhibit Tollip's binding to PtdIns3*P*. The membrane-free protein is available for cytosolic commitments.

The viceversa is also true, increased pool of PtdIns3*P* in the cellular membrane induce the protein to bind to the membrane, which has higher affinity to PtdIns3*P* than cellular ubiquitin. The protein is now available to participate in endosomal trafficking.

Thus, to conclude we propose that this non-covalent ubiquitin-Tollip UBD interaction partitions the protein into membrane-free and membrane-bound states, a function that contributes to Tollip's engagement in both membrane trafficking and cytosolic functions. Collectively, our work brings a molecular insight into Tollip's ligand recognition, which will help to define Tollip's role in basic cellular processes such as endosomal trafficking or innate immune pathways.

This study sets the groundwork for numerous future studies that can be done to conclude Tollip's role in endosomal trafficking. I) In our study we found that Tollip interacts with PtdIns3*P* in a Ca^{2+}-independent manner. This raises the question, what is the biological significance of Ca^{2+} binding by this protein? Experiments can be designed in order to find out the significance of Ca^{2+} binding in full length Tollip protein. II) Tollip K162A and the surrounding region was found to be important in lipid binding, Ubiquitin binding and for a potential protein sumoylation target. Hence, it will be intriguing to perform cell biological experiments with this mutant and decipher how it disrupts the endosomal trafficking/protein sumoylation in cell. III) Another interesting aspect will be to compare the polyubiquitin vs noncovalent monoubiquitin binding in Tollip. Several key

players of TLR signaling pathways undergo Lys63-mediated polyubiquitination (such as IRAK-1, TRAF-6, NEMO, etc.), that precisely activate the proteins to perform their respective functions during signaling process. Therefore, it will be intriguing to test the same phenomenon in Tollip and compare that to ubiquitin binding by the Tollip C2 and CUE domains.

APPENDICES

Appendix A

LIST OF PRIMERS

TOLLIP

Forward primer: 5'-CGC GGA TCC GGC GGC GGC ATG GCG ACC ACC GTC AGC-3'

Reverse primer: 5'-CCG GAA TTC CTA TGG CTC CTC CCC CAT CTG-3'

TOLLIP C2

Forward primer: 5'-GCG TFT CGA CAC CGT GGG CCG ACT GAA C-3'

Reverse primer: 5'-ATT CTT ATG CGG CCG CCT ACA TCA CCA TGG CAG CTG G-3'

TOLLIP C2 R78A

Forward primer: 5'-GAC CCC TAC TGC GCA CTG CGC CTG GGC-3'

Reverse primer: 5'-GCC CAG GCG CAG TGC GCA GTA GGG GTC-3'

TOLLIP C2 K102A

Forward primer: 5'-CCC CGC TGG AAT GCG GTC ATC CAC TGC-3'

Reverse primer: 5'-GCA GTG GAT GAC CGC ATT CCA GCG GGG-3

TOLLIP C2 R123A

Forward primer: 5'-GAG ATC TTC GAT GAG GCA GCC TTC TCC ATG GAC-3'

Reverse primer: 5'-GTC CAT GGA GAA GGC TGC CTC ATC GAA GAT CTC-3'

TOLLIP C2 H135A

Forward primer: 5'-GAC CGC ATT GCC TGG ACC GCC ATC ACC ATC CCG GAG TCC-3'

Reverse primer: 5’-GGA CTC CGG GAT GGT GAT GGC GGT CCA GGC AAT GCG GTC-3’

TOLLIP C2 L142A

Forward primer: 5’-CAC ATC ACC ATC CCG GAG TCC GCG AGG CAG GGC AAG GTG GAG GAC-3’

Reverse primer: 5’-GTC CTC CAC CTT GCC CTG CCT CGC GGA CTC CGG GAT GGT GAT GTG-3’

TOLLIP C2 K150A

Forward primer: 5’-CAA GGT GGA GGA CGC GTG GTA CAG CCT G-3’

Reverse primer: 5’-CAG GCT GTA CCA CGC GTC CTC CAC CTT G-3’

TOLLIP C2 R157A

Forward primer: 5’-TGG TAC AGC CTG AGC GGG GCG CAG GGG GAC GAC AAG GAG-3’

Reverse primer: 5’-CTC CTT GTC GTC CCC CTG CGC CCC GCT CAG GCT GTA CCA-3’

TOLLIP C2 K162A

Forward primer: 5’-CAG GGG GAC GAC GCG GAG GG ATG ATC-3’

Reverse primer: 5’-GAT CAT GCC CTC CGC GTC GTC CCC CTG-3’

TOLLIP CUE DOMAIN

Forward primer: 5’-CGC GGA TCC CCC CCG GCC GCC-3’

Reverse primer: 5’-CCG GAA TTC CTA TGG CTC CTC CCC CAT CTG C-3’

TOLLIP CUE D239A

Forward primer: 5’-AAA GCC ATC CAG GCG ATG TTC CCC AAC ATG GAC-3’

Reverse primer: 5’-GTC CAT GTT GGG GAA CAT CGC CTG GAT GGC TTT-3’

TOLLIP CUE M240A

Forward primer: 5’-AAA GCC ATC CAG GAC GCG TTC CCC AAC ATG GAC-3’

Reverse primer: 5’-GTC CAT GTT GGG GAA CGC GTC CTG GAT GGC TTT-3’

TOLLIP CUE F241A

Forward primer: 5’-AAA GCC ATC CAG GAC ATG GCG CCC AAC ATG GAC-3’

Reverse primer: 5’-GTC CAT GTT GGG CGC CAT GTC CTG GAT GGC TTT-3’

TOLLIP CUE N243A

Forward primer: 5’-CAG GAC ATG TTC CCC GCG ATG GAC CAG GAG GTG-3’

Reverse primer: 5’-CAC CTC CTG GTC CAT CGC GGG GAA CAT GTC CTG-3’

TOLLIP CUE G271V

Forward primer: 5’-TCC CTG CTG CAG ATG GTG GAG GAG CCA-3’

Reverse primer: 5’-TGG CTC CTC CAC CAT CTG CAG CAG GGA-3’

UBIQUITIN

Forward primer: 5’-CGC GGA TCC ATG CAG ATC TTC GTC AAG ACG-3’

Reverse primer: 5’-AAG GAA AAA AGC GGC CGC TTA ACC ACC ACG AAG TCT TAA GAC-3’

UBIQUITIN K6A

Forward primer: 5’-ATG CAG ATC TTC GTC GCG ACG TTA ACC GGT AAA ACC-3’

Reverse primer: 5’-GGT TTT ACC GGT TAA CGT CGC GAC GAA GAT CTG CAT-3’

UBIQUITIN L8A

Forward primer: 5’-ATC TTC GTC AAG ACG GCG ACC GGT AAA ACC ATA ACT C-3’

Reverse primer: 5’-GAG TTA TGG TTT TAC CGG TCG CCG TCT TGA CGA AGA T-3’

UBIQUITIN I44A

Forward primer: 5’-GAT CAA CAA AGA TTG GCG TTT GCC GGT AAG CAG CTC-3’

Reverse primer: 5’-GAG CTG CTT ACC GGC AAA CGC CAA TCT TTG TTG ATC-3’

UBIQUITIN K63A

Forward primer: 5’-TCT GAT TAC AAC ATT CAG GCG GAG TCG ACC TTA CAT CTT GTC-3’

Reverse primer: 5’-GAC AAG ATG TAA GGT CGA CTC GCG CTG AAT GTT GTA ATC AGA-3’

UBIQUITIN H68A

Forward primer: 5’-CAG AAG GAG TCG ACC TTA GCG CTT GTC TTA AGA CTT CGT G-3’

Reverse primer: 5’-CAC GAA GTC TTA AGA CAA GCG CTA AGG TCG ACT CCT TCT G-3’

UBIQUITIN L69A

Forward primer: 5’-AAG GAG TCG ACC TTA CAT GCG GTC TTA AGA CTT CGT G-3’

Reverse primer: 5’-CAC GAA GTC TTA AGA CCG CAT GTA AGG TCG ACT CCT T-3’

UBIQUITIN L43A

Forward primer: 5’-CCT GAT CAA CAA AGA GCG ATC TTT GCC GGT AAG-3’

Reverser primer: 5’-CTT ACC GGC AAA GAT CGC TCT TTG TTG ATC AGG-3’

UBIQUITIN E51A

Forward primer: 5’-GCCGGT AAG CAG CTC GCG GAC GGT AGA ACG CTG-3’

Reverse primer: 5’-CAG CGT TCT ACC GTC CGC GAG CTG CTT ACC GGC-3’

UBIQUITIN L71A

Forward primer: 5’-GAG TCG ACC TTA CAT CTT GTC GCG AGA CTT CGT GGT GG-3’

Reverse primer: 5’-CCA CCA CGA AGT CTC GCG ACA AGA TGT AAG GTC GAC TC-3’

UBIQUITIN L71A/L73A

Forward primer: 5’-ACC TTA CAT CTT GTC GCG AGA GCG CGT GGT GGT -3’

Reverse primer: 5’-ACC ACC ACG CGC TCT CGC GAC AAG ATG TAA GGT-3’

Appendix B

MODELS USED FOR SPR FITTING

Two different models were used in our study: i) Two state conformational change model and ii) Bivalent analyte model.

i) Two state conformational change model was used to fit

a) Tollip C2 domain binding to PtdIns*3*P and PtdIns(4,5)P_2

b) GST-Tollip binding to PtdIns3*P*

c) Tollip C2 domain binding to his-tagged ubiquitin and

d) Tollip CUE domain binding to his-tagged ubiquitin

The model describes a binding mechanism consisting of 1:1 interaction that is stabilized or destabilized by a secondary process such as conformational change. The secondary process us assumed to be slower than the initial binding. The rate equation for this model is as follows:

The KD value was calculated using the formula:

$$K_D = Ka_1 (1 + Kd_1)$$

ii) Bivalent analyte model was used to fit the GST-Tollip binding to histagged ubiquitin. The model describes the binding of a bivalent analyte to a monovalent ligand. The rate reaction is as follows:

The KD value for the initial binding event was calculated using the formula:

$$K_{D1} = Kd_1/Ka_1$$

Appendix C

LITERATURE REVIEW REFERENCES

1. Janeway, C. A., Jr., and Medzhitov, R. (2002) Innate immune recognition, *Annu Rev Immunol 20*, 197-216.
2. Hooper, L. V., Littman, D. R., and Macpherson, A. J. (2012) Interactions between the microbiota and the immune system, *Science 336*, 1268-1273.
3. Geijtenbeek, T. B., and Gringhuis, S. I. (2009) Signalling through C-type lectin receptors: shaping immune responses, *Nature reviews. Immunology 9*, 465-479.
4. Kawai, T., and Akira, S. (2008) Toll-like receptor and RIG-I-like receptor signaling, *Ann N Y Acad Sci 1143*, 1-20.
5. Kanneganti, T. D. (2010) Central roles of NLRs and inflammasomes in viral infection, *Nature reviews. Immunology 10*, 688-698.
6. Kawai, T., and Akira, S. (2006) TLR signaling, *Cell Death Differ 13*, 816-825.
7. Kagan, J. C. (2012) Defining the subcellular sites of innate immune signal transduction, *Trends in immunology 33*, 442-448.
8. McGettrick, A. F., and O'Neill, L. A. (2010) Localisation and trafficking of Toll-like receptors: an important mode of regulation, *Curr Opin Immunol 22*, 20-27.
9. Tokisue, T., Watanabe, T., Tsujita, T., Nishikawa, S., Hasegawa, T., Seya, T., Matsumoto, M., and Fukuda, K. (2008) Significance of the N-terminal histidine-rich region for the function of the human toll-like receptor 3 ectodomain, *Nucleic Acids Symp Ser (Oxf)*, 203-204.

10. Watanabe, T., Tokisue, T., Tsujita, T., Matsumoto, M., Seya, T., Nishikawa, S., Hasegawa, T., and Fukuda, K. (2007) N-terminal binding site in the human toll-like receptor 3 ectodomain, *Nucleic Acids Symp Ser (Oxf)*, 405-406.

11. Choe, J., Kelker, M. S., and Wilson, I. A. (2005) Crystal structure of human toll-like receptor 3 (TLR3) ectodomain, *Science 309*, 581-585.

12. Yamamoto, M., and Takeda, K. (2010) Current views of toll-like receptor signaling pathways, *Gastroenterol Res Pract 2010*, 240365.

13. Lim, K. H., and Staudt, L. M. (2013) Toll-like receptor signaling, *Cold Spring Harb Perspect Biol 5*, a011247.

14. Kawai, T., and Akira, S. (2010) The role of pattern-recognition receptors in innate immunity: update on Toll-like receptors, *Nature immunology 11*, 373-384.

15. Gay, N. J., Gangloff, M., and Weber, A. N. (2006) Toll-like receptors as molecular switches, *Nature reviews. Immunology 6*, 693-698.

16. Chen, L. Y., Zuraw, B. L., Zhao, M., Liu, F. T., Huang, S., and Pan, Z. K. (2003) Involvement of protein tyrosine kinase in Toll-like receptor 4-mediated NF-kappa B activation in human peripheral blood monocytes, *Am J Physiol Lung Cell Mol Physiol 284*, L607-613.

17. Medvedev, A. E., Piao, W., Shoenfelt, J., Rhee, S. H., Chen, H., Basu, S., Wahl, L. M., Fenton, M. J., and Vogel, S. N. (2007) Role of TLR4 tyrosine phosphorylation in signal transduction and endotoxin tolerance, *The Journal of biological chemistry 282*, 16042-16053.

18. Doyle, S. L., Jefferies, C. A., Feighery, C., and O'Neill, L. A. (2007) Signaling by Toll-like receptors 8 and 9 requires Bruton's tyrosine kinase, *The Journal of biological chemistry 282*, 36953-36960.

19. Watters, T. M., Kenny, E. F., and O'Neill, L. A. (2007) Structure, function and regulation of the Toll/IL-1 receptor adaptor proteins, *Immunology and cell biology 85*, 411-419.

20. Aderem, A., and Ulevitch, R. J. (2000) Toll-like receptors in the induction of the innate immune response, *Nature 406*, 782-787.

21. Bae, Y. S., Lee, J. H., Choi, S. H., Kim, S., Almazan, F., Witztum, J. L., and Miller, Y. I. (2009) Macrophages generate reactive oxygen species in response to minimally oxidized low-density lipoprotein: toll-like receptor 4- and spleen tyrosine kinase-dependent activation of NADPH oxidase 2, *Circ Res 104*, 210-218, 221p following 218.

22. Kagan, J. C., and Medzhitov, R. (2006) Phosphoinositide-mediated adaptor recruitment controls Toll-like receptor signaling, *Cell 125*, 943-955.

23. Valkov, E., Stamp, A., Dimaio, F., Baker, D., Verstak, B., Roversi, P., Kellie, S., Sweet, M. J., Mansell, A., Gay, N. J., Martin, J. L., and Kobe, B. (2011) Crystal structure of Toll-like receptor adaptor MAL/TIRAP reveals the molecular basis for signal transduction and disease protection, *Proceedings of the National Academy of Sciences of the United States of America 108*, 14879-14884.

24. Kenny, E. F., and O'Neill, L. A. (2008) Signalling adaptors used by Toll-like receptors: an update, *Cytokine 43*, 342-349.

25. Li, S., Strelow, A., Fontana, E. J., and Wesche, H. (2002) IRAK-4: a novel member of the IRAK family with the properties of an IRAK-kinase, *Proceedings of the National Academy of Sciences of the United States of America 99*, 5567-5572.

26. Janssens, S., and Beyaert, R. (2003) Functional diversity and regulation of different interleukin-1 receptor-associated kinase (IRAK) family members, *Mol Cell 11*, 293-302.

27. Kawagoe, T., Sato, S., Matsushita, K., Kato, H., Matsui, K., Kumagai, Y., Saitoh, T., Kawai, T., Takeuchi, O., and Akira, S. (2008) Sequential control of Toll-like receptor-dependent responses by IRAK1 and IRAK2, *Nature immunology 9*, 684-691.

28. Lin, S. C., Lo, Y. C., and Wu, H. (2010) Helical assembly in the MyD88-IRAK4-IRAK2 complex in TLR/IL-1R signalling, *Nature 465*, 885-890.

29. Keating, S. E., Maloney, G. M., Moran, E. M., and Bowie, A. G. (2007) IRAK-2 participates in multiple toll-like receptor signaling pathways to NFkappaB via activation of TRAF6 ubiquitination, *The Journal of biological chemistry 282*, 33435-33443.

30. Gohda, J., Matsumura, T., and Inoue, J. (2004) Cutting edge: TNFR-associated factor (TRAF) 6 is essential for MyD88-dependent pathway but not toll/IL-1 receptor domain-containing adaptor-inducing IFN-beta (TRIF)-dependent pathway in TLR signaling, *J Immunol 173*, 2913-2917.

31. Jiang, X., and Chen, Z. J. (2012) The role of ubiquitylation in immune defence and pathogen evasion, *Nature reviews. Immunology 12*, 35-48.

32. Banerjee, A., and Gerondakis, S. (2007) Coordinating TLR-activated signaling pathways in cells of the immune system, *Immunology and cell biology 85*, 420-424.

33. Palsson-McDermott, E. M., and O'Neill, L. A. (2004) Signal transduction by the lipopolysaccharide receptor, Toll-like receptor-4, *Immunology 113*, 153-162.

34. Liu, G., Park, Y. J., and Abraham, E. (2008) Interleukin-1 receptor-associated kinase (IRAK) -1-mediated NF-kappaB activation requires cytosolic and nuclear activity, *FASEB journal : official publication of the Federation of American Societies for Experimental Biology 22*, 2285-2296.

35. West, A. P., Koblansky, A. A., and Ghosh, S. (2006) Recognition and signaling by toll-like receptors, *Annu Rev Cell Dev Biol 22*, 409-437.

36. Tanimura, N., Saitoh, S., Matsumoto, F., Akashi-Takamura, S., and Miyake, K. (2008) Roles for LPS-dependent interaction and relocation of TLR4 and TRAM in TRIF-signaling, *Biochemical and biophysical research communications 368*, 94-99.

37. Kagan, J. C., Su, T., Horng, T., Chow, A., Akira, S., and Medzhitov, R. (2008) TRAM couples endocytosis of Toll-like receptor 4 to the induction of interferon-beta, *Nature immunology 9*, 361-368.

38. Lasker, M. V., and Nair, S. K. (2006) Intracellular TLR signaling: a structural perspective on human disease, *J Immunol 177*, 11-16.

39. Kondo, T., Kawai, T., and Akira, S. (2012) Dissecting negative regulation of Toll-like receptor signaling, *Trends in immunology 33*, 449-458.

40. Lang, T., and Mansell, A. (2007) The negative regulation of Toll-like receptor and associated pathways, *Immunology and cell biology 85*, 425-434.

41. Liew, F. Y., Xu, D., Brint, E. K., and O'Neill, L. A. (2005) Negative regulation of toll-like receptor-mediated immune responses, *Nature reviews. Immunology 5*, 446-458.

42. Janssens, S., Burns, K., Vercammen, E., Tschopp, J., and Beyaert, R. (2003) MyD88S, a splice variant of MyD88, differentially modulates NF-κB- and AP-1-dependent gene expression, *FEBS Letters 548*, 103-107.

43. Palsson-McDermott, E. M., Doyle, S. L., McGettrick, A. F., Hardy, M., Husebye, H., Banahan, K., Gong, M., Golenbock, D., Espevik, T., and O'Neill, L. A. (2009) TAG, a splice variant of the adaptor TRAM, negatively regulates the adaptor MyD88-independent TLR4 pathway, *Nature immunology 10*, 579-586.

44. Burns, K., Clatworthy, J., Martin, L., Martinon, F., Plumpton, C., Maschera, B., Lewis, A., Ray, K., Tschopp, J., and Volpe, F. (2000) Tollip, a new component of the IL-1RI pathway, links IRAK to the IL-1 receptor, *Nature cell biology 2*, 346-351.

45. Capelluto, D. G. (2012) Tollip: a multitasking protein in innate immunity and protein trafficking, *Microbes Infect 14*, 140-147.

46. Lo, Y. L., Beckhouse, A. G., Boulus, S. L., and Wells, C. A. (2009) Diversification of TOLLIP isoforms in mouse and man, *Mammalian genome : official journal of the International Mammalian Genome Society 20*, 305-314.

47. Didierlaurent, A., Brissoni, B., Velin, D., Aebi, N., Tardivel, A., Kaslin, E., Sirard, J. C., Angelov, G., Tschopp, J., and Burns, K. (2006) Tollip regulates proinflammatory responses to interleukin-1 and lipopolysaccharide, *Molecular and cellular biology 26*, 735-742.

48. Zhang, G., and Ghosh, S. (2002) Negative regulation of toll-like receptor-mediated signaling by Tollip, *The Journal of biological chemistry 277*, 7059-7065.

49. Li, T., Hu, J., and Li, L. (2004) Characterization of Tollip protein upon Lipopolysaccharide challenge, *Molecular immunology 41*, 85-92.

50. Kanzler, H., Barrat, F. J., Hessel, E. M., and Coffman, R. L. (2007) Therapeutic targeting of innate immunity with Toll-like receptor agonists and antagonists, *Nature medicine 13*, 552-559.

51. Ulevitch, R. J. (2004) Therapeutics targeting the innate immune system, *Nature reviews. Immunology 4*, 512-520.

52. Cook, D. N., Pisetsky, D. S., and Schwartz, D. A. (2004) Toll-like receptors in the pathogenesis of human disease, *Nature immunology 5*, 975-979.

53. Frantz, S., Ertl, G., and Bauersachs, J. (2007) Mechanisms of disease: Toll-like receptors in cardiovascular disease, *Nature clinical practice. Cardiovascular medicine 4*, 444-454.

54. Lakoski, S. G., Li, L., Langefeld, C. D., Liu, Y., Howard, T. D., Brosnihan, K. B., Xu, J., Bowden, D. W., and Herrington, D. M. (2007) The association between innate immunity gene (IRAK1) and C-reactive protein in the Diabetes Heart Study, *Experimental and molecular pathology 82*, 280-283.

55. Arroyo, D. S., Soria, J. A., Gaviglio, E. A., Rodriguez-Galan, M. C., and Iribarren, P. (2011) Toll-like receptors are key players in neurodegeneration, *International immunopharmacology 11*, 1415-1421.

56. Standiford, T. J., and Keshamouni, V. G. (2012) Breaking the tolerance for tumor: Targeting negative regulators of TLR signaling, *Oncoimmunology 1*, 340-345.

57. Doherty, G. J., and McMahon, H. T. (2009) Mechanisms of endocytosis, *Annu Rev Biochem 78*, 857-902.

58. Mukherjee, S., Ghosh, R. N., and Maxfield, F. R. (1997) Endocytosis, *Physiological reviews 77*, 759-803.

59. Kumari, S., Mg, S., and Mayor, S. (2010) Endocytosis unplugged: multiple ways to enter the cell, *Cell Res 20*, 256-275.

60. Conner, S. D., and Schmid, S. L. (2003) Regulated portals of entry into the cell, *Nature 422*, 37-44.

61. Lamb, C. A., Dooley, H. C., and Tooze, S. A. (2013) Endocytosis and autophagy: Shared machinery for degradation, *Bioessays 35*, 34-45.

62. Ciechanover, A., and Iwai, K. (2004) The ubiquitin system: from basic mechanisms to the patient bed, *IUBMB Life 56*, 193-201.

63. Wiborg, O., Pedersen, M. S., Wind, A., Berglund, L. E., Marcker, K. A., and Vuust, J. (1985) The human ubiquitin multigene family: some genes contain multiple directly repeated ubiquitin coding sequences, *EMBO J 4*, 755-759.

64. Sloper-Mould, K. E., Jemc, J. C., Pickart, C. M., and Hicke, L. (2001) Distinct functional surface regions on ubiquitin, *The Journal of biological chemistry 276*, 30483-30489.

65. Hilt, W., and Wolf, D. H. (2004) The ubiquitin-proteasome system: past, present and future, *Cell Mol Life Sci 61*, 1545.

66. Sadowski, M., Suryadinata, R., Tan, A. R., Roesley, S. N., and Sarcevic, B. (2012) Protein monoubiquitination and polyubiquitination generate structural diversity to control distinct biological processes, *IUBMB Life 64*, 136-142.

67. David, R. (2011) Endocytosis: One ubiquitin does the trick, *Nat Rev Mol Cell Biol 12*, 135.

68. MacGurn, J. A., Hsu, P. C., and Emr, S. D. (2012) Ubiquitin and membrane protein turnover: from cradle to grave, *Annu Rev Biochem 81*, 231-259.

69. Tachiyama, R., Ishikawa, D., Matsumoto, M., Nakayama, K. I., Yoshimori, T., Yokota, S., Himeno, M., Tanaka, Y., and Fujita, H. (2011) Proteome of ubiquitin/MVB pathway: possible involvement of iron-induced ubiquitylation of transferrin receptor in lysosomal degradation, *Genes Cells 16*, 448-466.

70. Hicke, L., and Dunn, R. (2003) Regulation of membrane protein transport by ubiquitin and ubiquitin-binding proteins, *Annu Rev Cell Dev Biol 19*, 141-172.

71. Husnjak, K., and Dikic, I. (2012) Ubiquitin-binding proteins: decoders of ubiquitin-mediated cellular functions, *Annu Rev Biochem 81*, 291-322.

72. Slagsvold, T., Aasland, R., Hirano, S., Bache, K. G., Raiborg, C., Trambaiolo, D., Wakatsuki, S., and Stenmark, H. (2005) Eap45 in mammalian ESCRT-II binds ubiquitin via a phosphoinositide-interacting GLUE domain. *J Biol Chem* 280, 19600-19606

73. Hirano, S., Suzuki, N., Slagsvold, T., Kawasaki, M., Trambaiolo, D., Kato, R., Stenmark, H., and Wakatsuki, S. (2006) Structural basis of ubiquitin recognition by mammalian Eap45 GLUE domain. *Nat Struct Mol Biol* 13, 1031-1032

74. Searle, M. S., Garner, T. P., Strachan, J., Long, J., Adlington, J., Cavey, J. R., Shaw, B., and Layfield, R. (2012) Structural insights into specificity and diversity in mechanisms of ubiquitin recognition by ubiquitin-binding domains, *Biochemical Society transactions 40*, 404-408.

75. Randles, L., and Walters, K. J. (2012) Ubiquitin and its binding domains, *Front Biosci 17*, 2140-2157.

76. Sokratous, K., Roach, L. V., Channing, D., Strachan, J., Long, J., Searle, M. S., Layfield, R., and Oldham, N. J. (2012) Probing affinity and ubiquitin linkage selectivity of ubiquitin-binding domains using mass spectrometry, *J Am Chem Soc 134*, 6416-6424.

77. Katoh, Y., Shiba, Y., Mitsuhashi, H., Yanagida, Y., Takatsu, H., and Nakayama, K. (2004) Tollip and Tom1 form a complex and recruit ubiquitin-conjugated

proteins onto early endosomes, *The Journal of biological chemistry 279*, 24435-24443.

78. Ponting, C. P. (2000) Proteins of the endoplasmic-reticulum-associated degradation pathway: domain detection and function prediction, *The Biochemical journal 351 Pt 2*, 527-535.

79. Shih, S. C., Prag, G., Francis, S. A., Sutanto, M. A., Hurley, J. H., and Hicke, L. (2003) A ubiquitin-binding motif required for intramolecular monoubiquitylation, the CUE domain, *EMBO J 22*, 1273-1281.

80. Prag, G., Misra, S., Jones, E. A., Ghirlando, R., Davies, B. A., Horazdovsky, B. F., and Hurley, J. H. (2003) Mechanism of ubiquitin recognition by the CUE domain of Vps9p, *Cell 113*, 609-620.

81. Yamakami, M., Yoshimori, T., and Yokosawa, H. (2003) Tom1, a VHS domain-containing protein, interacts with tollip, ubiquitin, and clathrin, *The Journal of biological chemistry 278*, 52865-52872.

82. Brissoni, B., Agostini, L., Kropf, M., Martinon, F., Swoboda, V., Lippens, S., Everett, H., Aebi, N., Janssens, S., Meylan, E., Felberbaum-Corti, M., Hirling, H., Gruenberg, J., Tschopp, J., and Burns, K. (2006) Intracellular trafficking of interleukin-1 receptor I requires Tollip, *Curr Biol 16*, 2265-2270.

83. Zhu, L., Wang, L., Luo, X., Zhang, Y., Ding, Q., Jiang, X., Wang, X., Pan, Y., and Chen, Y. (2012) Tollip, an intracellular trafficking protein, is a novel modulator of the transforming growth factor-beta signaling pathway, *The Journal of biological chemistry 287*, 39653-39663.

84. Cullen, P. J. (2011) Phosphoinositides and the regulation of tubular-based endosomal sorting, *Biochemical Society transactions 39*, 839-850.

85. Falkenburger, B. H., Jensen, J. B., Dickson, E. J., Suh, B. C., and Hille, B. (2010) Phosphoinositides: lipid regulators of membrane proteins, *The Journal of physiology 588*, 3179-3185.

86. Gruenberg, J. (2003) Lipids in endocytic membrane transport and sorting, *Current opinion in cell biology 15*, 382-388.

87. Saiardi, A., Sciambi, C., McCaffery, J. M., Wendland, B., and Snyder, S. H. (2002) Inositol pyrophosphates regulate endocytic trafficking, *Proceedings of the National Academy of Sciences of the United States of America 99*, 14206-14211.

88. Di Paolo, G., and De Camilli, P. (2006) Phosphoinositides in cell regulation and membrane dynamics, *Nature 443*, 651-657.

89. Roth, M. G. (2004) Phosphoinositides in constitutive membrane traffic, *Physiological reviews 84*, 699-730.

90. De Matteis, M. A., and Godi, A. (2004) PI-loting membrane traffic, *Nature cell biology 6*, 487-492.

91. Downes, C. P., Gray, A., and Lucocq, J. M. (2005) Probing phosphoinositide functions in signaling and membrane trafficking, *Trends in cell biology 15*, 259-268.

92. Balla, T. (2005) Inositol-lipid binding motifs: signal integrators through protein-lipid and protein-protein interactions, *Journal of cell science 118*, 2093-2104.

93. Mayinger, P. (2012) Phosphoinositides and vesicular membrane traffic, *Biochimica et biophysica acta 1821*, 1104-1113.

94. Catimel, B., Schieber, C., Condron, M., Patsiouras, H., Connolly, L., Catimel, J., Nice, E. C., Burgess, A. W., and Holmes, A. B. (2008) The PI(3,5)P2 and PI(4,5)P2 interactomes, *Journal of proteome research 7*, 5295-5313.

95. Catimel, B., Yin, M. X., Schieber, C., Condron, M., Patsiouras, H., Catimel, J., Robinson, D. E., Wong, L. S., Nice, E. C., Holmes, A. B., and Burgess, A. W. (2009) PI(3,4,5)P3 Interactome, *Journal of proteome research 8*, 3712-3726.

96. Moravcevic, K., Oxley, C. L., and Lemmon, M. A. (2012) Conditional peripheral membrane proteins: facing up to limited specificity, *Structure 20*, 15-27.

97. Nishizuka, Y. (1988) The molecular heterogeneity of protein kinase C and its implications for cellular regulation, *Nature 334*, 661-665.

98. Ponting, C. P., and Parker, P. J. (1996) Extending the C2 domain family: C2s in PKCs delta, epsilon, eta, theta, phospholipases, GAPs, and perforin, *Protein science : a publication of the Protein Society 5*, 162-166.

99. Cho, W., and Stahelin, R. V. (2006) Membrane binding and subcellular targeting of C2 domains, *Biochimica et biophysica acta 1761*, 838-849.

100. Nalefski, E. A., and Falke, J. J. (1996) The C2 domain calcium-binding motif: structural and functional diversity, *Protein science : a publication of the Protein Society 5*, 2375-2390.

101. Fukuda, M., Kojima, T., Aruga, J., Niinobe, M., and Mikoshiba, K. (1995) Functional diversity of C2 domains of synaptotagmin family. Mutational analysis

of inositol high polyphosphate binding domain, *The Journal of biological chemistry 270*, 26523-26527.

102. Montaville, P., Coudevylle, N., Radhakrishnan, A., Leonov, A., Zweckstetter, M., and Becker, S. (2008) The PIP2 binding mode of the C2 domains of rabphilin-3A, *Protein science : a publication of the Protein Society 17*, 1025-1034.

103. Stahelin, R. V., and Cho, W. (2001) Roles of calcium ions in the membrane binding of C2 domains, *The Biochemical journal 359*, 679-685.

104. Nalefski, E. A., McDonagh, T., Somers, W., Seehra, J., Falke, J. J., and Clark, J. D. (1998) Independent folding and ligand specificity of the C2 calcium-dependent lipid binding domain of cytosolic phospholipase A2, *The Journal of biological chemistry 273*, 1365-1372.

105. Sutton, R. B., Davletov, B. A., Berghuis, A. M., Sudhof, T. C., and Sprang, S. R. (1995) Structure of the first C2 domain of synaptotagmin I: a novel Ca2+/phospholipid-binding fold, *Cell 80*, 929-938.

106. Ciarrocchi, A., D'Angelo, R., Cordiglieri, C., Rispoli, A., Santi, S., Riccio, M., Carone, S., Mancia, A. L., Paci, S., Cipollini, E., Ambrosetti, D., and Melli, M. (2009) Tollip is a mediator of protein sumoylation, *PLoS One 4*, e4404.

107. Geiss-Friedlander, R., and Melchior, F. (2007) Concepts in sumoylation: a decade on, *Nat Rev Mol Cell Biol 8*, 947-956.

108. Steenholdt, C., Andresen, L., Pedersen, G., Hansen, A., and Brynskov, J. (2009) Expression and function of toll-like receptor 8 and Tollip in colonic epithelial cells

from patients with inflammatory bowel disease, *Scand J Gastroenterol 44*, 195-204.

109. Schimming, T. T., Parwez, Q., Petrasch-Parwez, E., Nothnagel, M., Epplen, J. T., and Hoffjan, S. (2007) Association of toll-interacting protein gene polymorphisms with atopic dermatitis, *BMC Dermatol 7*, 3.

110. Hu, Y., Li, T., Wang, Y., Li, J., Guo, L., Wu, M., Shan, X., Que, L., Ha, T., Chen, Q., Kelley, J., and Li, Y. (2009) Tollip attenuated the hypertrophic response of cardiomyocytes induced by IL-1beta, *Front Biosci 14*, 2747-2756.

111. Shah, J. A., Vary, J. C., Chau, T. T., Bang, N. D., Yen, N. T., Farrar, J. J., Dunstan, S. J., and Hawn, T. R. (2012) Human TOLLIP regulates TLR2 and TLR4 signaling and its polymorphisms are associated with susceptibility to tuberculosis, *J Immunol 189*, 1737-1746.